CLAUDIN-1 IS THE DIRECT TARGET OF *RUNX3* IN GASTRIC EPITHELIAL CELLS

CHANG TI LING

NATIONAL UNIVERSITY OF SINGAPORE

2009

CLAUDIN-1 IS THE DIRECT TARGET OF *RUNX3* IN GASTRIC EPITHELIAL CELLS

CHANG TI LING

(M.Sc., National University of Malaysia)

A THESIS SUBMITTED

FOR THE DEGREE OF DOCTOR OF PHILOSOPHY

DEPARTMENT OF MEDICINE

NATIONAL UNIVERSITY OF SINGAPORE

2009

ACKNOWLEDGEMENTS

My gratitude goes to both my supervisors, Prof. Yoshiaki Ito and A/P Kosei Ito for their patient guidance and discussions throughout my PhD study. I thank them for critically reviewing my work during our progress report sessions, as well as their useful advice for improvements.

I would also like to specially thank my ex-supervisor, A/P Evelyn Koay, the Director of Molecular Diagnosis Centre, NUH for her constant support and encouragement. Without her nurturing and many opportunities given, I will not be where I am today.

My gratitude also goes to the Singapore Millennium Foundation for providing me the SMF scholarship during the first three years of my PhD project and the sponsored trip to the Gordon Research Conferences, as well as to the NUS for my final year of scholarship. I also thank the Oncology Research Institute common grant for supporting my PhD work throughout.

My sincere appreciation also goes to all my fellow colleagues and friends at ORI (Tomoko, Tada-san, TK, Angela, KumChew, PeiYi, FenYi, BeeKeow, Michelle, Kathryn, Dr. LihWen, Dr. Vidya, Baidah, Diyanah, Erna, Judy, Mei Xian and ShenKiat) and IMCB *RUNX* group (Cecilia, Dominic, Anthony, Dr. Osato, YungKiang, Eunice, Ida, Yano and Ken-ichi) for their kind assistance and constructive advice along my PhD journey. I thank them for their friendship. Many thanks also to the ORI administrative team, Selena Gan, Deborah, Ivy, Alexis and Siew Hong for their kind help.

Last but not least, I would like to specially thank my beloved husband, Andy Yip for his loving care, trust, sacrifice and constant moral support and encouragement to make my PhD journey a possible one. I thank God for our baby Jasper who brought much joy and hope towards the end of my PhD project. Endless gratitude also goes to

my beloved parents, family members, cell members (Doris, BoonLay & FeeYoon, Selena & Willie, PohChoo, Anna & Charles, SiorPeng & ChekLeong, Winnie & ShenKong) and friends (Hazel, Eileen, HueyFen, HongLing, Maisy, Tony and JennHui) for their patient support, understanding, constant encouragement and prayers.

To God be the Glory! He is my pillar of support in times of troubles.

Chang Ti Ling
January 2009

TABLE OF CONTENTS

SUMMARY

The genes controlling cell-cell contact and cellular polarity are known to be heavily involved in cancer progression. Tumorigenic mouse GIF cells isolated from *Runx3*$^{-/-}$ gastric epithelium attached weakly to each other and did not form glandular structures on collagen gels as previously reported, suggesting that cellular polarity could not be established in the *Runx3*$^{-/-}$ cells. In a search for *RUNX*3 target genes functioning in gastric carcinogenesis, *claudin-1*, a gene from the tight junction protein family which functions in cell-cell contact and cellular polarity was found to be expressed at high level in *Runx3*$^{+/+}$ mouse gastric epithelial cells, but at very low level in *Runx3*$^{-/-}$ ones.

In human gastric cancer cell line, SNU16, RUNX3 is expressed in the cytoplasm in an inactive form and, upon treatment of cells by TGF-β, RUNX3 translocates into the nucleus and functions as a tumor suppressor. In SNU16, claudin-1 is expressed after the treatment of cells with TGF-β. The TGF-β-dependent expression of claudin-1, however, was not observed in *RUNX3*-knocked-down SNU16 cells. Furthermore, *hclaudin-1* promoter activity was dose-dependently up-regulated by expression of *RUNX3*. Chromatin immunoprecipitation assay showed that RUNX3 is bound to the cognate RUNX3 binding site in the promoter region of *hclaudin-1*.

SNU16 cells express claudin-1 and knock-down of claudin-1 expression enhanced tumorigenicity in nude mice. Furthermore, the tumorigenicity of *Runx3*$^{-/-}$ GIF clones stably expressing claudin-1 was significantly less than parental cell lines.

Altogether, these results showed that claudin-1 has a tumor suppressor activity in gastric epithelial cells. Consistent with these observations, expression of claudin-1 and RUNX3 expression were found to be correlated in the human gastric cancer specimens.

For the first time, *claudin-1* was identified as a novel downstream target of *RUNX3* in the TGF-β pathway. Strong evidence showed that *RUNX3* transcriptionally regulates the expression of *claudin-1*. Since *claudin-1* exhibits tumor suppressive activity, a part of tumor suppressor activity of *RUNX3* is likely to be mediated by *claudin-1*.

LIST OF TABLES

LIST OF FIGURES

LIST OF ABBREVATIONS

AJ	adheren junction
APS	ammonium persulfate
AS	anti-sense
bp	base pair
BS	binding site
CBF	core-binding factor
cDNA	complementary DNA
ChIP	chromatin immunoprecipitation
DAPI	4',6-Diamidino-2-phenylindole dihydrochloride
DMEM	Dulbecco's modified eagle's medium
dNTP	deoxynucleotide triphosphate
EMSA	electrophoresis mobility shift assay
FBS	fetal bovine serum
G	gauge
GAPDH	glyceraldehyde-3-phosphate dehydrogenase
GI	gastro-intestinal
GIF	gastric Ito-Fukamachi cells
kb	kilo base
kDa	kilo Dalton
LDS	lithium dodecyl sulfate
mAb	monoclonal antibody
min	minute
mRNA	messenger RNA
ORF	open reading frame
PBS	phosphate buffered saline
PBST	phosphate buffered saline with tween-20
PCR	polymerase chain reaction
PEBP	polyomavirus enhancer-binding protein
pmol	pico mole
PVDF	polyvinylidene fluoride

RT	room temperature
S	sense
SDM	site-directed mutagenesis
SDS	sodium dodecyl sulfate
TBE	Tris, Boric Acid, EDTA
TJ	tight junction
TEMED	N,N,N,N-Tetramethyl-Ethylenediamine
Tgf-β	transforming growth factor-beta
V	volt
wt	wild type
ZO	zonula occluden

CHAPTER 1 OBJECTIVE

The aim of the study is to understand the full potential of *RUNX3* as a tumor suppressor. Since *RUNX3* is a transcription factor, the identification of the target genes that are induced or suppressed by *RUNX3* should provide important insights into the molecular mechanism behind its tumor suppressor activity. Since *RUNX3* is a nuclear effecter of TGF-β pathway and TGF-β pathway is considered to be a tumor suppressor pathway, it is important to identify TGF-β dependent, *RUNX3* mediated target genes.

Based on a previous observation that the loss of *RUNX3* affects cell-cell contact and polarity, I would like to examine whether *RUNX3* regulates genes involve in this function and its possible link to gastric carcinogenesis. Previously, it was observed that *claudin-1*, a member of the tight junction protein family exhibited a similar knockout phenotype as those of *Runx3*$^{-/-}$. As *RUNX3* functions as a tumor suppressor under the TGF-β pathway, it would be feasible to observe if tight junction genes are regulated under this pathway in the gastric epithelial cells, which is an area yet to be examined. Findings of possible connections between RUNX3 and tight junction proteins in the gastric system may enable the development of useful molecular markers for diagnostic purposes.

CHAPTER 2 INTRODUCTION

2.1 Gastric Cancer

With the steady decline in the incidence of gastric cancer worldwide, it has become the fourth most common cancer, after cancers of the lung, breast, and colorectal. This is in comparison to its ranking as the second most common cancer worldwide in the past (1). However, gastric cancer remains a major public health problem as it remains the second most common type of fatal cancer worldwide (1, 2). There has been little improvement in survival as gastric cancer is too often diagnosed at an advanced stage, despite the extensive diagnostic and therapeutic investigations of gastric cancer.

Although gastric cancer frequencies have been clearly linked to environmental factors, such as *Helicobacter pylori* infection and diet, the genetic basis for gastric cancer development is still largely unclear. It is evident that transformation of a normal epithelial cell to a malignant cell is a result from the accumulation of several gene abnormalities which involves multiple steps. Correa postulated a model involving histomorphological changes that leads to gastric cancer (3). In this model, development of chronic gastritis, atrophy, intestinal metaplasia and eventually dysplasia results in gastric cancer. However, this model is still open to debate as it remains unclear whether these changes follow each other step by step, or whether some histomorphological changes directly precede gastric cancer development (3, 4).

2.1.1 Genetics of Gastric Cancer

Over the years, various genetic and epigenetic alterations have been associated with the development and progression of gastric cancer. These include microsatellite instability (MSI), reactivation of telomerase, inactivation of tumor suppressor genes and activation of oncogenes.

Due to DNA mismatch repair deficiency, replication errors in simple repetitive microsatellite sequences may occur which is defined as MSI. MSI can be classified as high-frequency (MSI-H), low-frequency (MSI-L), or stable (MSS). MSI has been recognized as one of the earliest changes in carcinogenesis, resulting in genomic instability. It was discovered that gastric cancer cases with MSI-H often show hypermethylation of CpG islands in the promoter region of the *hMlh1* gene which is associated with decreased *hMlh1* protein expression. This indicates that epigenetic inactivation of *hMlh1* due to promoter methylation could be the underlying cause of MSI (5, 6). A subset of gastric cancers including gastric tumors was found to harbor MSI (7, 8). Various genes involved in the regulation of cell-cycle progression and apoptotic signaling that have been found to be specifically altered in gastric cancer displaying MSI include *BAX*, *hMSH3*, *hMSH6*, *E2F-4*, TGF-β receptor II, and insulin-like growth factor receptor II (7). In view of this, MSI has been suggested as a genetic marker for the development of multiple gastric cancers (9).

Tumor suppressor genes and oncogenes play a general role in regulating the developmental and differentiation processes. Deregulation of these genes enables the development of cancer. Inactivation of tumor suppressor genes is frequently discovered in gastric carcinogenesis (10). It is known that at least two independent 'hits' are required to fully inactivate a tumor suppressor. The attention in cancer research has typically been on two of the mechanisms that inactivate tumor suppressors, namely loss of heterozygosity (LOH) or homozygous deletion. LOH in chromosomal loci such as 1p, 2q, 4p, 5q, 6p, 7q, 11q, 12q, 14q, 17p, 18q and 21q have been discovered in differentiated type of gastric cancer (11-14). However, it remained unclear which are the genes that are specifically involved in gastric carcinogenesis. It was then found that DNA methylation is also a powerful mechanism that suppresses gene transcription, which represents an alternative mechanism of tumor suppressor inactivation in cancer. Genes that are inactivated by DNA methylation include *RB*, the von Hippel-Lindau gene (*VHL*), CDKN2A ($p16^{INK4A}$), CDKN2B ($p15^{INK4B}$), E-cadherin (*E-cad*), *hMLH1*, *APC*, *RASSF1* and *caspase-8* (15-17).

The group of activated oncogenes consists primarily of various growth factors and growth factor receptors. *c-met*, a proto-oncogene which encodes a tyrosine kinase receptor for the hepatocyte growth factor, was overexpressed in 50% of diffuse and intestinal-type of gastric cancers. Tumors overexpressing c-met also display increased invasiveness and are poorly differentiated (18). The overexpression of *c-erB2* (*HER-2/neu*) gene, a proto-oncogene and a transmembrane tyrosine kinase receptor was also

found to associate with approximately one-fourth of all gastrointestinal tract malignancies (19), and has been implicated as a potential marker for the prognosis in gastric cancers (20). Oncogenes, such as cyclin E and and *c-myc* were also discovered to be amplified and overexpressed in gastric carcinoma (21, 22).

Though numerous genetic abnormalities associated with gastric cancer have been described, they were either associated with a limited number of cases or were still poorly understood. The molecular mechanisms underlying the pathogenesis of gastric cancer have only been characterized recently with the discovery of *RUNX3* and its role in gastric carcinogenesis. The reason why *RUNX3* was not identified as a tumor suppressor earlier could be because this gene is inactivated mainly by epigenetic modification and genetic alteration of both alleles is very rare. *RUNX3* appears to be a new addition to the list of genes that are inactivated by DNA methylation. Since its discovery as a strong candidate tumor suppressor in gastric carcinogenesis (23), the underlying mechanisms of *RUNX3* regulation and its downstream target genes in gastric carcinogenesis became the subject of active investigations.

2.2 RUNX Protein Family

RUNX genes encode the α subunits called the polyomavirus enhancer-binding protein 2 (*PEBP2*)*α*/core binding factor (*CBF*)*α* of the Runt domain transcription factors. The α subunit heterodimerizes with the β subunits (*PEBP2β/CBFβ*) to form the

heterodimeric transcription factor, initially discovered as the PEBP2, or the CBF, which interacts with the enhancer core of Moloney murine leukemia virus. RUNX proteins alone are unstable, as they are subjected to ubiquitination followed by proteolytic degradation by proteasome enzymes (24). Heterodimerization with the β subunit prevents ubiquitination, thus stabilizing RUNX proteins (Figure 2.1).

However, RUNX heterodimers are relatively weakly acting transcriptional regulators. Associations with transcriptional co-activators, such as MYB, ETS, and p300/CBP, or co-repressors such as TLE1 and mSin3A however can induce the potency of its transcriptional function (25). Due to the low expression level of RUNX proteins, subcellular localization of RUNX proteins has been studied largely using exogenously expressed RUNX proteins in fibroblasts and leukemic cells. Immunocytochemistry shows that RUNX proteins are localized in the nucleus, whereas exogenously expressed PEBP2β/CBFβ is in the cytoplasm.

To date, three *RUNX* genes, namely *RUNX1*, *RUNX2* and *RUNX3* have been identified in mammals, whereby all three genes contain a conserved region, termed the Runt domain (26). By comparing between the mouse PEBP2αA1 (Runx2), mouse PEBP2αB1 (Runx1), and human PEBP2αC1 (RUNX3) as well as *Drosophila* Runt proteins, PEBP2αA1 and PEBP2αC1 was found to be 93.8% identical in homology, whereas PEBP2αB1 and PEBP2αC1 was 93.0% identical in homology. Besides, all three Runt domain proteins also have a C-terminal end containing a unique five amino-acid sequence, identified as VWRPY, which is 100% conserved from

Drosophila to human (27). This C-terminal part of the RUNX molecule plays a role in transcription regulation (28, 29).

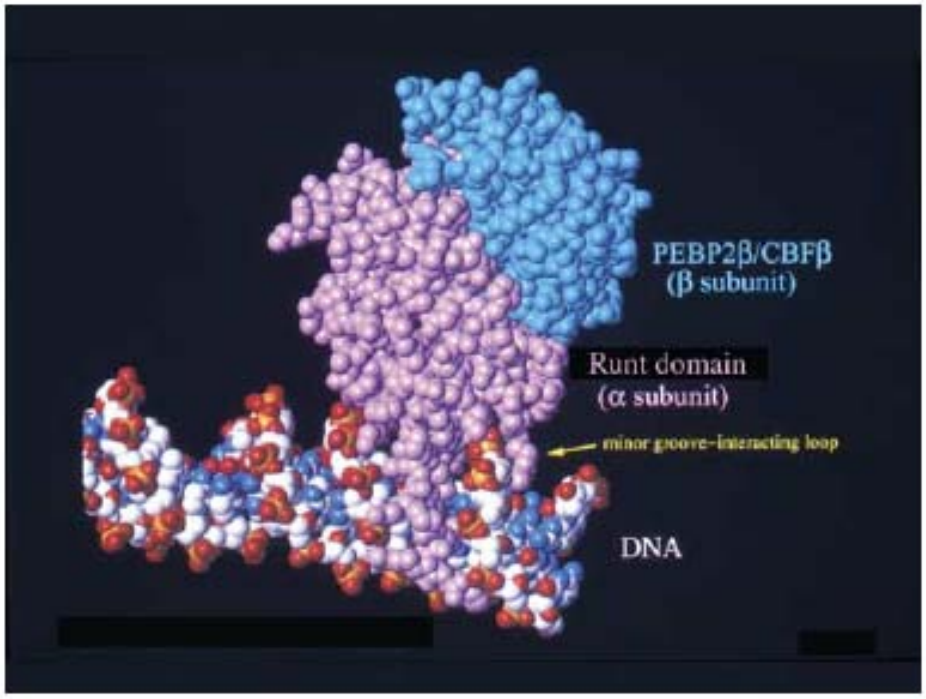

Figure 2.1: Crystal structure of the Runt domain heterodimerized with the 134 amino-acid region of PEBP2/CBF bound to DNA. [Ref. 23]

2.2.1 Nomenclature of *RUNX*

The runt-domain transcription factors *RUNX1, RUNX2* and *RUNX3* have previously been assigned various designations by different laboratories. The designation acute myelogenous leukemia (AML) factors (ie. AML1, AML2 and AML3) was generated

based on the genetic studies of leukemia-related chromosomal translocations. Core-binding factor alpha (CBFA) was initially characterized as sequence specific DNA-binding proteins that interact with the enhancers of retroviruses. PEBP2 was named after the murine cDNAs polyoma enhancer-binding proteins. Other aliases, such as nuclear matrix protein 2 (NMP2), osteoblast-specific complex (OBSC) and osteoblast-specific factor 2 (OSF2) were also generated. In November 1999, the Nomenclature Committee of the Human Genome Organization (HUGO) adopted the use of the term 'RUNX' to refer to the genes encoding the runt-related proteins, also an abbreviation for the term 'runt-related protein'. The mammalian RUNX proteins and their synonyms as well as their locus are as listed in Table 2.1. The order of the numbers was given according to the order in which the knock-outs for each of the mouse *Runx* genes were published (*Runx1/Aml1* in 1996 (30, 31), *Runx2/Cbfa1* in 1997 (32, 33) and *Runx3/Pebp2αC* in 2002 (23).

Table 2.1: The mammalian RUNX genes synonyms and their locus
(Adapted from Oncogene 2004; 23:4209-10)

RUNX1	CBFA2	AML1	PEBP2alphaB	21q22
RUNX2	CBFA1	AML3	PEBP2alphaA	6p21
RUNX3	CBFA3	AML2	PEBP2alphaC	1p36

2.2.2 Evolutionary Conservation of *RUNX*

Besides the three *RUNX* genes in mammals, four genes have been reported in *D. melanogaster* (34), (35), (36), one in sea urchin (37), one in Xenopus (38), four in zebra fish (39), (40), (41), and one in *C. elegens* (42). *RUNX* genes also appear to be conserved throughout in metazoa, the most primitive organism described so far, with the findings of RUNX homologs in basal metazoans such as starlet sea anemone (*Nematostella vectensis*) (43) and sponge (*Oscarella carmela*) (44). This shows that *RUNX* genes were highly conserved throughout the evolution, and very likely to play an important role in the early metazoan development and evolution. Like their counterparts in *D. melanogaster* and *C. elegans*, mammalian *RUNX* family transcription factors also play important roles in cell fate determination during development. As reported for *Runx1* (30), *Runx2* (32, 33) and *Runx3* (23), genetic ablation of all these genes have profound effects on development processes.

2.3 Role of *RUNX* Protein Family

2.3.1 *RUNX1*

RUNX1 is known to play a critical role in hematopoietic development and is genetically altered in leukemia. RUNX1 is the most frequent target of chromosomal translocations associated with human leukemia, with the TEL-AML t(12;21) fusion

accounting for 20% of acute lymphoblastic leukemia (ALL) cases and the AML-ETO t(8;21) fusion accounting for 12% of acute myeloid leukemias (AML) (45). Heterozygous loss-of-function mutations which cause haploinsufficiency of *RUNX1* are associated with familial platelet disorder with predisposition to acute myeloid leukemia (FPD-AML) (46). This supported the hypothetical function of *RUNX1* as tumor suppressor for AML. Besides, sporadic heterozygous mutations and point mutations of *RUNX1* are also leukemogenic (47, 48). Its association with several autoimmune diseases, namely, systemic lupus erythematosus, rheumatoid arthritis and psoriasis has also been reported (49), (50).

In mouse model, genetic ablation of *Runx1* results in embryonic lethality and a complete lack of fetal liver hematopoiesis (30), (31). *Runx1* is also essential for the generation of hematopoietic stem cells (HSCs) (51, 52). *Runx1*-deficient hematogenic endothelial cells are incapable of producing hematopoietic stem cells (HSCs), supporting its role in the initiation of the hematopoietic system. However, *Runx1* is not necessary for the maintenance of HSCs in the adult stage or expansion of HSC/progenitor cells (HSC/Ps). Instead, lack of *Runx1* induces myeloproliferative disease and T-cell lymphoma. It was thus suggested that *Runx1* plays a role as a global regulator of hematopoiesis, from initiation to terminal differentiation.

2.3.2 *RUNX2*

RUNX2 is essential in osteogenesis. In human and mice, deletions, insertions or mutations that inactivates one allele of the *RUNX2* gene causes the autosomal dominant bone disorder, called cleidocranial dysplasia (33, 53, 54). *Runx2* gene product is necessary for osteoblast differentiation and bone ossification as *Runx2*-knockout mice display complete bone loss, whereas *Runx2* heterozygous mice displayed hypoplasia of the clavicle and delayed development of membranous bones which were all typical features of cleidocranial dysplasia (32, 33). 2Interestingly however, *Runx2* has also been described as an oncogene whereby the overexpression of *Runx2* pertubates T cell development in lymphomagenesis by its cooperation with *c-myc* (55). However, the oncogenic property of *Runx2* is something yet to be fully understood since both *RUNX1* and *RUNX3* are well-documented tumor suppressors.

2.3.3 *RUNX3*

As compared to *RUNX1* and *RUNX2*, *RUNX3* is involved in more diverse biological pathways. Besides playing a role in gastric carcinogenesis as shown by targeted deletion of *Runx3* in mice (23), its role in CD8-lineage T-cells development (56, 57) and in dendritic cells (58) have also been reported. Besides, absence of *Runx3* also affects the biological function of the TrkC-dependent dorsal root ganglion neurons as reported by Inoue et al. (2002) (59) and Levanon et al. (2002) (60). Possible

involvement of *RUNX3* in the cancers of the lung, colon, pancreas, liver, prostate, bile duct, breast, larynx, esophagus, endometrium, uterine cervix and testicular yolk sac was also reported (61-75). Since *RUNX3* is involved in so many different cancer types, it may also be playing critical roles in different aspects of carcinogenesis.

2.4 RUNX and TGF-β Tumor Suppressor Pathway

Transforming growth factor-β (TGF-β) is a family of multifunctional cytokines that regulate the growth, differentiation, apoptosis and matrix accumulation of wide varieties of cells (76). It is a member of the TGF-β superfamily which includes bone morphogenetic proteins (BMPs), activins, Nodal, myostatin, and anti-Mullerian hormone (AMH). TGF-β, activin, Nodal and myostatin activates the TGF-β-like signals, whereas BMPs and AMH activates BMP-like signals.

TGF-β is essential in many development and physiological processes. It acts as a potent growth inhibitor of most cell types, such as the epithelial cells, endothelial cells, hematopoietic cells, and lymphocytes. Abnormalities in the TGF-β receptor affect downstream signal transduction pathways involved in the control of cell growth and differentiation, which often results in tumor progression, thus is regarded as a tumor suppressor pathway (77-79). Heterozygously disrupted TGF-β1 displayed increased hepatocyte proliferation and decreased apoptosis in liver and lung, which induced liver and lung cancer when challenged with chemical carcinogen (80). TGF-

β1 knockout mice also show hyperplasia in the epithelial cells of glandular stomach (81).

It is interesting to note that some functions of the TGF-β superfamily cytokines are similar to those of RUNX proteins. For example, TGF-β acts on B lymphocytes and induces synthesis of IgA, and Runx1 exhibits a similar effect. BMPs induce bone formation, which is similar to the function of Runx2. TGF-β also regulates growth and apoptosis of gastric epithelial cells, which are also regulated by Runx3. True enough, Runt domain transcription factors were found to be important targets of TGF-β superfamily signaling. Smad2 and Smad3 which acts as signal transducers in the TGF-β signaling pathway were shown to interact with RUNX1, RUNX2 and RUNX3 *in vitro* (82). Physiologically, endogenous RUNX2 also interacts with endogenous Smad3 in 10T1/2 and ROS17/2.8 cells (83).

In the TGF-β signaling pathway, members of the TGF-β superfamily bind to two distinct transmembrane receptors, the type I, which is a threonine kinase receptor, and type II, which is a serine kinase receptor (84). Upon binding of their corresponding ligand to type I and type II receptors, type II receptor kinases transphosphorylate the juxtamembrane domains of the type I receptor kinases, forming a heterotetramers. This activated form of receptor then phosphorylates the receptor-regulated Smads (R-Smads), namely Smad2 and Smad3, which will then form hetero-oligomeric complexes with the common-partner Smad (Co-Smads), Smad4. The R-Smad-Co-Smad complexes then translocate into the nucleus and binds to transcription factors to regulate the transcription of target genes. These

transcription factors would act along with other transcription factors, co-activators and co-repressors to regulate various genes upon stimulation by members of the TGF-β superfamily (Figure 2.2).

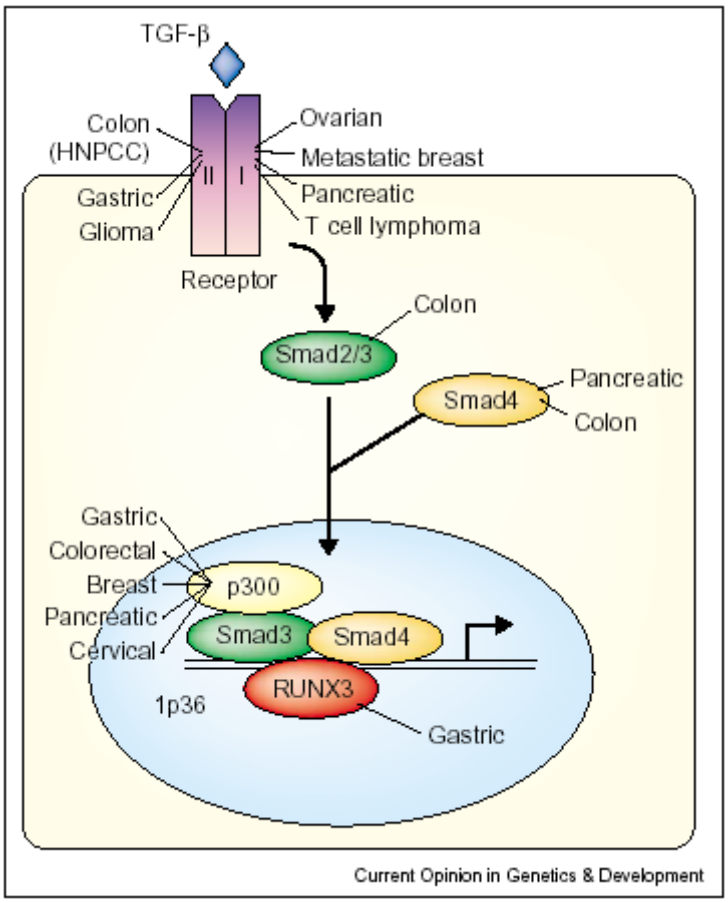

Figure 2.2: The TGF-β tumor suppressor pathway. Mutations in the genes encoding TGF-β type I and type II, Smad2/3 and Smad4 are linked to various cancers as indicated. The transcriptional co-activator p300 is also mutated in several cancers. RUNX3 is a target of TGF-β tumor suppressor pathway. [Ref. 100]

Both TGF-β signaling components and RUNX establish a functional relationship by working synergistically to regulate the downstream target genes. Figure 2.2 shows a schematic diagram of the transcription regulation by RUNX3 under the TGF-β tumor suppressor pathway. Various cancers linked to mutations in the gene encoding TGF-β type I and type II receptors, Smad2/3, Smad4 (DPC4) and the transcriptional co-activator p300 were depicted in the diagram (78, 85-87).

2.5 *RUNX3* and Gastric Cancer

Identification of *Runx3* expressing tissues has been challenging and complicated since results generated from different methods of detection were different. Besides, temporal and spatial changes of expression also add to the complexity. However, *Runx3* appears to be expressed ubiquitously in many cell types including epithelial cells, mesenchymal cells and blood cells. Expression in peripheral nervous system including dorsal root ganglion neurons, epithelial cells in the adult gastrointestinal tract and hematopoietic cells are especially prominent (88).

RUNX3 has been identified as the smallest gene in the family, which span about 67kb with six exons. Based on the genomic structure complexity, Bangsow et al. (2001) (89) proposed that *RUNX3* is the most primitive of the three genes though the precise chronology of evolutional diversification of the genes still remains to be determined (36). However, it is still interesting to note that *Runx3* is involved in the development of primitive monosynaptic neurons (59, 60). Both *C. elegens* and sea

urchins also contain one *Runx* gene, which are expressed in the intestine and foregut respectively (42, 90). In mouse, *Runx3* is expressed in the gastrointestinal organs of the developing embryo and throughout the adulthood of the mouse. *RUNX3* function in the stomachs of mammals may therefore be evolutionarily conserved.

In human, *RUNX3* is found in locus *1p36*, a region that is frequently deleted in many type of cancers, and was postulated to contain other important tumor suppressor gene(s) (91). Several lines of evidence have demonstrated that *RUNX*3 is a tumor suppressor of gastric cancer (23, 92). Work by Li et al (2002) shows that while *Runx3* knockout mice are born in Mendelian ratios, they die soon after birth, possibly due to starvation. The gastric epithelium of *Runx3* knockout mice displays hyperplasia due to an increase in cell proliferation and a reduced apoptosis rate (23, 93). A reduced sensitivity to TGF-β1 was also shown in *Runx3* knockout mice, suggesting that *RUNX3* operates downstream of the TGF-β signaling pathway, which is a well-known tumor suppressive pathway. *Runx3*-/- gastric epithelial cells in a *p53*-/- background are tumorigenic in nude mice, whereas those from *Runx3*+/+*p53*-/- mice are not. This suggests that *Runx3* functions in keeping cell proliferation under control, which is a typical feature of a tumor suppressor.

Studies in mice have implicated the importance of *Runx3* in the growth and differentiation of mouse gastric epithelial cells (93-95). Observation of the *Runx3*+/+*p53*-/- and *Runx3*-/-*p53*-/- cells using phase contrast microscopy showed that both types of cells were relatively homogenous in appearance, and exhibited polygonal morphology, a characteristic of epithelial cells (Fig. 2.3A and B). Further

examination of the *Runx3*+/+ and *Runx3*-/- gastric epithelial cells revealed that when cultured between collagen gels, *Runx3*+/+ cells formed simple columnar epithelia with occasional glandular structures. The cells showed polarity with positive staining for PAS, which stains mucus localized on the luminal surface, a characteristic of mucous neck cells, indicating that they retain the phenotype of relatively undifferentiated gastric epithelial cells (Fig. 2.3C) In contrast, *Runx3*-/- cells attached weakly to each other and did not form glandular structures, but piled between collagen gels. Some cells were weakly stained with PAS, indicating that they synthesized and secreted mucus, but mucus droplets were evenly distributed in their cytoplasm, suggesting that cellular polarity could not be established when cells were combined with collagen gels (Fig. 2.3D) (95).

Besides, it was also found that primary gastric cancer specimens express significantly lower levels of *RUNX3* due to a combination of hemizygous deletion and hypermethylation of the *RUNX3* promoter region. Of 46 primary human gastric cancer specimens, 30% displayed hemizygosity of *RUNX3*. Intragenic mutation in the remaining allele was however very rare. Instead, *RUNX3* gene was silenced by DNA methylation on the CpG island located in the proximal (P2) promoter region, which resulted in reduced *RUNX3* level in 45-60% of the primary human gastric tumors analyzed, which further rised to nearly 90% among the late stage, representing highly metastatic tumors. One incidence of a single point mutation involving a single-nucleotide transition of arginine 122 to cysteine (R122C) within the conserved Runt domain was also discovered in the 119 human tumors investigated. When tested on

nude mice, exogenous *RUNX3* greatly reduced tumor growth, while the R122C mutation abolished the tumor-suppressor activity of *RUNX3* (23).

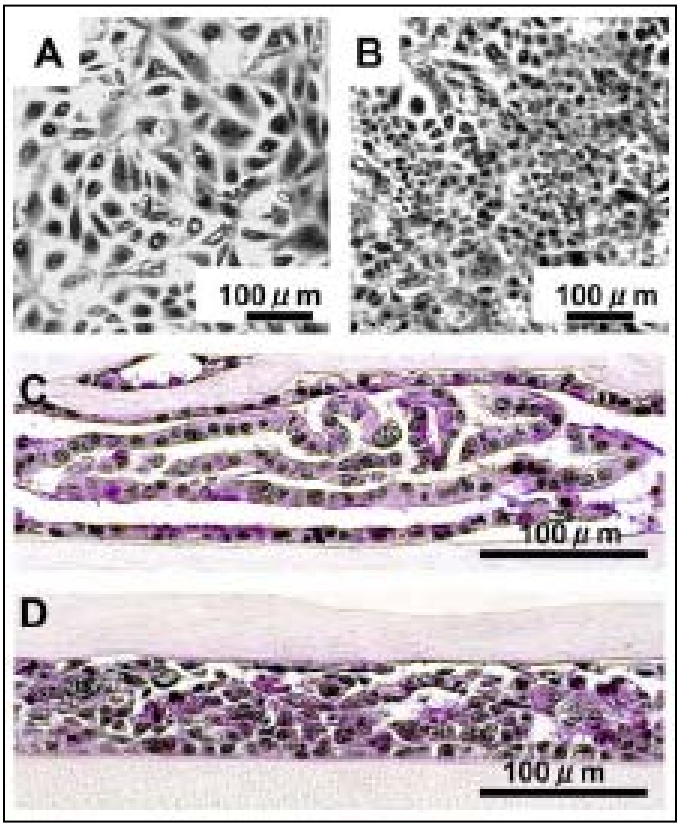

Figure 2.3: Characteristic of mouse gastric epithelial cell lines *in vitro*. Phase contrast micrographs of *Runx3+/+p53-/-* GIF9 cell line (A), and *Runx3-/-p53-/-* GIF5 cell line (B) in culture. Light micrographs of *Runx3+/+p53-/-* GIF9 (C) and *Runx3-/-p53-/-* GIF5 cells (D) cultured between collagen gels, and stained with PAS-hematoxylin. [Ref. 95]

In *N*-methyla-*N*-nitrosourea (MNU)-treated mice that developed gastric cancer, *Runx3* was also inactivated by DNA methylation (92). Although the exact mechanism by which MNU induces gastric carcinomas remains unknown, *Runx3*

appeared to be the major target of the carcinogen, since CpG islands in the *Runx1* and *Runx2* promoter regions were not methylated (92). *Ras* and *p53* genes also do not appear to play important role in these changes (96). Collectively, these results provided strong evidence that *RUNX3* is a tumor suppressor in gastric cancer, whereby inactivation of *RUNX3* is causally associated with human gastric carcinogenesis.

On a separate investigation, the authors also found that *RUNX3* was inactivated in more than 80% of gastric cancer not only by gene silencing but also by protein mislocalization (97). In a total of 97 gastric cancer samples tested, 44% did not express RUNX3. From the remaining 56% that expressed RUNX3, 38% were detected exclusively in the cytoplasm, and only 18% showed nuclear localization. Unlike RUNX3 in nuclear, those that were expressed in the cytoplasm of cancer cells were inactive as tumor suppressor. Several other groups also reported the role of *RUNX3* in gastric cancer, whereby the lack of *RUNX3* function is linked to the genesis and progression of gastric cancer (68, 70, 98). Collectively, all these observations indicate the importance of *RUNX3* in the normal function of stomach as well as its role as tumor suppressor in gastric carcinogenesis.

2.5.1 Tumor Suppressive Mechanism of *RUNX3* in Gastric Cancer

RUNX3 is a downstream target of the TGF-β signaling pathway, whereby *RUNX3* forms complexes with *Smads* which in turn regulates target gene expression (99, 100).

Runx3 knockout mice which displayed a reduced sensitivity to TGF-β supported the notion that *RUNX3* operates downstream of the TGF-β signaling pathway (23).

Apoptosis induced by TGF-β is a well-documented phenomenon that occurs in many different cell types (101). The activation of Smad proteins seems to play a crucial role in the TGF-β-induced apoptosis, as shown by the induction of apoptosis with the overexpression of *Smad4* (102), whereas overexpression of a dominant-negative *Smad3* inhibits TGF-β-dependent apoptosis (103). Several proapoptotic target genes regulated by the TGF-β signaling pathyway, such as *Bcl-2, Bcl-xL, Bax* and the zinc-finger trasnscription factor (*TIEG*) were also reported (104-106). However, the underlying mechanism mediated by TGF-β that regulates these proapoptotic genes was not understood. Recently, *Bim* was discovered as a downstream target of *RUNX3*. *RUNX3* was shown to transcriptionally upregulates *Bim* which functions in the TGF-β induced apoptosis in gastric epithelial cells (107). This indicates that *RUNX3* plays a role in apoptosis to regulate proliferation of gastric epithelial cells.

TGF-β mediated growth arrest works through two classes of antiproliferative gene responses namely the inactivation of cyclin-dependent kinases (*cdks*) through the induction of cdk inhibitors, and the downregulation of *c-Myc* (108). It was recently reported that *RUNX3* mediates the TGF-β induced cell growth arrest in gastric epithelial cells by activating the cyclin-dependent kinase inhibitor, $p21^{WAF1/Cip1}$. The authors showed that the overexpression of *RUNX3* potentiates TGF-β-dependent endogenous *p21* induction. *RUNX3* also cooperates synergistically with Smad to

activate the *p21* promoter. This associates the *RUNX3* tumor suppressor function to its ability to induce cdk inhibitors (109). Taken together, these findings pointed to the ability of *RUNX3* in inhibiting proliferation, further support the role of *RUNX3* as a tumor suppressor under the TGF-β pathway in the gastric system.

2.6 Tight junction (TJ) Protein Family

Tight junctions are one of the four main structures regulating cell-to-cell interactions in the epithelial and endothelial cells. Adherens junctions (AJ) and desmosomes are mainly involved in cell to cell adhesion, and gap junctions in cell to cell communication, whereas TJs provide cell to cell contact with a seal between the apical portions of adjacent basolateral membranes (110). On ultrathin section electron micrographs, TJs are viewed as a series of fusion points between the plasma membranes of adjacent cells located at the most apical regions of the junctional complex. TJs contain aqueous pores that are permeable to small molecules, such as inorganic ions, with size and charge selectivity (111). In normal epithelial tissues, various tight junction proteins are connected through protein-protein interactions to form a complex that provide tight sealing of the cellular sheets and to control paracellular ion flux, thereby maintaining tissue homeostasis. Besides, tight junctions help to maintain cell polarity by forming a barrier that prevents diffusion of membrane proteins and lipids from the apical to the basolateral cell membrane (112).

Three integral proteins that are found at the TJ include the transmembrane proteins, namely occludin, claudins and junctional adhesion molecules (JAMS) (113). Occludin and claudins constitute the backbone of TJ strands and are found abundantly in the epithelial and endothelial cells, while JAM appears to be important for the routine trafficking of T-lymphocytes, neutrophiles and dendritic cells from the lymphoid and vascular compartments to the tissues during immune surveillance and inflammatory responses (114). There are also TJ proteins found within the myelin sheaths, such as the OSP / claudin-11 (115) and PMP22 / gas-3 (116) that play a role in the establishment and maintenance of TJs in epithelia of the central nervous system (CNS). JAM as its role suggests, belong to the immunoglobulin superfamily of the TJ tetraspan proteins (117).

Besides, TJ proteins can also be classified into those containing PDZ domains such as the MAGUK (membrane associated guanylate kinase homologues) family proteins ZO-1 (118), ZO-2 (119) and ZO-3 (120), the PAR (partitioning-defective proteins) (121-123), the MUPP1 (multi-PDZ domain protein 1) (124), and the AF-6 / Afadin protein, which is found both at the TJs (125) and AJs (126). Other TJ proteins that lack PDZ domain include cingulin (127) and symplekin (128). Through protein-protein interactions, ZOs, AF-6 and cingulin are recruited to form a complex with the TJ on the plasma membrane, providing a link to the actin cytoskeleton for transducing regulatory signals to and from tight junctions.

2.7 Claudin Superfamily

2.7.1 Emergence of Claudin Superfamily

In 1991, a novel and unique sequence named RVP.1 was found during the studies of genes that were up-regulated in rat ventral prostate epithelial cells in response to androgen withdrawal (129). Six years later, a receptor for the *Clostridium perfringens* enterotoxin (CPE-R) was characterized (130). With this, the high homology between the RVP.1 and CPE-R was revealed. RVP.1 and CPE-R were since renamed as claudin-3 and claudin-4 respectively and were functionally deomonstrated to be the low affinity and high affinity receptor for CPE respectively (131). In 1996, an oligodendrocyte-specific protein, which was renamed claudin-11, with homology to claudin-3 and claudin-4 was discovered (132, 133). In 1998, with the findings of two homologous novel molecules, named claudin-1 and claudin-2, which was discovered to form normal appearing, functional tight junctions in the absence of occludins, the claudins were recognized as a new superfamily of homologous protein that contributes to the major structural and functional components of tight junctions (134). Claudins were named after the Latin word ‘claudere’ – to close. To date, at least 23 members of the claudin family have been identified in mouse and human, mainly through database searches, each having its own characteristic sequence and expression pattern.

2.7.2 Evolution of Claudin Genes Family

Claudins are crucial members of the transmembrane tetraspan family that constitute the tight junctions, usually present on the membranes of epithelial and endothelial cells and thus are found throughout the body (135). Individual claudin family members can be expressed ubiquitously or is cell-type specific (136). Besides, individual cells can express either multiple claudin family members or a single claudin species (135, 136).

Invertebrates such as *C. elegans* or *D. melanogaster* only possess four to five claudin-related genes (137, 138). This is in contrast to the many claudin genes present in mammals. This, together with the frequently observed tissue- and cell-type specific expression of individual claudins in mammals (136, 139), indicates that the expansion of the claudin gene family in parallel with the evolution of increasingly complex tissue and organs was probably to accommodate new or overlapping functions. A total of 56 Fugu claudin genes have also been identified in the teleost fish, *Fugu rubripes* (*Fugu*), with 35 of them having orthology to 17 mammalian claudin genes, and the remaining 21 genes being specific to the fish lineage. The more or less tissue-specific or developmental stages-specific expression of Fugu claudin genes supported the notion that the expansion of claudin gene family during evolution was probably to allow acquisition of novel functions and to contribute to the distinct physiology of fishes and mammals (140).

2.7.3 Claudin Protein Structure and Functions

A typical claudin superfamily protein has a molecular weight of ~21 kDa. The putative protein structure of claudins is predicted to consist the cytoplasmic N- and C-termini, four transmembrane domains, and two extracellular loops (Figure 2.4c). Among the claudins, the amino acid sequences of the first and fourth transmembrane segments and the first and second extracellular loops are highly conserved, whereas the sequence of the second and third transmembrane segments are more diversified. The first extracellular loop is larger and more hydrophobic than the second extracellular loop and is believed to bridge the intercellular space. Claudins on adjacent cells interact with each other through these extracellular loops (141).

The tight junction protein occludin has the same tetraspanning structure like claudins. However, claudins are the main tight junction proteins that function in the sealing of the TJ (142). The crucial task of claudins in the TJs was highlighted by the following evidence. Firstly, claudin-1 co-localizes with occludin in the most apical regions of the second layer of the stratum granulosum in the skin. Epidermal barrier of claudin-1 deficient mice was severely affected leading to dehydration, wrinkled skin and death of mice within 1 day of birth. In the wild-type epidermis which was positive for both claudin-1 and occludin, TJs efficiently prevented the diffusion of subcutaneously injected tracer. The claudin-1 deficient and occludin positive epidermis however failed to prevent this diffusion from happening, indicating that claudin-based TJs in combination with occludin are crucial for the barrier function

(143). Secondly, transfection of claudin into human breast cancer cells that have lost the expression of claudin-1 decreases the paracellular flux of tracer despite the absence of occludin (144).

Claudins function by limiting the exchange of lipids between the apical and basal membranes of epithelial and endothelial cells, hence define the membrane polarity, provide a continuous intercellular seal, and regulate the paracellular transport of water, solutes and immune cells (112, 145-147) (Figure 2.4a and b). The tight sealing function of claudins is also probably mediated through phosphorylation at the cytoplasmic C-terminus of claudins which has the consensus motifs of protein kinase C (PKC), casein kinase II and cyclin adenosine monophosphate (cAMP)-dependent kinase. Different claudin species possess different type and number of phosphorylation site, suggesting the role of C-terminus in different functions between claudin species. Phosphorylation at this region by proteins such as mitogen-activated protein kinase (MAPK) and cAMP-dependent kinase, resulted in increased permeability of tight junctions, probably through the removal of claudin from the tight junction (148, 149).

Claudins being the major component of tight junctions, interact directly with occludin and zonula occludens (ZO), and indirectly with AF-6 and the myosin-binding molecule cingulin (150-152). Claudins bind to the PDZ-domain-containing proteins such as ZO-1, -2 and -3 through its PDZ-binding motif at the C-terminal region. As ZO proteins function as scaffolding proteins which are able to bind to cytoskeletal proteins, interactions between claudins and ZO proteins promote

scaffolding of the tight junction transmembrane proteins, providing a link to the actin cytoskeleton for transducing regulatory signals to and from tight junctions (153). Due to its crucial role in regulating signaling pathways, loss of normal tight junction functions, especially those that are related to claudins has been widely linked to a hallmark of cancers (154-159).

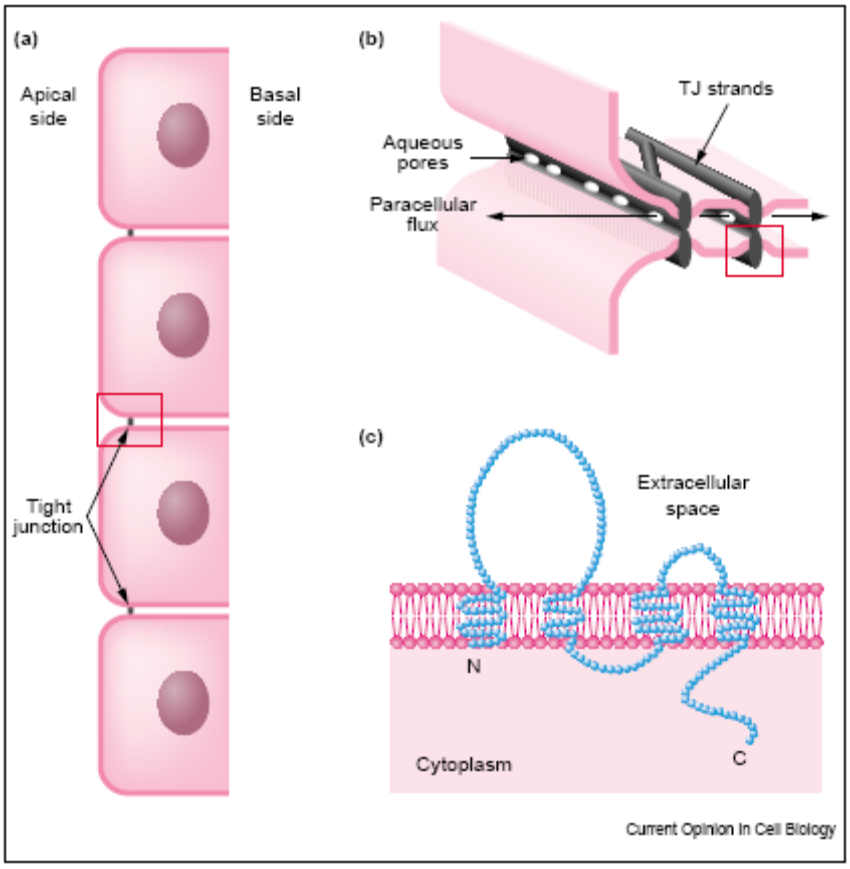

Figure 2.4: Claudin-based tight junctions in simple epithelia. (a) Location of TJs at the most apical region of lateral membranes. (b) Enlargement of the boxed area in (a). TJ strands are embedded within the lipid bilayer of each membrane. Each TJ strand tightly associates with another TJ strand in the opposing membrane of adjacent cells to form a paired strand. (c) Enlargement of the boxed area in (b). Structure of claudins. It bears four transmembrane domains with a short cytoplasmic tail and two extracellular loops. [Ref. 147]

2.8 Claudin and Cancer

Depending upon the cancer type, expression of claudins were observed to be diminished or elevated in cancer cells compared to normal adjacent cells or tissue (Table 2.2). Although the aberrant expression of claudins in cancer has been well established, whether claudins play a functional role in tumorigenesis and cancer progression remains unclear.

Based on its primary role in the formation of tight junctions, it has been hypothesized that the loss of claudin expression may reduce cell adhesion, hence increase tumor cell motility and invasive potential. In line with this hypothesis, a correlation has been established between the loss of tight junction protein claudin-7 and the invasiveness of ductal carcinoma of the breast (158). Besides, the loss of claudin expression was also associated with increased motility and invasiveness during epithelial mesenchymal transition (160, 161). In vitro studies by overexpression claudin-4 in gastric and pancreatic cancer cell lines also showed decreased motility, invasiveness and anchorage-independent growth (162, 163). In addition, mice injected with pancreatic cancer cells overexpressing claudin-4 formed fewer pulmonary metastases (163).

Table 2.2: Claudin expression in human cancer

Cancer type	**Claudin involved**	**Expression pattern**	**References**
Colon	1	Elevated	(164)
Gastric	1, 3, 4, 18, 23 4, 7	Diminished Elevated	(155, 165-167) (162, 168)
Prostate	3, 4	Elevated	(159)
Breast	1, 2, 4, 7 3, 4	Diminished Elevated	(158, 169, 170) (171)
Hepatocellular carcinoma	10	Elevated	(172)
Ovarian	3, 4	Elevated	(173)
Head and neck	7	Diminished	(174)
Melanoma	1	Diminished	(175)
Pancreatic	4	Elevated	(176)

Paradoxically, small interfering RNA (siRNA) knock-down of claudin-3 and claudin-4 in ovarian cancer cell lines inhibited invasive ability, consistent with the increase of motility and invasiveness when these two genes were overexpressed in human ovarian surface epithelial cells (177). Overexpression of claudin-1 in colon cancer cells resulted in increased tumor growth and metastasis in vivo, whereas siRNA knock-down of claudin-1 in metastatic colon cancer cells inhibited migration and invasion (178). This apparently contradicting role of claudins in different cancers

suggests that claudins may have cell-specific effects and that a balance of claudin expression is physiologically necessary. A shift in either direction may result in the disruption of the function and alterations in cellular behavior. This phenomenon could well be demonstrated whereby both claudin-1 knock-down and claudin-6 overexpression were lethal due to defect in epithelial barrier function (143, 179).

2.8.1 Claudin and Gastric Cancer

Among the claudin family members, claudin-1, -3, -4, -7, -18 and -23 have been reported to play a role in gastric cancer. It was reported that diffuse type of gastric carcinomas shows lack of claudin-1 and claudin-4 expression (169). A tissue microarray study also shows a lower expression of claudin-1, -3 and -4 in diffuse type of gastric cancer (165). Study by Lee et al. observed that loss of claudin-4 promotes the advancement of gastric adenocarcinoma (155). Quantitative RT-PCR and immunostaining method also revealed the down-regulation of claudin-18 in intestinal type of gastric cancer, which was postulated to be an early event in gastric carcinogenesis (166). Claudin-23 on the other hand, was found to be down-regulated in the intestinal type of gastric cancer (167). All these reports pointed to the link of the diminished level of claudins and gastric carcinogenesis. On the contrary, reports also show the up-regulation of claudin-4 and -7 in gastric cancer (139, 162). Despite all these findings, the mechanism by which various claudins are regulated and their function in gastric cancer is still poorly understood.

2.9 Crosstalk of TJ Components with Signaling Pathways

β-catenin was reported to regulate claudin-1 expression, evidenced by the decreased in *claudin-1* expression when intracellular β-catenin was reduced by adenovirus-mediated transfer of wild-type *APC* into the APC-deficient colon cancer cells. Two putative Tcf4 binding elements in the *claudin-1* promoter were tested to be responsible for activating its transcription. Primary colorectal cancers also expressed higher level of claudin-1 as compared to the adjacent noncancerous mucosa, indicating that claudin-1 is involved in the β-catenin-Tcf / LEF signaling pathway, and increased expression of claudin-1 may have some role in colorectal carcinogenesis (164). Likewise, activity of the claudin-2 promoter was elevated in mouse mammary epithelial C57 cells expressing Wnt-1. Expression of LEF-1 and beta-catenin also enhanced claudin-2 promoter activity, which was reduced when the LEF-1 binding sites within the claudin-2 promoter was mutated (180).

The beta-catenin signaling pathway is activated in the MDCK cells expressing (181) the mutant ZO-1 protein which encodes the PDZ protein, but no longer localizes at the plasma membrane. These cells also induce a dramatic epithelial to mesenchymal transition (EMT), indicating the loss of ZO-1 function in tumor metastasis initiation (182). Exogenous transfection of ZO-1 on the other hand was reported to activate the Membrane-type 1 Matrix Metalloproteinase (MT1-MMP) expression and cell invasiveness by concomitantly activating the beta-catenin / TCF / LEF signaling pathway in the human breast cancer cells (181).

Mitogen-activated protein (MAP) kinases are Ser / Thr protein kinases that respond to extracellular stimuli such as growth factors and stress. There are four distinct groups of MAPKs present in mammals. The first known as the classical MAP kinases or the extrcellular signal-regulated kinases (ERKs) is activated by growth factors and regulates cell proliferation and differentiation. c-Jun N-terminal kinases (JNKs) and p38 isoforms are two other groups of MAPKs activated by stress stimuli and involved in cell differentiation and apoptosis. The forth group, named ERK5 is activated by growth factors and stress stimuli and is involved in cell proliferation.

MAPK signaling pathway modulates TJ paracellular transport by up- or down-regulating the expression of several TJ proteins. Activation of the MAPK pathway can lead to TJ opening which perturbs the barrier function, or the assembly of TJ which promotes barrier function. Treatment with the cytokine IL-17 activated the ERK1/2 and increased the expression of claudin-1 and -2 in intestinal cells, which also increased the barrier function of TJs (183). Similarly, the expression of claudin-1 and ZO-2 which were upregulated by TGF-β in kidney and intestinal cells respectively through the activation of ERK1/2 also increased TJ barrier function (184, 185). On the other hand, Ras transfected MDCK cells show perturbs TJ barrier function due to the absence of occludin, claudin-1 and ZO-1 (186). In mouse hepatic cell lines, transfection with oncogenic Raf also decreased claudin-2 expression, altering the distribution of ZO-1 at cell borders and perturbs TJ barrier function (187).

The *Snail* family of transcription factors which function under the MAPK pathway were also identified to regulate claudin-1 expression. In human epithelial

cells and invasive human breast tumors, high levels of Snail and Slug were correlated with low levels of claudin-1 expression, indicating the *Snail* family transcription factors as repressors of claudin-1 (188). Other tight junction proteins including claudin-3, -4 and -7, occludin and ZO-1 were also reported to be down-regulated by Snail (160, 189).

Several growth factors and cytokines were also identified to affect claudin expression under the MAPK pathway. The tumor promoting factors hepatocyte growth factor (HGF) and epidermal growth factor (EGF) were shown to decrease claudin-7 expression and increase claudin-1, -3 and -4 expressions (158, 190). Exposure of the cytokines tumor necrosis factor α (TNF-α), interleukin 1β (IL-β) and IL-17 also cause increased claudin-1 expression (183).

2.10 TJ, AJ and Mechanism in Tumor Metastasis

Tight junctions are crucial players in the normal function of epithelial cells, such as the regulation of proliferation and differentiation. According to the theory proposed by Mullin (2004), when tight junction barrier functions are interrupted due to the loss of claudins expression, growth factors and cytokines freely penetrate from the surrounding tissue, increasing paracellular flux of growth factors, which subsequently give rise to auto- and paracrine stimulation of tumorigenic epithelial cells (Figure 2.5). This lowering of diffusion barrier leads to an improved nutrient supply and adds to the selective advantage for developing tumor cells (191, 192).

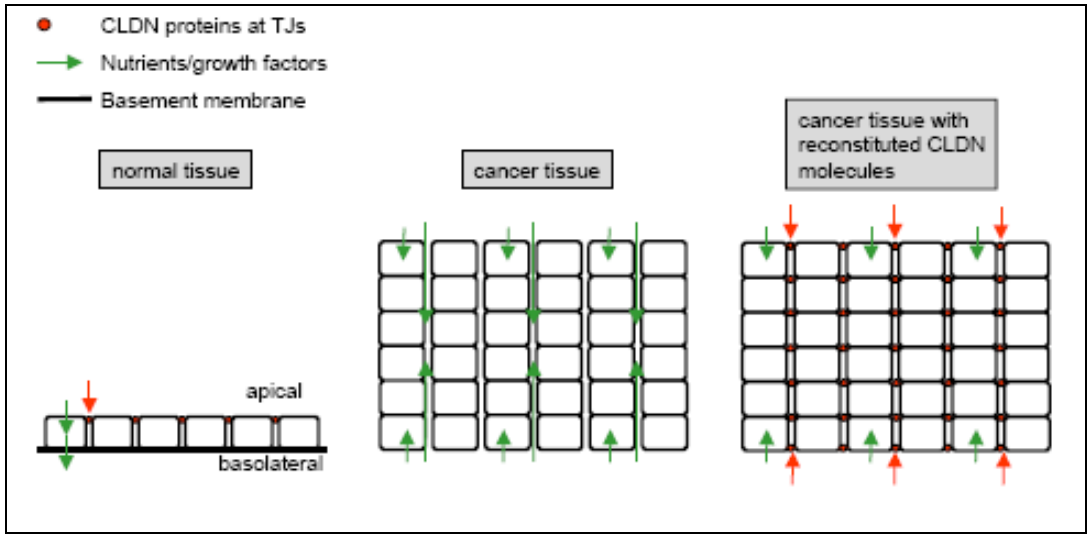

Figure 2.5: Model of claudin-based TJ and its alteration during cancer progression due to the loss of claudin expression and reconstitution in an experimental cancer model. In normal epithelial tissues, the passage of solutes including growth factors and cytokines, is regulated through the normal paracellular fence function of TJs, consisting of an intact basement membrane and endogenous claudin expression. Only a limited amount of these factors traverse the cell membrane to reach the tissue stromal. In in situ or invasive cancer, loss of claudin expression and breakdown of TJ barrier functions allow growth factors and cytokines to penetrate freely from the surrounding tissue. With the reconstitution of claudin expression, some or all the TJ functions are restored, resulting in a reduced paracellular flux of growth factors [Ref.191].

It is well-known that tumor metastasis can be initiated by epithelial-mesenchymal transition (EMT) (193). This cellular transformation results in the loss of cell adhesion and apical-basal polarity, followed by a shift in cytoskeletal dynamics from epithelial toward the mesenchymal phenotype. This alteration in cellular morphology is typically characterized by changes in cell polarity and loss of adhesion protein such as E-cadherin. Suppression of E-cadherin has been linked to various transcription factors such as Snail, Slug, SIP-1, ZEB-1, E12 / E47 (194, 195) and Twist (196).

It was known that up-regulation of Snail expression by MAPK and PI3K are responsible for suppressing approximately half of the total cellular E-cadherin (194). However, full repression of E-cadherin was shown to associate with nuclear localization and transcriptional activities of Smad4 and LEF-1, suggesting that both Snail and LEF-1 are necessary for complete loss of E-cadherin and completion of TGF-β1-induced EMT (Figure 2.6). Up-regulation of Snail also inhibits expression of claudin-1, claudin-2 and occludin. Both Smad-dependent and Smad-independent signaling pathways were shown to be necessary for EMT (161).

Downregulation of ZO-1 through the beta-catenin / TCF / LEF (182) and MAPK pathway (197) as well as suppression of occludin through the Snail transcription family (160, 198, 199) were also linked to the formation of EMT. Snail up-regulation through the MMP-3-Rac1-ROS pathway was also reported to promote EMT (200). Other pathways such as Notch (201, 202) and RhoA (203, 204), (205) have also been implicated in EMT.

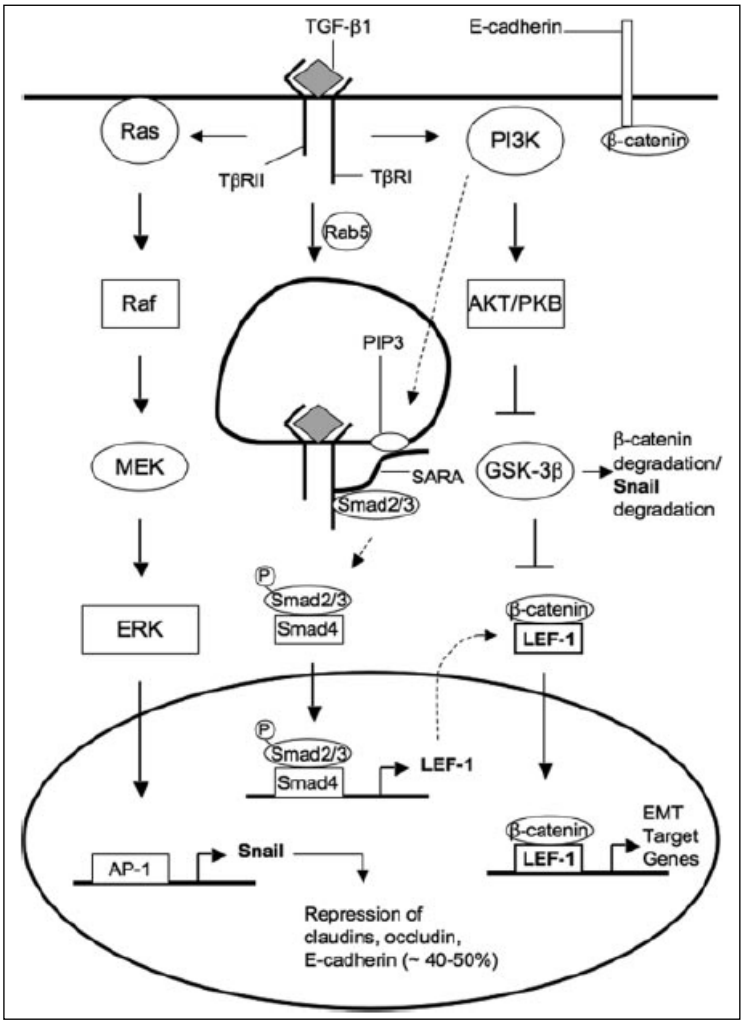

Figure 2.6: A schematic representation of the proposed TGF-β1 signaling mechanism that promotes EMT. Up-regulation of Snail expression happens in response to early signaling through Ras-Raf-MEK-ERK-AP-1. Snail then inhibits expression of claudin-1, claudin-2 and occludin. Snail causes partial loss of E-cadherin, decreasing the level of substrate for β-catenin. Further stabilization of cytoplasmic β-catenin is achieved through PI3K signaling, through phosphorylation and deactivation of p-GSK-3 β by AKT downstream of PI3K. Absence of p-GSK-3β inhibits the ubiquitin proteosome pathway and degradation of β-catenin and Snail. Smad signaling, controlled through endocytosis of TGF-β receptor complex, promotes transcription of LEF-1, an alternative substrate for β-catenin, through the Smad2/3-Smad4 transcription complexe. In early endosome, TβR1 phosphorylates Smad proteins upon their recruitment by SARA. SARA binds to PIP3 for proper association with the receptor. Formation of β-catenin / LEF-1 complexes acts to transcribe genes that promote EMT [Ref. 161].

The vascular endothelial (VE)-cadherin at AJ has recently been reported to up-regulate the gene encoding TJ protein claudin-5 by inducing the phosphorylation of FoxO1 through Akt activation and by limiting the translocation of beta-catenin to the nucleus (206). These results offer a molecular basis for the link between AJ and TJ in maintaining cell function. Although AJ and TJ can be functionally linked, reports have also shown that AJ assembly is not a pre-requisite for TJ formation (186, 207, 208). Inactivation of the *von Hippel-Lindau* (*VHL*) gene in the kidney epithelium triggers a downregulation of TJ molecules occludin and claudin-1, resulting in a dismantling of intercellular junctions and EMT. However, the disruption of these TJ proteins is not dependent on E-cadherin downregulation as re-expression of E-cadherin in *von Hippel-Lindau* (*VHL*) defective cells did not rescue TJ formation nor restore an epithelial-like cell shape (209).

Another mechanism of EMT was recently reported by Lehembre et al. (2008) (210) (Fig. 2.7). The authors demonstrated that the loss of E-cadherin function up-regulates expression of the neuronal cell adhesion molecule (NCAM). A subset of NCAM translocates from the fibroblast growth factor receptor (FGFR) complexes outside lipid rafts into lipid rafts where it stimulates the non-receptor tyrosine kinase p59 (Fyn), leading to the phosphorylation and activation of the focal adhesion kinase (FAK) and the assembly of β1-integrin-dependent focal adhesion assembly in cells that retain epithelial-mesenchymal plasticity. NCAM is not only needed for induction of EMT but also for maintenance of the mesenchymal state. Enforced expression of NCAM promotes mesenchymal-like properties in some epithelial cells in culture.

High NCAM expression is also correlates with tumor invasion. On the contrary, abolition of NCAM expression during EMT inhibits focal adhesion assembly, cell spreading and EMT. This proposed model established a link between the loss of E-cadherin expression, NCAM function, focal adhesion and cell migration and invasion.

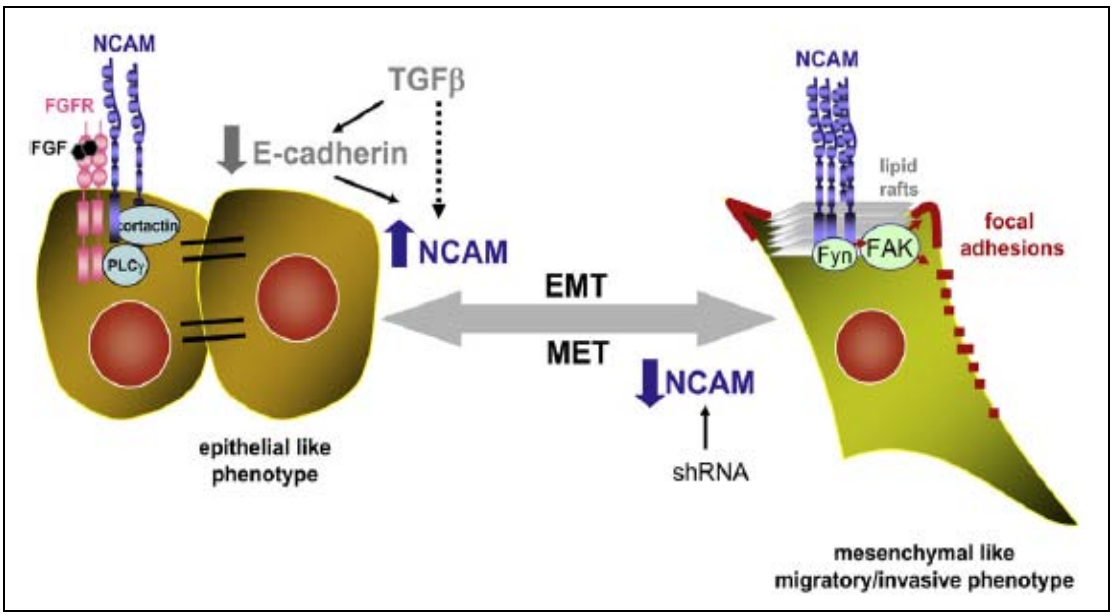

Figure 2.7: Putative NCAM-associated signaling changes during EMT. Induction of EMT, induced via TGF-β or cadherin loss, causes NCAM-mediated weakening of cell-cell adhesions and also formation and dynamic turnover of focal adhesions. Elevation in NCAM expression leads to altered signaling complexes. NCAM binding to PLCγ and cortactin is diminished, and forms a complex with Fyn and FAK. These signaling induce a more mesenchymal and migratory phenotype associated with aggressive cancers of epithelial origin. Knockdown of NCAM induces the reversal of EMT [Ref. 210]

CHAPTER 3 MATERIALS AND METHODS

3.1 MATERIALS

3.1.1 Primers

Primers for semiquantitative RT-PCR

hCldn1-F: 5'-CCAACGCGGGGCTGCAGCT-3'

hCldn1-R: 5'-TTGTTTTTCGGGGACAGGA-3'

Hu_Gapdh-F: 5'-GGTCGGAGTCAACGGATTTGGTCG-3'

Hu_Gapdh-R: 5'-CCTCCGACGCCTGCTTCACCAC-3'

Primers for quantitative real time RT-PCR (pre-made by ABI)

hRUNX3 (Identifier, Hs00231709_m1)

hclaudin-1 (Identifier, Hs00221623_m1)

hGAPDH (Identifier, Hs99999905_m1)

Primers for cloning hclaudin-1 promoter

hclaudin-1 promoter 1530-F:

5'-CGGGGTACCCCCTGGGATACAACACG-3' (KpnI site at 5')

hclaudin-1 promoter 1530-R:

5'-CGAGCTCCCCAGGCTCGGGAACTGAG-3' (SacI site at 5')

Primers for cloning mclaudin-1 ORF with Myc-Tag into pcDNA3.1/HisC

mclaudin-1 ORF/Myc-F:

5'-CGAGATATCATGGCCAACGCGGGG-3' (EcoRV site at 5')

mclaudin-1 ORF/Myc-R:

5'-GTATGCGGCCGCGTCGACTCACAG-3' (NotI site at 5')

Primers for cloning AS hclaudin-1 ORF into pcDNA3.1/HisC

AShclaudin-1 ORF-F:

5'-CTATTGCGGCCGCATGGCCAACG-3' (NotI site at 5')

AShclaudin-1 ORF-R:

5'-GGCGGCCGATATCTCACACGTAGTC-3' (EcoRV site at 5')

Primers for SDM on 1st RUNX binding site on hclaudin-1 promoter

Cldn1PromMut1F:

5'-GCTTCCCCTCCCATTACACTCGCACCACACACAAAAAGCAG-3'

Cldn1PromMut1R:

5'-CTGCTTTT TGTGTGTGGTGCGAGTGTAATGGGAGGGGAAGC-3'

Primers for SDM on 2nd RUNX binding site on hclaudin-1 promoter

Cldn1PromMut2F:

5'-GCT TCCCCTCCCACCACACTCGCATTACACACAAAAAGCAG-3'

Cldn1PromMut2R:

5’-CTGCTTTTTGTGTGTAATGCGAGTGTGG TGGGAGGGGAAGC-3’

Primers for SDM on 3rd RUNX binding site on hclaudin-1 promoter

Cldn1PromMut3F:

5’-GCAGTT GGAAAAACATTTCAATGATTCCTAATTACAACAGCAC-3’

Cldn1PromMut3R:

5’- GTGCTGT TGTAATTAGGAATCATTGAAATGTTTTTCCAACTGC-3’

Primers for SDM on 1st + 2nd RUNX binding site on hclaudin-1 promoter

Cldn1PromMut1+2F:

5’-GCT TCCCCTCCCA TTACACTCGCATTACACACAAAAAGCAGTTGG 3’

Cldn1PromMut1+2R:

5’-CCAACTGCTTTTTGTGTGTAATGCGAGTGTAATGGGAGGGGAAGC-3’

Primers for mutagenesis check

Cldn1PromSeq-F:

5’-GGAAATGAAGGTGGTGGGGCTTGGCC-3’

Cldn1PromSeq-R:

5’-GGCAAAAGGACTGGGCTGGAGTTGAGG-3’

ChIP primers for amplifying hclaudin-1 (specific for hclaudin-1 promoter)

Cldn1CHIP-2F: 5’ AAAACCATAGAAGCTTCCCCTCCC 3’

Cldn1CHIP-2R: 5’ CCTCTATGTTTCTCCAAAGCTTCC 3’

ChIP primers for amplifying GAPDH (specific for GAPDH promoter)

FOR: 5’-TACTAGCGGTTTTACGGGCG-3’

REV: 5’-TCGAACAGGAGGAGCAGAGAGCGA-3’

3.1.2 Oligonucleotide probes for EMSA

Probes for site 1 and 2

WT-WT:

5’-TCCCCTCCCACCACACTCGCACCACACACAAAAAG-3’

5’-CTTTTTGTGTGTGGTGCGAGTGTGGTGGGAGGGGA-3’

WT-MT:

5’-TCCCCTCCCACCACACTCGCATTACACACAAAAAG-3’

5’-CTTTT TGTGTGTAATGCGAGTGTGGTGGGAGGGGA-3’

MT-WT:

5’-TCCCCTCCCATTACACTCGCACCACACACAAAAG-3’

5’-CTTTT TGTGTGTGGTGCGAGTGTAATGGGAGGGGA-3’

MT-MT:

5’-TCCCCTCCCATTACACTCGCATTACACACAAAAAG-3’

5’-CTTTTTGTGTGTAATGCGAGTGTAATGGGAGGGGA-3’

Probes for site 3

WT:

5’-TTCAATGATTCCTAACCACAACAGCACTTCTGACT-3’

5’-AGTCAGAAGTGCTGTTGTGGTTAGGAATCATTGAA-3’

MT:

5’-TTCAATGATTCCTAATTACAACAGCACTTCTGACT-3’

5’-AGTCAGAAGTGCTGTTGTAATTAGGAATCATTGAA-3’

3.1.3 Commercial kit

RNeasy mini kit, 74104, Qiagen

Omniscript reverse transcription kit, 205111, Qiagen

TaqMan Fast Universal PCR Master Mix, 4352042, Applied Biosystems

QuickChange XL site-directed mutagenesis kit, 200516, Stratagene

Dual-Luciferase Reporter Assay System, E1910, Promega

EnVision+ system (DAB), K4010; Dako

NE-PER Nuclear and Cytoplasmic Extraction Reagents, 78833, Pierce Biotechnology

LightShift Chemiluminescent EMSA kit, 20148, Pierce Biotechnology

EZ ChIP Chromatin Immunoprecipitation kit, 17-371, Upstate cell signaling solutions

ECL Direct Nucleic Acid Labelling and Detection System, RPN3000, Amersham Pharmacia Biotech

3.1.4 Antibodies

Anti-RUNX3 (R3-5G4), mAb, mouse IgG, 0.5 µg/ml; a monoclonal antibody against RUNX3 established in our laboratory

Anti-RUNX3 (R3-6E9), mAb, mouse IgG, 0.7 mg/ml; a monoclonal antibody against RUNX3 established in our laboratory

Anti-Claudin-1, pAb, rabbit IgG, 0.5 ml concentrate, 18-7362, Zymed

Anti-Claudin-2, pAb, rabbit IgG, 0.25 µg/µl, 51-6100; Zymed

Anti-Claudin-3, pAb, rabbit IgG, 0.25 µg/µl, 34-1700; Zymed

Anti-Claudin-4, pAb, rabbit IgG, 0.25 µg/µl, 36-4800; Zymed

Anti-Claudin-7, pAb, rabbit IgG, 0.25 µg/µl, 34-9100; Zymed

Anti-Claudin-11, pAb, rabbit IgG, 0.25 µg/µl, 36-4500; Zymed

Anti-Claudin-16, pAb, rabbit IgG, 0.25 µg/µl, 34-5400; Zymed

Anti-ZO-1, pAb, rabbit IgG, 0.25 µg/µl, 61-7300; Zymed

Anti-ZO-2, pAb, rabbit IgG, 0.25 µg/µl, 71-1400; Zymed

Anti-ZO-3, pAb, rabbit IgG, 0.25 µg/µl, 36-4100; Zymed

Anti-Occludin, pAb, rabbit IgG, 0.25 µg/µl, 71-1500; Zymed

Anti-E-cadherin, mAb, mouse IgG, 250 µg/ml, 610181; BD Pharmingen

Anti-β-actin, mAb, mouse IgG, AC-15; Sigma

Donkey Anti-Rabbit IgG, Horseradish Peroxidase linked whole antibody, 1 ml, NA934V; Amersham Pharmacia Biotech

Sheep Anti-Mouse IgG, Horseradish Peroxidase linked whole antibody, 1 ml, NA931V; Amersham Pharmacia Biotech

Normal Mouse IgG, 200 µg, sc-2025, Santa Cruz Biotechnology

Biotinylated Goat Anti-Rabbit IgG (H + L), 1.5 mg, BA-1000, Vector Labs

Fluorescein Avidin D, 5 mg, A-2001, Vector Labs

3.1.5 General Buffer Preparation

Phosphate buffered saline (PBS) [137 mM NaCl, 2.7 mM KCl, 4.3 mM Na_2HPO_4, 1.4 mM KH_2PO_4, pH7.4]

TE buffer [10 mM Tris-HCL, 1mM EDTA, pH 8.0]

Bacteria Transformation

LB broth [1% (w/v) Bacto-tryptone, 0.5% (w/v) Bacto-yeast extract, 0.5% (w/v) NaCl; pH 7.0]

LB agar [1% (w/v) Bacto-tryptone, 0.5% (w/v) Bacto-yeast extract, 0.5% (w/v) NaCl, 2% (w/v) Bacto-agar]

SOC media [2% Bacto-tryptone, 0.5% yeast extract, 10 mM NaCl, 2.5 mM KCL, 10 mM $MgCl_2$, 10 mM $MgSO_4$, 20 mM glucose]

NZY broth [1.0% NZ amine (Casein hydrolysate), 0.5% NaCl, 0.5% Yeast Extract, 0.2% $MgSO_4$, 0.2% $MgCl_2$, 20 mM glucose]

Agarose Gel Electrophoresis

10X TBE [0.89 M Tris, 0.89 M Boric Acid, 0.02 M EDTA]

6X Sample loading buffer [0.25% (w/v) Bromophenol blue, 0.25% (w/v) Xylene cyanol, 30% (v/v) Glycerol]

SDS-PAGE and Western Blotting

Tris, pH 8.8 [1.5 M Tris base, 0.4% (w/v) SDS, pH adjusted to 8.8 with concentrated HCl]

Tris, pH 6.8 [0.5 M Tris base, 0.4% (w/v) SDS, pH adjusted to 6.8 with concentrated HCl]

10X Laemli running buffer [0.25 M Tris base, 1.92 M Glycine, 1% (w/v) SDS]

Towbin transfer buffer [10% (v/v) 10X Laemli buffer, 20% (v/v) Methanol]

Blocking buffer [5% skim milk powder in 1X PBS]

Wash buffer [1X PBS, 0.1% Tween 20]

Stripping buffer [0.1X SSC, 0.1% (w/v) SDS, 0.2 M Tris-HCl, pH 7.5]

SDS-PAGE Gel

10% Resolving Gel:

30% Acrylamide	3.3 ml
1.5 M Tris (pH 8.8)	2.5 ml
10% APS	0.1 ml
10% SDS	0.1 ml
TEMED	0.004 ml
dH_2O	4.0 ml
Total volume	10.0 ml

6% Resolving Gel:

30% Acrylamide	2.0 ml
1.5 M Tris (pH 8.8)	2.5 ml
10% APS	0.1 ml
10% SDS	0.1 ml
TEMED	0.008 ml
dH_2O	5.3 ml
Total volume	10.0 ml

5% Stacking Gel:

30% Acrylamide	0.17 ml
1.0 M Tris (pH 6.8)	0.13 ml

10% APS	0.01 ml
10% SDS	0.01 ml
TEMED	0.001 ml
dH_2O	0.68 ml
Total volume	1.0 ml

Tissue Fixation

4% PFA [Add 16 g of PFA to approximately 300 ml of preheated dH_2O; Use NaOH to dissolve mixture and add 40 ml of 10X PBS; measure pH and adjust with 1 M HCl till pH reaches 7.2-7.4; top up to 400 ml with dH_2O and filter]

Protein Extraction

Lysis buffer [9 M Urea; 2% Triton-X; 5% final concentration of 2-mercaptoethanol is added freshly before use]

EMSA

0.5X TBE Gel (1.5 mm SDS-PAGE plate)

30% polyacrylamide	2.2 mL
1X TBE	6.6 mL
10% APS	110 µL
TEMED	11 µL
dH_2O	4.4 mL

Annealing buffer [20 mM Tris (pH7.5), 50 mM NaCl and 10 mM $MgCl_2$]

3.2 METHODS

3.2.1 Establishment of Gastric Epithelial Cell Lines

Runx3 knock out mice was collaboratively generated by Drs. Kosei Ito (Kyoto University, Japan) and Suk-Chul Bae (Chungbuk National University, South Korea) as described in Li et al. (2002). In brief, A phage DNA clone containing exon 3 of the *Runx3* gene was isolated from a 129/SvJ mouse genomic library (Stratagene). The *LacZ* gene was introduced into the Sma1 site (12^{th} codon in-frame) of exon 3 of the phage clone to generate a gene-targeting vector (appendix 1). The generated plasmid was transfected by electroporation into the E14 mouse ES cells. Correctly targeted ES cells were injected into C57BL/6 blastocysts, and the resulting chimeras were crossed with C57BL/6 females. *p53*-deficient mice with C57BL/6 genetic background was provided by Drs. Aizawa S and Katsuki M and generated as described previously by Tsukada T et al. (1994) (211).

All mouse gastric epithelial cell lines used in this experiment were generated and provided by Dr. Hiroshi Fukamachi (University of Tokyo, Japan) through crossing the *Runx3* and *p53* knock out mice. All animal experiments were carried out in accordance with the guidelines for the care and use of laboratory animals of University of Tokyo. $Runx3^{+/-}p53^{+/-}$ mice were mated to obtain $Runx3^{-/-}p53^{-/-}$ and $Runx3^{+/+}p53^{-/-}$ fetuses (Figure 3.1). Gastric epithelial cells from 16.5-day fetuses were separated from attaching mesenchymes by treating gastric tissues with 30 mM

EDTA-Hanks' solution and cultured separately in wells precoated with rat tail collagen gels. Cells were seeded in Ham's F12 medium (Sigma) supplemented with 10% horse serum (Trace Biosciences), bovine pituitary extract (100 μg/ml; Gibco-BRL), epidermal growth factor (10 ng/ml; Upstate Biotechnology), insulin (3 μg/ml; Sigma), cholera toxin (300 ng/ml; List Biological Laboratories), and hydrocortisone (3 μg/ml; Sigma), and cultured in a humidified atmosphere of 5% CO_2 in air at 37°C.

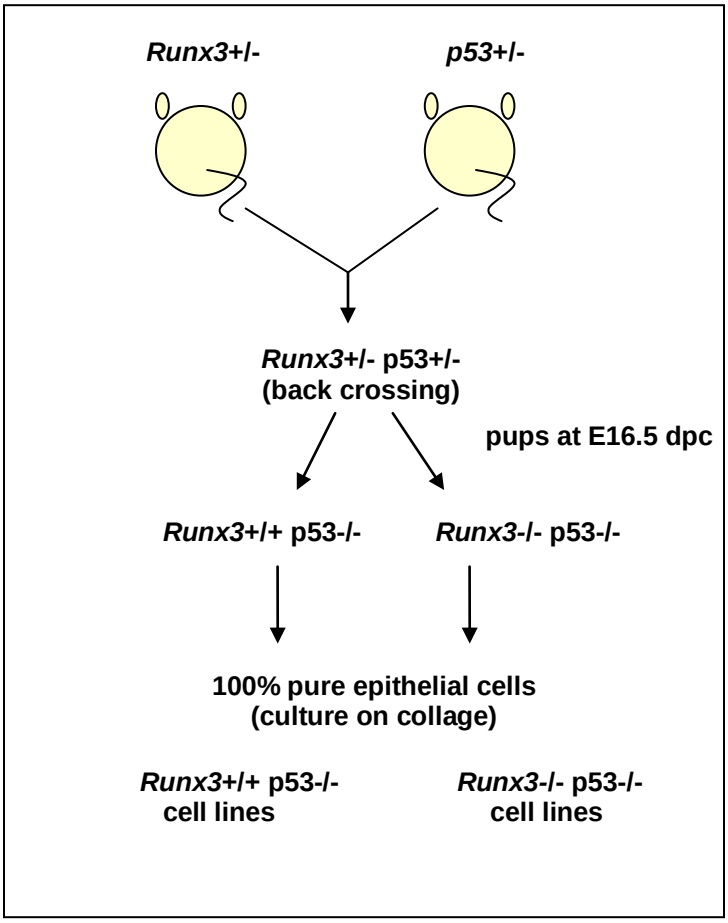

Figure 3.1: Schematic diagram showing the generation of *Runx3*+/+*p53*-/- and *Runx3*-/-*p53*-/- cell lines.

Rapidly growing cells were treated with trypsin-EDTA and dispersed cells were re-seeded on new collagen gels in the first 5-7 passages, and on plastic substratum after 6-8 passages. Once the cells began to proliferate rapidly on plastic substratum, at about passage number 12, the culture medium was changed to Dulbecco's modified Eagle's medium (Sigma) supplemented with 10% fetal bovine serum (Sigma), as cells grow faster in this medium. GIF5 and 14 cells were established from *Runx3*$^{-/-}$*p53*$^{-/-}$ mice while GIF9 and 13 cells were established from *Runx3*$^{+/+}$*p53*$^{-/-}$ mice.

3.2.2 Cell Lines and Cell Culture

SNU16 gastric cancer cell line was maintained in RPMI-1641 medium supplemented with 10% fetal bovine serum (BDH Biosciences). AGS and 293T cells were cultured in DMEM supplemented with 10% fetal bovine serum. GIF cells (Runx3+/+ and Runx3-/-) were maintained in Ham's F-12 medium (Sigma) supplemented with 10% horse serum (Trace Biosciences), bovine pituitary extract (100 μg/ml; Gibco-BRL), epidermal growth factor (10 ng/ml; Upstate Biotechnology), insulin (3 μg/ml; Sigma), cholera toxin (300 ng/ml; List Biological Laboratories), and hydrocortisone (3 μg/ml; Sigma), and cultured in a humidified atmosphere of 5% CO_2 in air at 37°C. When the cells reach passage number 12, the culture medium was changed to Dulbecco's modified Eagle's medium (Sigma) supplemented with 10% fetal bovine serum (BDH Biosciences).

3.2.2.1 Treatment of Cells by TGF-β1

Regulation of target genes by TGF-β was observed by treating cells with the recombinant human TGF-β1 (R&D systems, USA). SNU16 and ASSNU16 cells were treated with 3 ng/ml of TGF-β1. Cells at 0 hr before treatment and 6, 12 and 24 hr after treatment were collected for protein extraction, followed by Western blot analysis.

To observe the effect of TGF-β inhibitor on the expression of claudin-1, same number of SNU16 cells was seeded and grown overnight in three separate 75 cm^3 flask. One flask of cells was added 3 ng/ml of TGF-β1, another flask with same amount of TGF-β1 and 1 μg/ml of TGF-β inhibitor (SB431542) (GlaxoSmithKline Pharmaceuticals). The flask without any treatment was used as control. After 24 hr treatment, cells were collected and protein extraction from these cells was performed. Protein samples were used for Western blot analysis.

3.2.3 Semiquantitative RT-PCR, Quantitative RT-PCR

Total RNA was extracted from SNU16 cells and AS SNU16 cells using the RNeasy mini kit (Qiagen) and cDNAs were synthesized from total RNA using the Omniscript reverse transcription kit (Qiagen) according to the manufacturer's protocol. Semiquantitative reverse transcription-PCR (RT-PCR) for the detection of *hClaudin-*

1 was carried out using the hCldn1-F and hCldn1-R primers, whereas detection of *GAPDH* was carried out using the Hu_Gapdh-F and Hu_Gapdh-R primers.

Quantitative RT-PCR was performed on cDNA from SNU16 control cells stably expressing pcDNA3 and SNU16 stable cells expressing Flag-Runx3 using the real-time TaqMan Fast Universal PCR Master Mix system on an ABI PRISM 7900HT instrument (Applied Biosystems) for the detection of *hRUNX3* (identifier, Hs00231709_m1) and *hclaudin-1* (identifier, Hs00221623_m1). *hGAPDH* (identifier, Hs99999905_m1) was used for normalization. Analysis was performed using the SDS database (version 2.2.1).

3.2.4 Protein Isolation

Adherent cells with 90% confluency were washed twice with ice-cold PBS. 10% of ice-cold TCA (in PBS) was added to the cells and incubation at 4 ºC for 20 minutes was carried out. Cells were rinsed with ice-cold PBS twice and harvested into a 1.5 ml eppendorf tube using a rubber policeman. Cells were centrifuged to collect cell pellet. Protein lysis buffer were added to the cell pellet followed by sonication twice for approximately 10 sec each on ice until cells were completely lysed. 1 µl of protein lysate was used for protein concentration measurement using the Bradford method on the Beckman Coulter DU530 machine. The remaining protein lysate were added 10% lithium dodecyl sulphate (LDS) to a final concentration of 2%. Samples were kept on ice and were ready to load. Suspension cells were collected from culture flask into

falcon tube and centrifuged to collect cell pellet, which was then rinsed twice with ice-cold PBS. Washed pellet was added protein lysis buffer and the same extraction procedure was carried out as above.

3.2.5 SDS-PAGE and Western Blot Analysis

SDS-PAGE was run in 1X Laemli buffer at 100 V for approximately 1.5 hr until the bromophenol blue dye migrated out of the gel. Proteins on SDS-PAGE gel were transferred to the PVDF membrane (pretreated with methanol) using the Western blotting apparatus (BioRad). Western blot was carried out in transfer buffer at 70 V for 90 min at 4 ºC. Transferred membrane was blocked with 5% skim milk in PBS for 1 hr, rinsed once with PBST and incubated with the respective primary antibody at 4 ºC overnight. Membrane was washed three times for 5 min each with 1X PBST, followed by incubation with HRP-conjugated secondary antibody for 1 hr at RT. Membrane was washed again three time for 5 min each with 1X PBST, and develop with the chemiluminescence detection solutions (Amersham Pharmacia Biotech.) using an X-ray film developer (Kodak).

Western blot for the detection of claudin-1, claudin-2, claudin-3, claudin-4, claudin-7, claudin-11, claudin-16, ZO-1, ZO-2, ZO-3, occludin, E-cadherin and β-actin expression in GIF cells and SNU16 cells was performed using a final concentration of 1:200 dilution for anti-claudin-1, 1 µg/ml for anti-claudin-2, 1 µg/ml for anti-claudin-3, 1 µg/ml for anti-claudin-4, 1 µg/ml for anti-claudin-7, 2 µg/ml for

anti-claudin-11, 2 µg/ml for anti-claudin-16, 0.5 µg/ml for anti-ZO-1, 1 µg/ml for anti-ZO-2, 2 µg/ml for anti-ZO-3, 0.25 µg/ml for anti-occludin, 1:2500 dilution for anti-E-cadherin (BD Pharmingen) and 1:10000 dilution for β-actin (Sigma) antibodies, respectively. Expression of RUNX3 in SNU16 and AS SNU16 cells were detected using 0.05 ug/ml of anti-RUNX3 (R3-5G4) (97).

3.2.6 Promoter Assay

3.2.6.1 Cloning of *hclaudin-1* Promoter

The promoter region of human *claudin-1*, which span a segment of 1.53 kb upstream from the *claudin-1* transcription start site (appendix 2), was amplified from the SNU16 genomic DNA by PCR using the hclaudin-1 promoter 1530-F and hclaudin-1 promoter 1530-R primers. PCR was carried out at 94ºC for 1 min, and 35 cycles of 94ºC for 30 sec, 68ºC for 30 sec, 72ºC for 2 min and a final cycle at 72ºC for 5 min using the Pfu Ultra polymerase (Stratagene). The amplified DNA segment was cloned into the pGL3-Basic vector (Promega) (appendix 3) between the KpnI and SacI sites. Ligation product was transformed into the *E. coli* DH5α strain. Positive clones were picked and checked by sequencing. One clone with the right sequence was selected and used as the wt *hclaudin-1* promoter.

3.2.6.2 Site-Directed Mutagenesis

Three RUNX binding sites found within the *hclaudin-1* promoter were mutated (point-mutation) using the QuikChange XL site-directed mutagenesis kit (Stratagene) with the following primers: Cldn1PromMut1F and Cldn1PromMut1R for site 1, Cldn1PromMut2F and Cldn1PromMut2R for site 2, Cldn1PromMut3F and Cldn1PromMut3R for site 3, and Cldn1PromMut1+2F and Cldn1PromMut1+2R for sites 1+2. Reporter plasmid with mutated site 2 was used as template to generate reporter plasmid with mutated sites 2+3 using primers set for site 3. Reporter plasmid with all sites being mutated were generated using reporter plasmid with mutated sites 1+2 and primers set for site 3.

An overview of QuikChange XL site-directed mutagenesis method is illustrated in Figure 3.2. Generally, site-directed mutagenesis can be used to create point mutations, switch amino acids, delete or insert single or multiple amino acids. In this approach, *PfuTurbo* DNA polymerase, which has a 6-fold higher fidelity in DNA synthesis than *Taq* DNA polymerase was used. It is able to replicate both plasmid strands in a supercoiled double-stranded DNA (dsDNA) vector without displacing the mutant oligonucleotide primers. Incorporation of the oligonucleotide primers generates a mutated plasmid containing staggered nicks. As plasmid DNA isolated from almost all of the commonly used *E. coli* strains (dam+) is methylated, the *Dpn* I endonuclease which is specific for methylated and hemimethylated DNA is used to digest the parental DNA template for selection of mutation-containing

synthesized DNA. The XL1-Gold ultracompetent cells repair the nicks in the mutated plasmid upon transformation of the mutated form of dsDNA into these cells. Being endonuclease deficient (*endA1*) and recombinant deficient (*recA*), XL10-Gold ultracompetent cells greatly improves the quality of plasmid miniprep DNA, and also to ensure insert stability upon transformation.

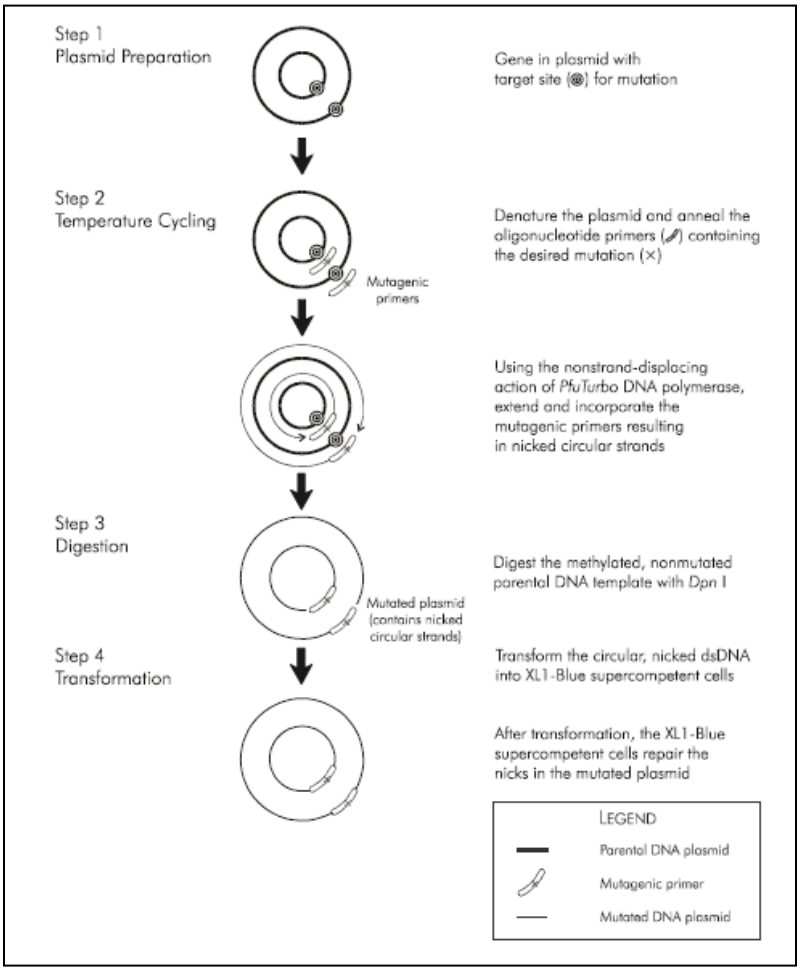

Figure 3.2: Overview of QuikChange XL site-directed mutagenesis procedure. (Adapted from the Stratagene QuikChange XL Site-Directed Mutagenesis kit manual)

3.2.6.3 Dual-Luciferase Reporter Assay

Transfections into the SNU16 and AGS cell lines were carried out using the Lipofectamine 2000 (Invitrogen) and Fugene 6 (Roche) respectively according to the manufacturer's protocol. Fugene 6:DNA amount of 3:1 ratio was used throughout the experiment. Upon transfection, SNU16 cells were incubated at 37 ºC for approximately 36 hrs. After incubation, 50% of each transfected sample, labeled as 0 hr time point, were collected and stored as cell pellet at -20ºC. The remaining cells were added 3 ng/ml of TGF-β and incubated for 12-18 hrs before cell pellets were harvested. These cells were labeled as 12-18 hr time point samples. Similarly, the transfected AGS cells were incubated at 37 ºC for approximately 36 hrs before cells were harvested.

All cells were subjected to the luciferase assay using a Dual-Luciferase Reporter Assay system (Promega) according to the manufacturer's protocol. Active lysis was carried out for SNU16 cell pellets collected in 1.5 ml eppendorf tubes. AGS cells on the other hand were harvested using the passive lysis method. Cells were pelleted after cell lysis and 20 µl of cell supernatant was used for the luciferase assay. Luciferase assay was carried out as depicted in Figure 3.3 using the Sirius luminometer (Berthold Detection System) in triplicates. All firefly luciferase activity was normalized by the renilla luciferase activity of the promoterless pRL-SV40 vector (appendix 4).

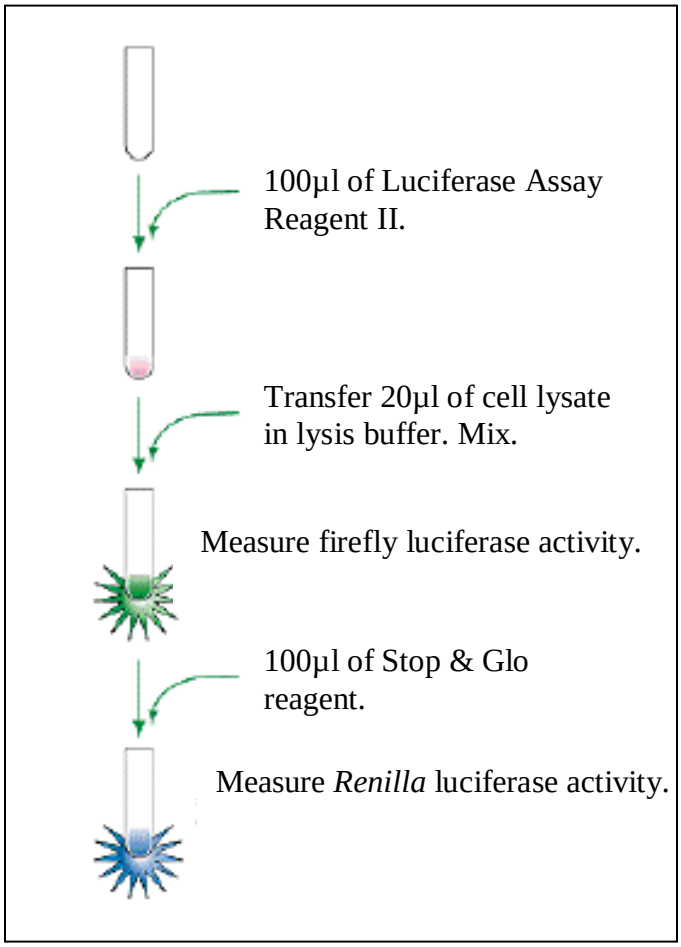

Figure 3.3: Format of the Dual-Luciferase Reporter Assay. The firefly reporter assay is initiated by mixing an aliquot of lysate with the Luciferase Assay Reagent II. Upon completion of the firefly luciferase assay, the firefly luminescence is quenched and Renilla luminescence is simultaneously activated by adding Stop & Glo Reagent to the sample tube. (Adapted from the Dual-Luciferase Reporter Assay kit manual)

3.2.7 Generation of Stable Cell Line

3.2.7.1 Plasmids and Stable Cell Line

The AS RUNX3 plasmid construct was generated by inverting the *RUNX3* cDNA (RUNX3 coding region + 5' and 3' UTR) (appendix 5), followed by cloning into the pEFBos/Neo vector between the XbaI site by blunt end ligation (generated and provided by Dr. Suk Chul Bae from Chungbuk National University, South Korea). This expression construct was transfected into the SNU16 cells to generate AS SNU16 stable cell line. *RUNX3* cDNA was also cloned into the Flag-tagged pcDNA3/Neo vector (Invitrogen). This expression construct was transfected into the SNU16 cells to generate SNU16 stable cell line harboring exogenous *RUNX3*.

Mouse claudin-1 ORF (666 bp) (appendix 6) was amplified from pBIG-mClaudin-1/Myc (kindly provided by Dr. Eveline Schneeberger, University of Harvard, USA) using the mclaudin-1 ORF/Myc-F and mclaudin-1 ORF/Myc-R primers. The amplified product was cloned into the pcDNA3.1/Hygro vector (Invitrogen) between the EcoRV and NotI sites. The expression construct and pcDNA3.1/Hygro vector alone was transfected seperately into GIF5 and GIF14 cells. hclaudin-1 ORF (636 bp) (appendix 7) was inverted and cloned into pcDNA3.1/Hygro between the EcoRV and NotI sites using the AShclaudin-1 ORF-F and AShclaudin-1 ORF-R primers. This expression construct and the pcDNA3.1/Hygro vector alone were transfected separately into the SNU16 cells.

Transfections into SNU16 cells were carried out using Lipofectamine 2000 (Invitrogen), whereas transfections into GIF5 and GIF14 cells were carried out using Fugene 6 (Roche).

3.2.7.2 Stable Transfection and Stable Cloning

Transfection into the SNU16 cell line was carried out using Lipofectamine 2000 (Invitrogen), whereas transfection into the AGS, GIF5 and GIF14 cell lines were carried out using Fugene 6 reagent (Roche). All transfections were carried out in 6-well plates. Cells were allowed to grow for 48 hrs, followed by the addition of antibiotic for selection of transfected cells. 0.6 mg/ml of Neomycin or 125 µg/ml of Hygromycin was used depending on the antibiotic selection of the vector used. Cell growth was monitored in the presence of antibiotic.

For attachment cells like AGS, GIF5 and GIF14, dead floating cells were discarded and fresh medium was changed every 2-3 days to allow attached cells to grow till at least 50% confluency. Cells were then trypsinized and well-suspended cells were subcultured into multiple 10 cm dish in dilutions of 1:500, 1:1000 and 1:2000. Dispersed single cells were allowed to attach on dish and grow. Expansion of attached cell colonies was monitored in the presence of antibiotic. When cell colonies grow to approximately 2-3 mm in size, cells were trypsinized in cloning ring and subcultured to 12-well plates. Cells that continue to grow in the presence of antibiotic were again subcultured to 6-well plates and allowed to grow to approximately 90%

confluency. Cells were harvested and divided into three portions: for protein extraction, subculturing and storage purposes. Presence of selected genes in stable clones was determined using western blotting. For SNU16 suspension cells, selection of stable clones was carried out in 96-well plates using the serial dilution method. Wells that contained 1-3 cells that continued to grow in the presence of antibiotic were monitored and new medium was added every 2-3 days. Expended cells were subcultured to 24-well plates, followed by 12-well and 6-well plates. Cells were harvested and divided as mentioned above. Positive stable clones were determined through western blotting.

3.2.8 Xenografts in Nude Mice

Each of GIF5+pcDNA3.1 and GIF5+mclaudin-1, GIF14+pcDNA3.1 and GIF14+mclaudin-1 as well as SNU16+pcDNA3.1 and SNU16+AShclaudin-1 stable cell lines (5 x 10^6 cells respectively in PBS) were injected subcutaneously into the flanks and back of 10 approximately 2-mth old female nude mice using a 27 ½ gauge needle (Figure 3.4). When the tumors grow to approximately 1 cm of size, they were cut out and weight (gm) was measured. Tumors were kept in 80% ethanol for long term storage or future use.

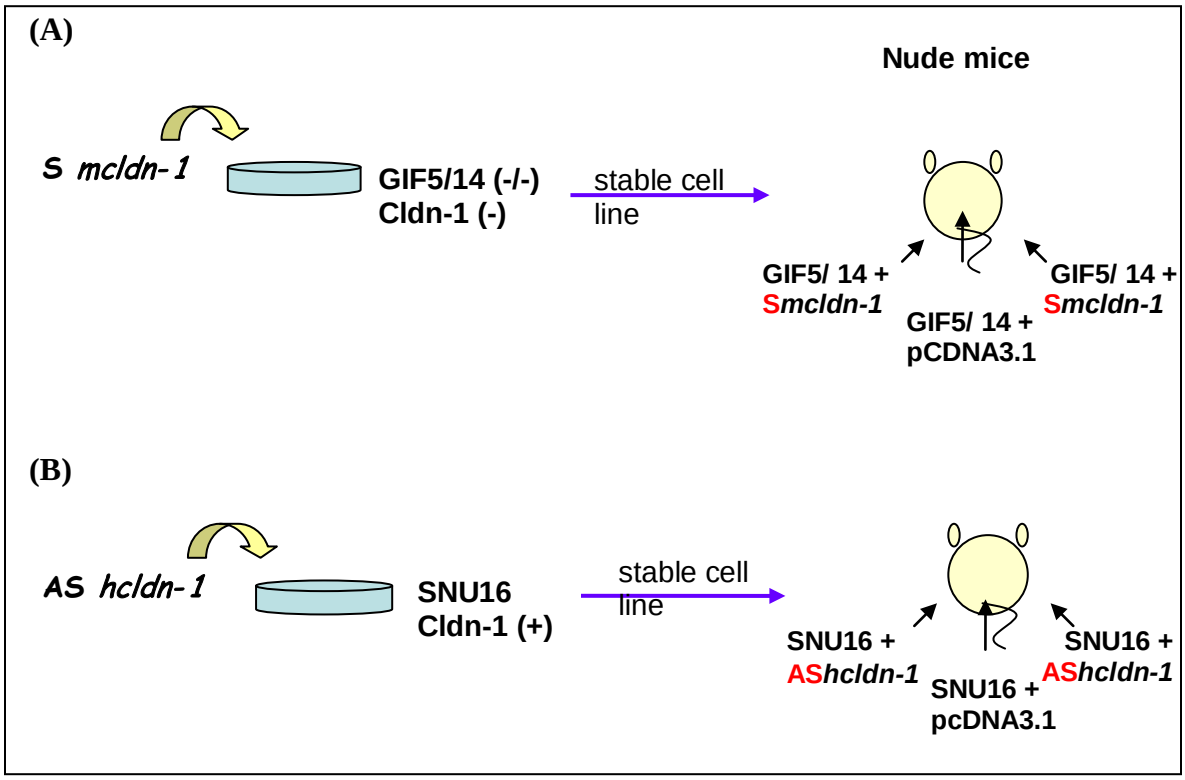

Figure 3.4: Nude mice assay in *Runx3*-/- GIF and SNU16 cell lines. (A) Rescue experiment to observe if exogenous expression of mclaudin-1 in *Runx3*-/- GIF cells reduces tumorigenecity in nude mice. (B) Experiment to observe if knock-down of hclaudin-1 in tumorigenic SNU16 cells enhances tumorigenicity in nude mice.

3.2.9 Collection and Processing of Mouse and Human Tissue Samples

3.2.9.1 Fixing, Processing and Embedding of Mouse Stomach

Freshly dissected neonatal 0 day mice stomach was fixed in 4% paraformaldehyde (PFA) for approximately 2 hrs at 4ºC, briefly rinsed with dH_2O, followed by 70% ethanol overnight at RT. The specimen was then transferred to the tissue processor (Tissue Tek Citabel 2000) for dehydration and processing. The specimen was subjected to dehydration in a series of ethanol followed by xylene and paraffin as the following: 1X 80% ethanol for 1 hr, 1X 90% ethanol for 1 hr, 2X 100% ethanol at 1 hr each, 2X xylene at 1 hr each, 1X xylene + paraffin (1:1) for 2 hrs, 1X paraffin for 1 hr followed by a final immersion in paraffin until the specimen was taken out for embedding. The processed specimen was taken out and immediately embedded on a paraffin block which was then left to solidify. Paraffin blocks were kept at RT until ready to be sectioned.

3.2.9.2 Human Gastric Cancer Specimens

52 surgically resected gastric adenocarcinoma samples and their corresponding non-cancerous tissues were obtained from the Department of Pathology and Surgery, National University of Singapore under a protocol approved by the Institutional Review Board. According to Lauren's classification for gastric adenocarcinoma, there

were 29 differentiated/ intestinal type of gastric adenocarcinoma, and 23 diffuse type of gastric adenocarcinoma.

3.2.10 Microscopy Technique

3.2.10.1 Immunocytochemistry (IF)

GIF cells grown on cover slips in 6-well plates that reached approximately 90% confluency were fixed with 4% PFA for 10 min at RT. Cells were rinsed briefly with PBS, followed by permeabilization with 0.1% Triton X-100 for 10 min at RT, and rehydration with PBS. After blocking with hydrogen peroxide for 5 min at RT, cells were incubated with 1:100 of rabbit anti-claudin-1 diluted in antibody diluent for 1 hr at RT. Cells were washed three times for 5 min each with PBST at RT. Biotinylated anti-rabbit IgG (1:200 dilution) and fluorescein avidin D (1:2000 dilution) were used as secondary and tertiary antibody respectively and incubated for 1 hr each at room temperature. Cells were washed three times for 5 min each with PBST at RT in between the secondary and tertiary antibodies. Slides were counterstained with DAPI (D8417; Sigma) diluted to 0.2 µg/ml in PBS for 3 min at RT. Slides were washed three times with PBS for 3 min each at RT. Mounted slides were subsequently used for immunofluorescence imaging with Zeiss microscope (Axioplan 2 imaging system).

3.2.10.2 Immunohistochemistry (IHC)

Mouse tissues embedded in paraffin blocks were sectioned into 5 μm using a microtome (Leica RN2255) to obtain a series of approximately 10 continuous sections. Sections were placed on the surface of 80% Ethanol to facilitate separation of serial sections into single section. Each serial section was transfered to water bath at approximately 42ºC and left for few seconds for rehydation and fished out and displayed onto the poly-L-lysine coated slides. Slides were left on heating block set to 37ºC for approximately 1 hr until sections were dry. Deparaffinization was carried out in xylene followed by rehydration of specimen in ethanol. Deparaffinized tissues were incubated at 96°C for 40 min with antigen retrieval solution (S1700; Dako) and cooled down for 30 min at RT. After blocking with hydrogen peroxidase for 5 min, the specimens were incubated with rabbit anti-Claudin-1 (1:100 dilution) for 1 hr at RT, followed by three time washing for 5 min each with PBST at RT. Secondary antibody and chromogen-substrate for visualization were added according to the instructions given by the EnVision+ system (DAB) kit. After development with diaminobenzedine, the sections were counterstained with hematoxylin, dehydrated and mounted with coverslips.

52 human tissues were fixed with 10% neutral-buffered formalin, embedded in paraffin, and serially sectioned at 4 μm. After routine deparaffinization and rehydration, specimen was treated at 96°C for 40 min with antigen retrieval solution. Specimens were cool down for 30 min at room temperature. After blocking with

hydrogen peroxidase, the specimens were incubated with rabbit anti-Claudin-1 (1:100 dilution) and mouse anti-RUNX3 (1 μg/ml, R3-6E9) (97) for 1 hr at RT. The EnVision+ system (DAB) kit was used for visualization. After development with diaminobenzedine, the sections were counterstained with hematoxylin, dehydrated and mounted with coverslips. Cases showing RUNX3 expression in the nucleus were counted as positive. Cases with no expression or showing RUNX3 expression in the cytoplasm were counted as negative.

3.2.11 Electrophoresis Mobility Shift Assay (EMSA)

EMSA was carried out according to the manufacturer's protocol provided by the LightShift Chemiluminescent EMSA kit and the Chemiluminescent Nucleic Acid Detection Module. Labeled probes were prepared by annealing six pairs of 5' biotinylated oligomers with nonlabeled complementary oligomers; unlabeled competitor probes were prepared by annealing six pairs of two unlabeled complementary oligomers in annealing buffer comprising of 20 mM Tris (pH7.5), 50 mM NaCl and 10 mM $MgCl_2$. Complementary oligomers were denatured at 95°C for 5 min and left to cool down at room temperature to enable annealing to happen. First set of probes cover the first and second RUNX binding sites, whereas the second set of probes cover the third RUNX binding site. Four pairs of oligonucleotides that were used as probes for site 1 and 2 include WT-WT, WT-MT, MT-WT and MT-MT. Probes for site three include WT and MT. A final concentration of 30 fmol of labeled

probes and 4 pmol of unlabeled probes were used for the binding reactions in the presence of 1 μg/μl of poly (dI-dC) and 1x binding buffer. 200 ng of anti-RUNX3 (R3-5G4) were added to the control reaction to check the specificity of binding.

Briefly, binding reactions were prepared on ice with the addition of distilled water, 10X binding buffer, 1 μg/μl of poly (dI-dC), unlabeled probe and protein extract (293T cells with or without exogenous *RUNX3*) in sequence. The binding reaction was performed at RT for 20 min before the biotin-labeled probe was added. Loading buffer was mixed with the binding reactions and loaded into 0.5X TBE gel. Gel electrophoresis was carried out at 100 V until the bromophenol blue dye migrated ¾ down the length of the gel. DNA on gel was transferred to nylon membrane in ice-cold 0.5X TBE buffer at 100 V for 30 min. Cross-linking of DNA to membrane was performed twice for 1 min each at 120 mJ/cm^2 using a UV-cross-linker. Nylon membrane was then incubated with blocking buffer for 15 min with gentle shaking, followed by incubation with streptavidin-horseradish peroxidase conjugate for 15 min with gentle shaking. Membrane was washed four times for 5 min each with 1X wash solution with gentle shaking. Substrate equilibration buffer was added for 5 min with gentle shaking. Finally, membrane that has been removed from the substrate equilibration buffer was added the mixture of luminal/ enhancer solution and stable peroxide solution (1:1 ratio) and ready to be exposed to X-ray film.

3.2.12 Chromation Immunoprecipitation (ChIP)

Chromatin immunoprecipitation (ChIP) was performed according to the manufacturer's protocol provided by the EZ ChIP Chromatin Immunoprecipitation kit. Crosslinking of histones to DNA in formaldehyde was carried out for 5 min at 37°C. Sheering of DNA was done by sonication using 8 sets of 12-second pulses with 30% of maximum power on a sonicator (Sonifier 150; Branson). 5 μg of anti-RUNX3 (R3-6E9) was used to immunoprecipitate endogenous RUNX3 from the SNU16 cells. Protein G Agarose was used to collect the antibody/ histone complex. As control, 5 μg of mouse normal IgG (sc-2025; Sigma) was used in a separate reaction. Washing of protein G agarose/ antibody/ chromatin complex was carried out followed by elution in elution buffer (1% SDS, 0.1 M $NaHCO_3$).

The chromatin complex was reverse cross-linked and DNA was recovered by phenol/ chloroform extraction and ethanol precipitation. Primers Cldn1CHIP-2F and Cldn1CHIP-2R which are specific to the human claudin-1 promoter were used to amplify the DNA fragment comprising of all three RUNX binding sites. Primers FOR and REV specific for the GAPDH promoter were used to perform PCR on the pull-down DNA, acting as a negative control. PCR for claudin-1 was carried out at 94ºC for 5 min and for 32, 35 or 37 cycles each of 94ºC for 30 sec, 58ºC for 30 sec, 72ºC for 30 sec and final cycle of 72ºC for 10 min. PCR for GAPDH was carried out at 94ºC for 5 min and for 32 cycles each of 94ºC for 30 sec, 60ºC for 30 sec, 72ºC for 30

sec and final cycle of 72ºC for 10 min. PCR amplification product was visualized on a 2% agarose gel.

CHAPTER 4 RESULTS AND DISCUSSIONS

4.1 Results

4.1.1 Expression of TJ Proteins in Mouse Gastric Epithelial Cells

RUNX3 was found to be a strong candidate for gastric cancer tumor suppressor as loss of expression or mislocalization of RUNX3 protein are associated with gastric carcinogenesis (23, 97). In a previous report, *Runx3*$^{-/-}$ gastric epithelial cells were shown to attach weakly to each other, suggesting a loss of *Runx3* function may be responsible for the reduction of cell-cell contact and polarity (95). To investigate whether *RUNX3* plays a role in the regulation of cell-cell contact and polarity, Western blot analysis was performed on a series of mouse embryonic gastric epithelial cells (GIF cells), namely the GIF5 and GIF14 *Runx3*-null cells and the *Runx3* expressing GIF9 and GIF13 cells, to examine the relationship between Runx3 expression and expression of proteins involved in cell-cell contact.

The AJ and TJ proteins are known to function in the maintenance of cell-cell contact and polarity. Thus the expression level of E-cadherin, an AJ protein known to play a role in gastric carcinogenesis and TJ proteins including claudin-1, claudin-2, claudin-3, claudin-4, claudin-7, claudin-11, claudin-16, ZO-1, ZO-2, ZO-3 and occludin was examined using these cell lines.

Interestingly, the TJ proteins, claudin-1, claudin-3, ZO-3 and occludin were found to be expressed in high abundance in *Runx3* expressing GIF9 and GIF13 cells, whereas none or very low level were detected in *Runx3*-null GIF5 and GIF14 cells (Fig. 4.1). These results suggest that presence of *Runx3* has a direct or indirect effect on the expression of claudin-1, claudin-3, ZO-3 and occludin in the mouse embryonic gastric epithelial cells. In contrast, the expression of E-cadherin was not affected by the presence or absence of *Runx3*. Claudin-2, -4, -7, -11 and -16 however were not detected in GIF cell lines.

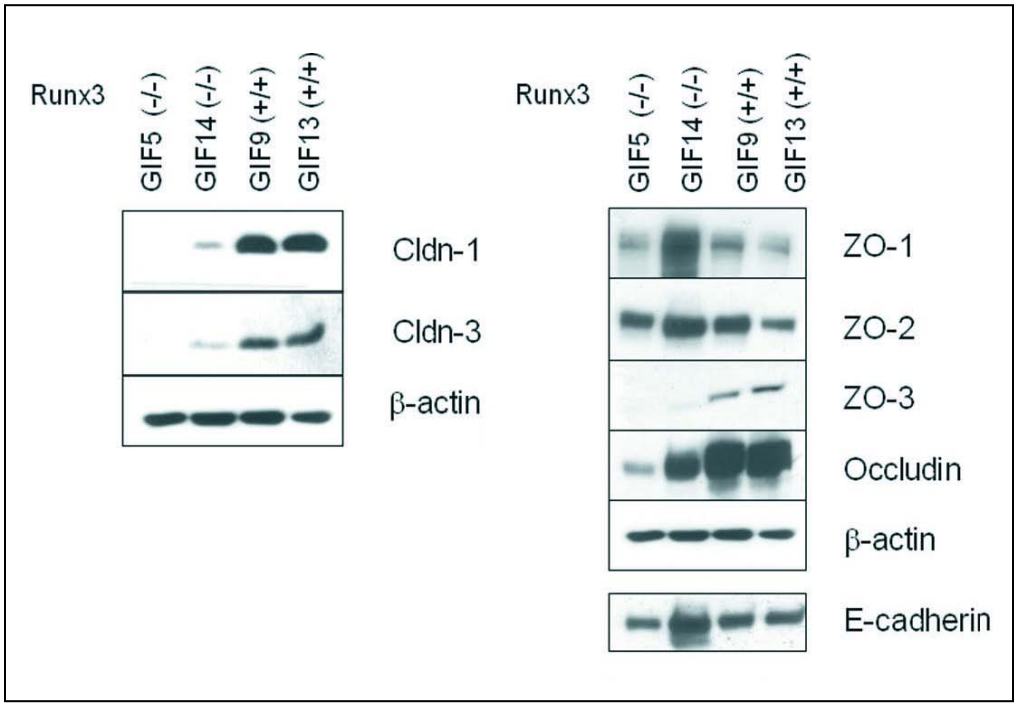

Figure 4.1: Western blot analysis of tight junction (TJ) and adhesion junction (AJ) proteins in *Runx3*$^{-/-}$ and *Runx3*$^{+/+}$ mouse gastric epithelial GIF cell lines. claudin-1, claudin-3, ZO-3 and occludin were expressed in high abundance in *Runx3* expressing GIF9 and GIF13 cells, whereas none or very low level were detected in *Runx3*-null GIF5 and GIF 14 cells. Claudin-2, claudin-4, claudin-7, claudin-11 and claudin-16 were not detectable using these cell lines.

4.1.2 TJ Proteins and TGF-β Pathway

RUNX3 functions as a tumor suppressor under the TGF-β pathway. To observe if the TJ proteins as well as E-cadherin tested in section 4.1 were regulated downstream of *RUNX3,* the expression level of these proteins in the presence and absence of TGF-β were observed. As *Runx3* expressing GIF cell lines expressed relatively low level of *Runx3,* it was not the best cell line to be used for this study. For this purpose, the SNU16 cell line which is a human gastric cancer cell line that expresses relatively high level of RUNX3 and responses to the treatment of TGF-β was used. SNU16 cell lysate was collected at 0 hr before addition of TGF-β and at 6, 12 and 24 hr after addition of TGF-β, followed by Western blot analysis with the antibody against the respective TJ proteins (Fig. 4.2).

From the series of TJ and AJ proteins tested, only claudin-1 showed responsiveness towards TGF-β, whereby its expression increased in a time dependent manner upon addition of TGF-β. This indicates that TGF-β is involved in the induction of claudin-1 expression in SNU16 gastric epithelial cells. This regulation pattern however was not observed in other TJ and AJ proteins. Hence, claudin-1 was selected for further analysis whereas claudin-3, ZO-3 and occludin were omitted even though their expression showed a positive correlation with *Runx3* in mouse embryonic gastric epithelial cells (Fig. 4.1).

4.1.3 RUNX3 and claudin-1 in TGF- β Pathway

To further confirm that claudin-1 expression is regulated by TGF-β, experiment in (Fig. 4.3A) was carried out. SNU16 cells that were treated with TGF-β for 24 hr showed a higher claudin-1 expression level as compared to the untreated one (Lane 1 & 2). When the TGF-β inhibitor was added to SNU16 cells in the presence of TGF-β, the induction of claudin-1 expression greatly diminished (Lane 3). This clearly shows that the TGF-β signaling pathway is involved in the regulation of claudin-1 expression in the SNU16 cell line.

To observe if *RUNX3* is involved in the regulation of *claudin-1* under the TGF-β pathway, the expression of *claudin-1* was compared between the SNU16 cell line and the AS SNU16 cell line, in which *RUNX3* was knocked-down by using the antisense DNA against *RUNX3* (Fig. 4.3B). Both RT-PCR and Western blot analysis showed a time-dependent increased of claudin-1 expression in SNU16 cell line upon treatment by TGF-β. This pattern of claudin-1 expression however was not observed in the AS SNU16 cell line. This shows that RUNX3 is necessary for the regulation of claudin-1 expression under the TGF-β pathway.

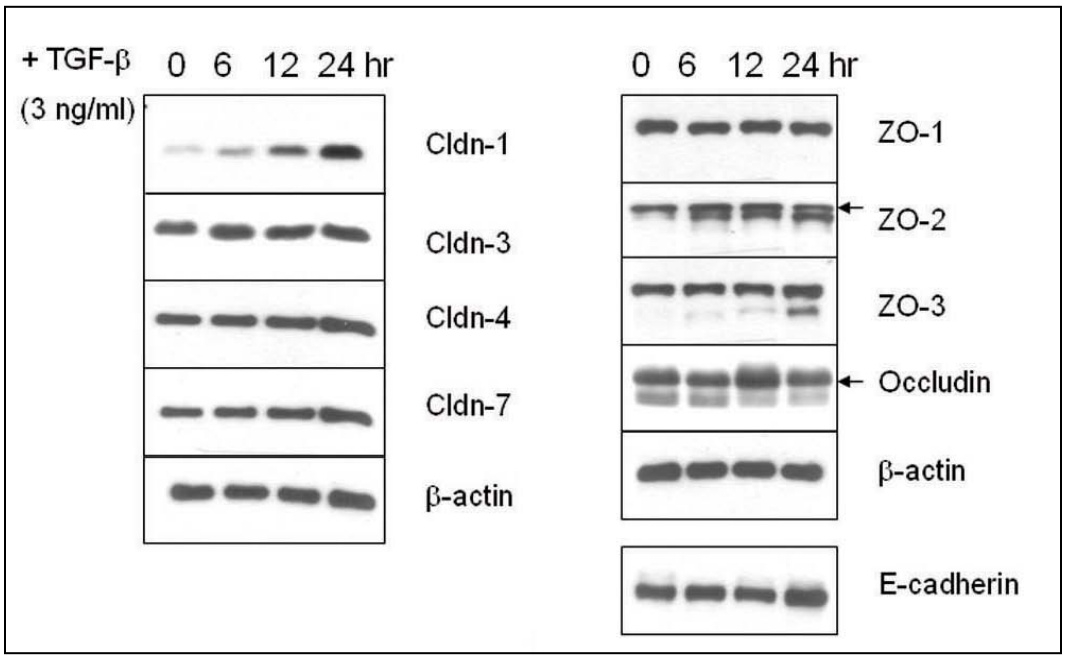

Figure 4.2: TGF-β treatment and expression of tight junction and adhesion junction proteins. SNU16 cell lysates were collected at 0 hr before treatment with TGF-β and at 6, 12 and 24 hr upon treatment with TGF-β. Western blot analysis was carried out using antibodies against the respective tight junction and adhesion junction proteins. claudin-1 expression increased in response to TGF-β, indicating that claudin-1 expression is regulated by the TGF-β signaling pathway. claudin-2, claudin-11 and claudin-16 were not detectable in these cell lines.

(A)

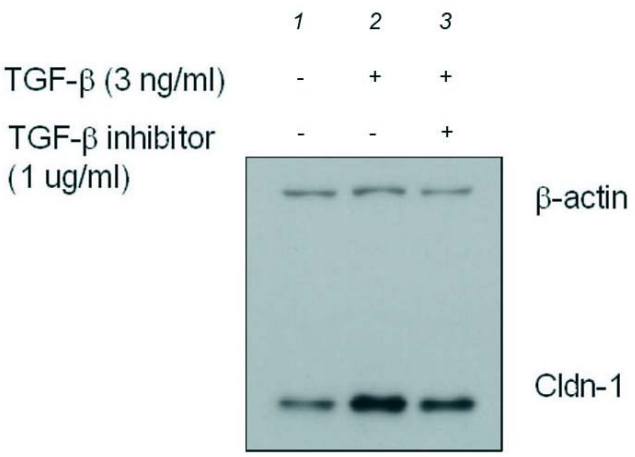

(B)

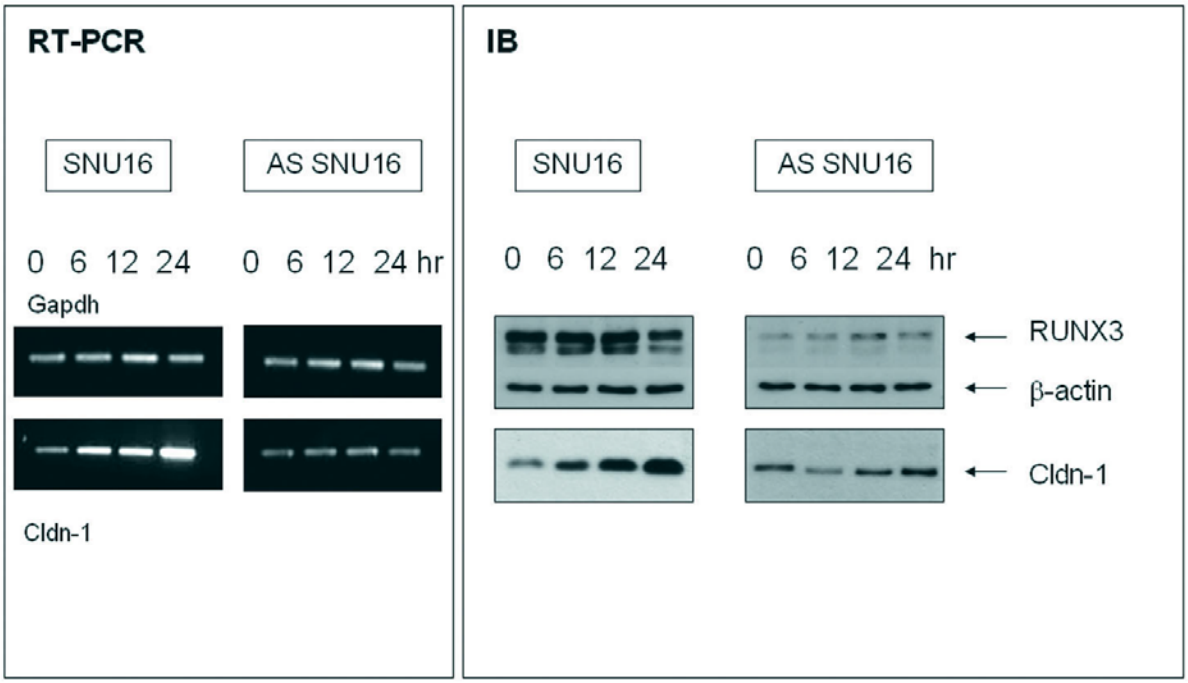

Figure 4.3: Regulation of claudin-1 by TGF-β. (A) Induction of claudin-1 by TGF-β was highly reduced in the presence of TGF-β inhibitor, confirming the involvement of TGF-β signaling pathway in the regulation of claudin-1 expression. (B) RT-PCR and Western blot analysis showing claudin-1 expression in the presence and absence of *RUNX3*. AS SNU16 is a *RUNX3*-knocked-down SNU16 cell line using the antisense DNA against *RUNX3*. Reduced level of RUNX3 was confirmed by Western blot analysis. The TGF-β dependent expression of claudin-1 was greatly reduced when majority of *RUNX3* was knocked-down, indicating the involvement of RUNX3 in the regulation of claudin-1 expression.

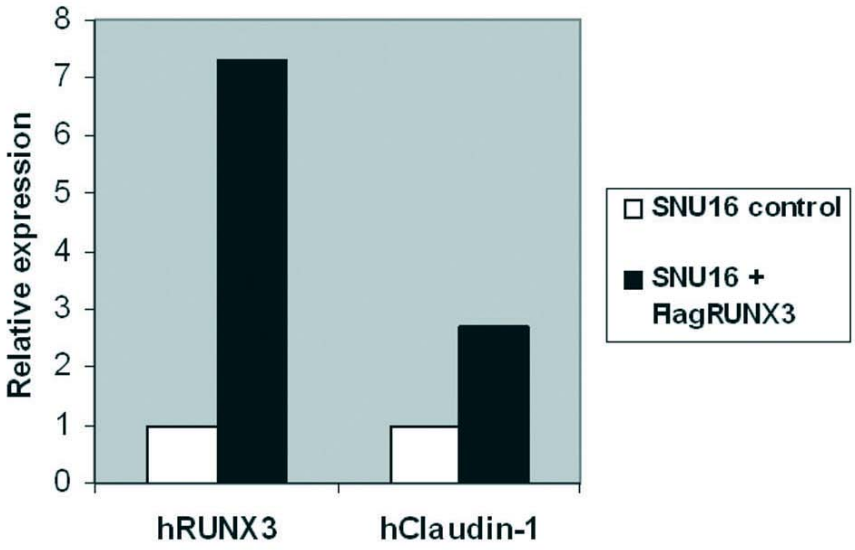

Figure 4.4: Quantitative RT-PCR analysis of claudin-1 expression upon induction by *RUNX3* in SNU16 cell line. Stable SNU16 cell line expressing exogenous *RUNX3* was assigned SNU16+FlagRUNX3 (*black bars*). Basal expression level of RUNX3 and claudin-1 in SNU16 were adjusted to 1 (*white bars*) for comparison purposes. Claudin-1 expression was increased by approximately 2.7 folds in the presence of exogenous RUNX3, indicating that RUNX3 is involved in the induction and regulation of claudin-1 expression in the SNU16 gastric epithelial cell line.

4.1.4 claudin-1 Expression in Mouse Gastric Epithelial Cells

The expression pattern of claudin-1 was further confirmed by immunofluorescence staining using the *Runx3*$^{+/+}$ and *Runx3*$^{-/-}$ GIF cell lines. *Runx3*$^{+/+}$ GIF9 and GIF13 cell lines were positively stained by claudin-1, whereas *Runx3*$^{-/-}$ GIF5 and GIF14 cell lines were either not stained, or stained at very low level by claudin-1 (Fig. 4.5A). These results correlated well with the results of Western blot analysis in Fig. 4.1.

(A)

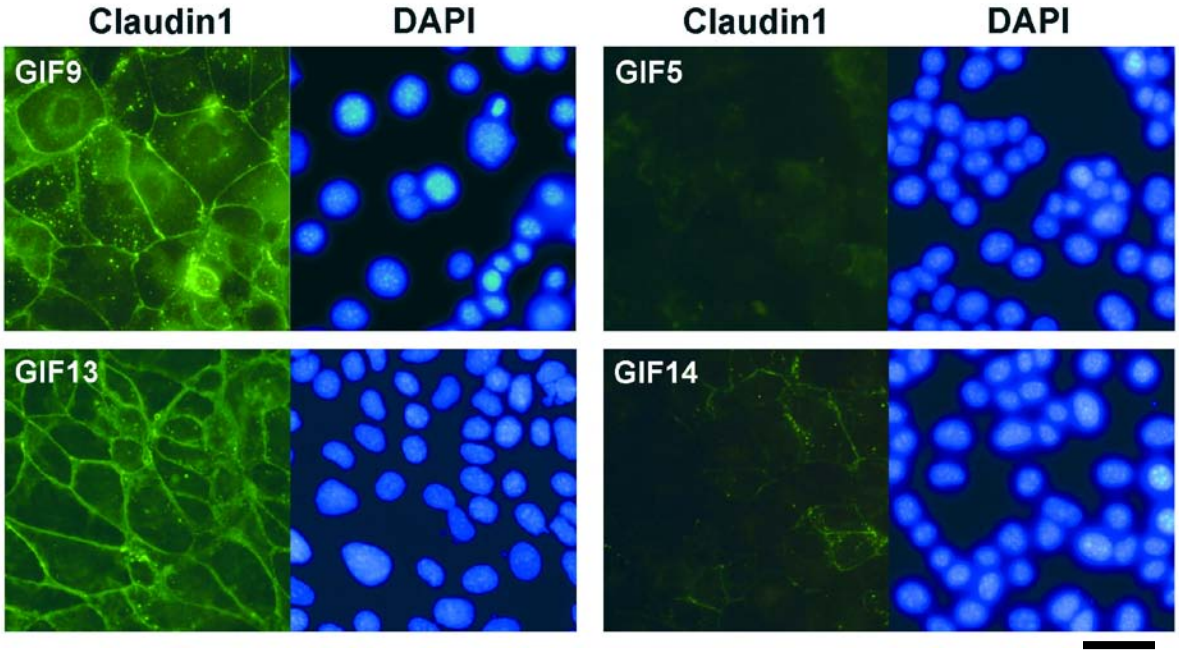

(B)

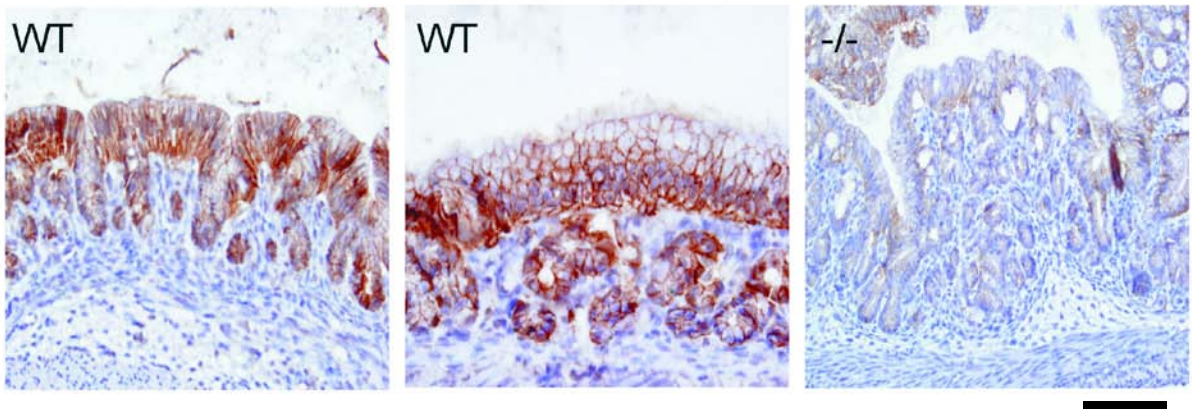

Figure 4.5: Immunodetection of claudin-1 in mouse gastric epithelial cells and tissue samples. (A) Immunofluorescence analysis of claudin-1 in *Runx3*-/- and *Runx3*+/+ GIF cell lines. *Runx3*+/+ cells showed clear claudin-1 staining at cell-cell boundaries. *Runx3*-/- GIF cells showed none or very low level of claudin-1 expression. Scale bar, 50 µm. (B) Immunohistochemistry analysis of neonatal 0 day mice stomach. Left and middle panels represent stomach sections from wild-type mice; right panel represents stomach section from *Runx3* knock-out mice. Scale bar, 100 µm.

Immunohistochemistry staining was also performed on sections of wt and *Runx3* knock-out mouse gastric epithelial tissues which were embedded into paraffin blocks. Results showed that claudin-1 stained positively on the surface membrane of wt mouse gastric epithelial cells. *Runx3* knock-out gastric epithelial cells on the other hand show greatly diminished level of claudin-1 expression (Fig. 4.5B). These results collectively show that claudin-1 expression is positively correlated to the expression of Runx3 in mouse gastric epithelial model.

4.1.5 claudin-1 Promoter Assay

Results from section 4.13 shows that *RUNX3* mediates induction of *claudin-1* transcription. In order to examine the direct involvement of *RUNX3* in the regulation of *claudin-1* expression, a human *claudin-1* promoter was examined. The constructed promoter contains three putative RUNX binding elements (Fig. 4.6A). The proposed consensus sequence for RUNX binding element was 5'-PuACCPuCA-3', or in the reverse orientation, 5'-TG(T/G)GGT-3', with 5'-AACCACA-3' being the regular type of sequence found in most bona fide RUNX target promoters (212). The second and third RUNX binding consensus, which happened to be the regular type, were found to be highly conserved in the mouse and human *claudin-1* promoter (Fig. 4.6B). Seven types of luciferase reporter plasmids were constructed, each containing one (M1, M2 & M3), two (M1+2, M1+3, M2+3) or three (M1+2+3) mutant binding elements, upstream of the luciferase gene. All reporter activity was normalized against the luciferase activity expressed by the promoterless pRL-SV40 vector.

Reporter assay was first performed using the SNU16 cell line. Figure 4.7 showed that the reporter activity of WT promoter increased in a dose dependent manner, both before and after the addition of TGF-β. In the AGS cell line in which RUNX3 is not expressed, the reporter activity of WT promoter increased in consistent with the addition of *RUNX3* and was *RUNX3*-dose-dependent (Fig.4.8A). In Figure 4.8B, the reporter activity increased for about 1.7 folds when *Smad3* and *Smad4* were added as compared to control. This was possible as there were six *Smad* binding elements found within the human *claudin-1* promoter downstream of the third RUNX binding site and this verifies the proper function of the promoter. The promoter activity increased by another 2.2 folds when *RUNX3* was added in addition to *Smad3* and *Smad4*, resulting in an approximately 4 folds increase of promoter activity compared to the control.

The reporter activity of wild type plasmid was also significantly higher than that of any reporter plasmid containing one or more mutant elements. When all three RUNX binding elements were mutated, the reporter activity was abolished (Fig. 4.8B). These results collectively indicate that *RUNX3* induces claudin-1 expression in cooperation with Smad proteins.

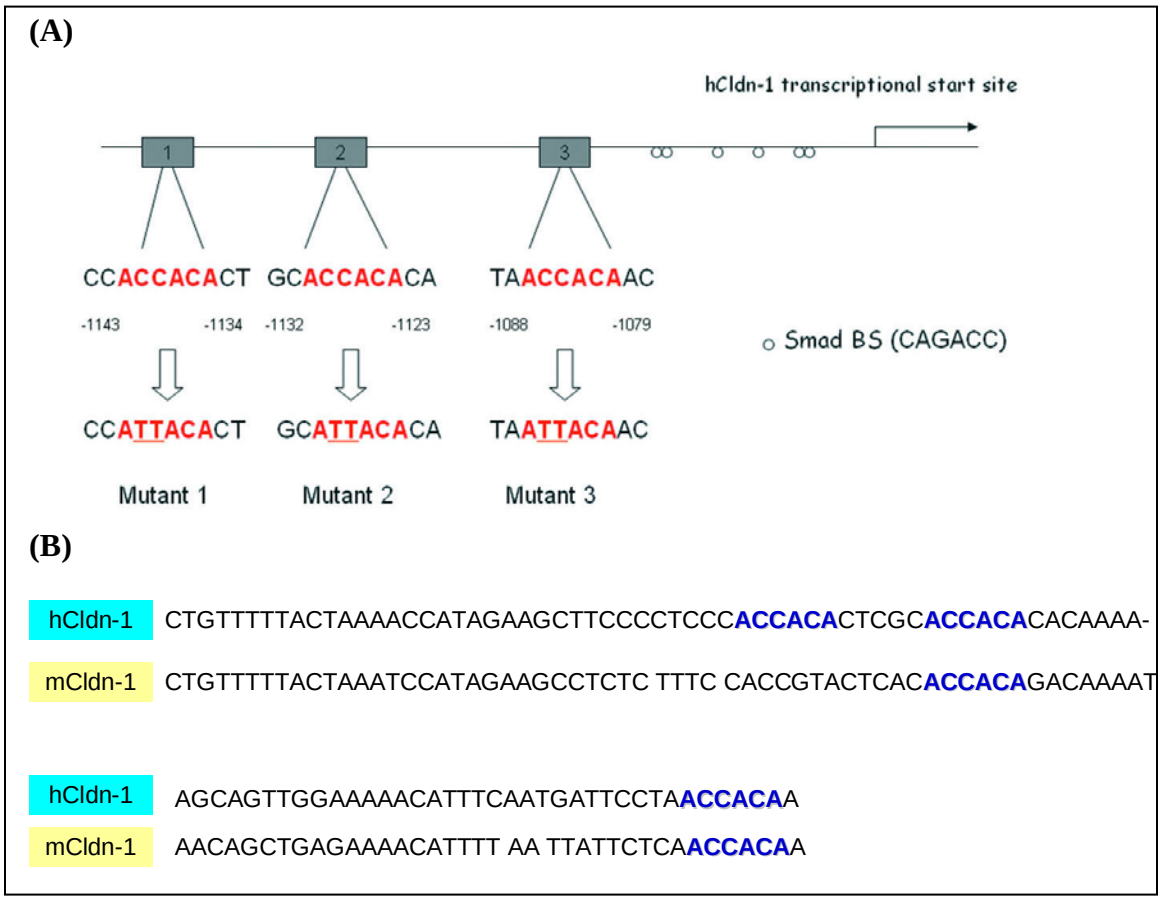

Figure 4.6: *hclaudin-1* promoter. (A) Schematic diagram of the *hclaudin-1* promoter, 1500 bp upstream of the transcriptional start site. Three *RUNX* consensus binding sequence, with their respective mutants were highlighted in red. Mutants were generated using the site-directed mutagenesis method. (B) Schematic diagram showing conservation of the second and third RUNX binding sites in the human and mouse claudin-1 promoter region.

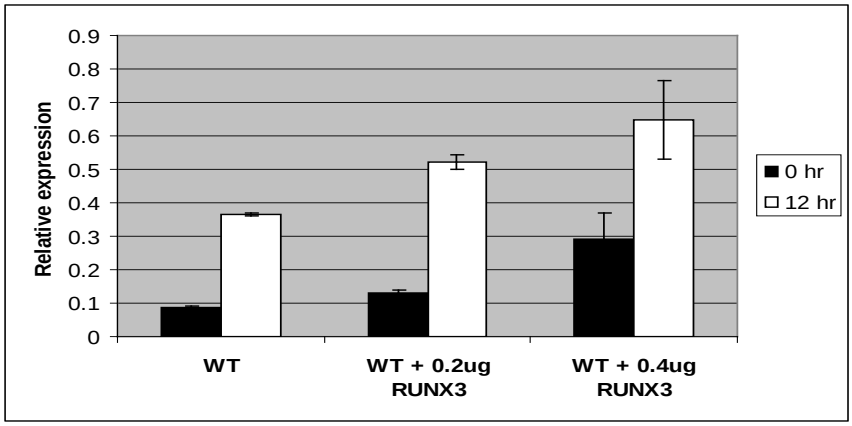

Figure 4.7: *hclaudin-1* reporter assay in SNU16 cell line. *hclaudin-1* promoter activity was up-regulated by the expression of *RUNX3* in a *RUNX3*-dose dependent manner. 0 hr represents sample before addition of TGF-β, 12 hr represents sample at 12 hr time point upon addition of TGF-β.

(A)

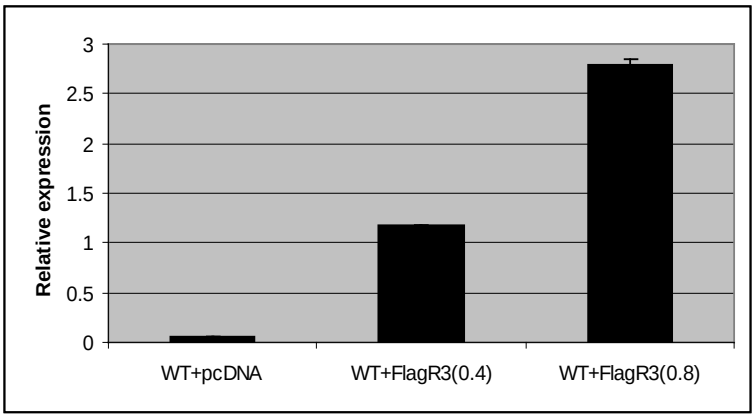

(B)

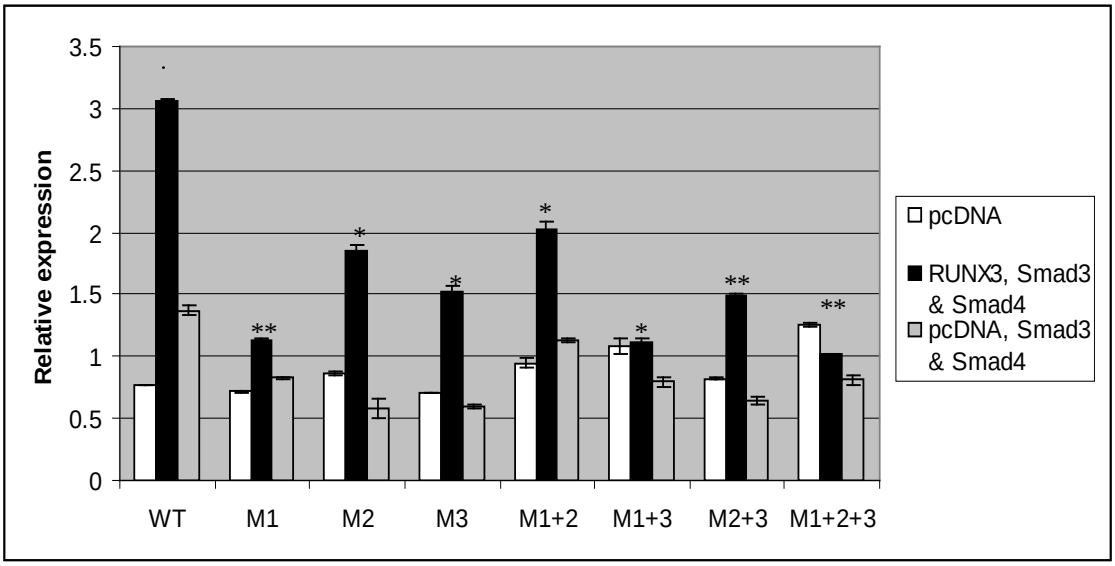

Figure 4.8: hclaudin-1 reporter assay in AGS cell line. (A) Up-regulation of promoter activity was *RUNX3*-dose-dependent. (B) WT represents wild-type reporter construct. M1, M2 and M3 represent reporter constructs with single mutant at first, second and third RUNX binding sites. M1+2, M1+3, M2+3 and M1+2+3 represent reporter constructs with compound mutants at RUNX binding sites. As compared to the WT promoter, single and compound mutants show significant reduction of promoter activity in the presence of *RUNX3* and *Smads*. Two tailed Student's *t* test: (*) $p<0.05$; (**) $p<0.01$.

4.1.6 Electrophoretic Mobility Shift Assay (EMSA)

To investigate the possibility of direct interaction between the putative binding elements in the claudin-1 promoter and RUNX3, EMSA was performed using double-stranded DNA probes containing either the wild type or mutant sequences of the binding elements (Fig. 4.9). Protein extracts were obtained from 293T cells which do not contain endogenous RUNX3, and 293T cells exogenously expressing RUNX3. IgC-alpha promoter region contains three RUNX binding sites, thus were used as the control probe in this assay (Lane 1-3). Four pairs of probes covering first and second RUNX binding elements, which contain both wild type (WT-WT), one wild type and one mutant (WT-MT; MT-WT) or both mutant (MT-MT), and 2 probes covering third RUNX binding element (WT and MT) were used.

A band corresponding to RUNX3 binding to probe containing two wild type RUNX binding elements was observed as shown in lane 6. Addition of unlabelled wild type competitor probe blocked this association (Lane 7), but not for unlabelled competitor probe containing both mutated RUNX binding sites (Lane 8). These results were likewise observed for probes with one wild type and one mutant RUNX binding sites (WT-MT and MT-WT) (Lane 16-19). These results collectively show that RUNX3 binds to the first and second RUNX binding sites in the *claudin-1* promoter. When either one of these RUNX binding sites was being mutated, the binding affinity of RUNX3 to the probe became weaker, as shown by the weaker bands in lane 16 and 18 as compared to lane 6. RUNX3 also binds to the third RUNX

binding site, with a stronger affinity, as shown by the stronger bands in Lane 11 & 13. To confirm the specificity of these shifts, the anti-RUNX3 (R3-5G4) monoclonal antibody which is specific for RUNX3 was added. A supershifted band was observed, confirming that RUNX3 protein was present in the DNA-protein complexes (Lane 20). These observations clearly show the direct binding of RUNX3 to *claudin-1* promoter *in vitro*.

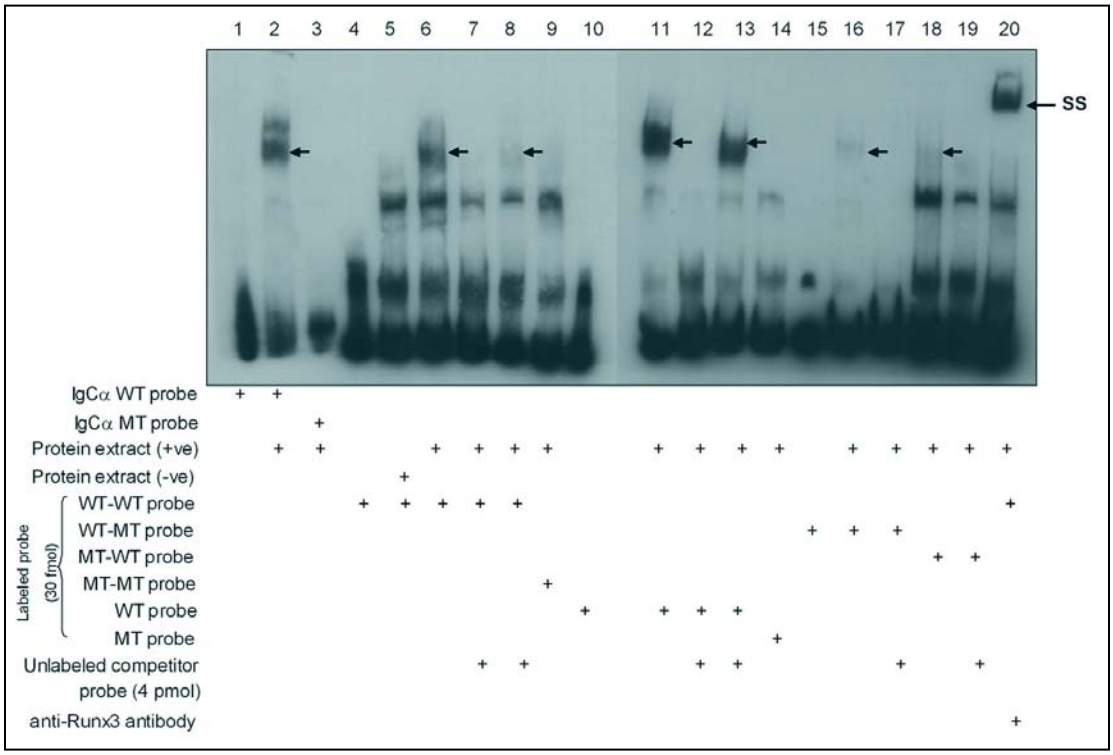

Figure 4.9: Electrophoretic Mobility Shift Assay (EMSA). Protein extract was obtained from 293T cells in the presence and absence of exogenous *RUNX3*. IgCα WT probe which contains *RUNX* binding sites acts as positive control. Both biotin-labeled and unlabeled probes of 35 mers were used. First set of probes contain either wild-type or mutated forms of first and second *RUNX* binding sites (*WT-WT*, *WT-MT*, *MT-WT*, *MT-MT*); second set of probes contain only wild-type or mutated form of third *RUNX* binding site (*WT*, *MT*). Results showed that RUNX3 binds to all 3 putative RUNX binding sites on hclaudin-1 promoter, with third RUNX binding site as the seemingly favorable binding site. Arrow; DNA-protein complex. SS; DNA-protein-antibody complex.

4.1.7 Chromatin Immunoprecipitation (ChIP)

To observe if RUNX3 also binds to claudin-1 *in vivo*, ChIP assay was carried out using the SNU16 cells containing endogenous RUNX3. As shown in Figure 4.10, the anti-RUNX3 (R3-6E9) monoclonal antibody was able to successfully pull down *claudin-1* promoter region. Upon TGF-β treatment, RUNX3 localized in the cytoplasm is translocated into the nucleus. Hence, more RUNX3 is available to bind to the claudin-1 promoter, resulting in the increase in immunoprecipitated claudin-1, as shown by the higher intensity of the PCR product. Quantitation of the ChIP band was done by increasing cycles of PCR. PCR using the *GAPDH* primers and pull-down by a normal mouse IgG acted as negative controls, to show that the pulled-down chromatins by the RUNX3 antibody was specific. Thus, the results show that RUNX3 binds to the *claudin-1* promoter *in vivo* and *claudin-1* is a direct target of *RUNX3* in SNU16 cells.

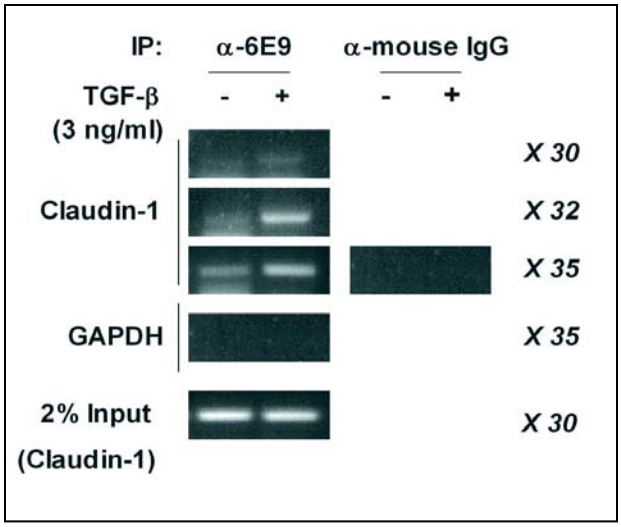

Figure 4.10: Chromatin Immunoprecipitation (ChIP) assay. PCR results with primers specific to *hclaudin-1* promoter indicates the specificity of pull-down product as well as specificity of antibody used. Figures on the right panel indicate number of PCR cycles. PCR for input is done using primers specific to *hclaudin-1* promoter. A smaller band detected below the claudin-1 band in the 6E9 precipitates is a result of primer dimer formation.

4.1.8 Nude Mice Assay

4.1.8.1 Restoration of claudin-1 Expression and Its Tumor Suppressive Effect

As shown in Fig. 4.1 and Fig. 4.5A, *Runx3*$^{-/-}$ GIF5 cell line does not express claudin-1 whereas *Runx3*$^{-/-}$ GIF14 cell line expresses very low level of claudin-1. A previous publication showed that GIF cells from *Runx3*$^{-/-}$ mice were tumorigenic in nude mice, whereas GIF cells from *Runx3*$^{+/+}$ mice were not (23). To check if *claudin-1* acts as a tumor suppressor in gastric epithelial cells, GIF5 and GIF14 stable cell lines expressing exogenous claudin-1 in the pcDNA3.1 vector were generated. Interestingly, restoration of exogenous claudin-1 in both GIF5 and GIF14 cells greatly suppress tumorigenicity in nude mice, and the tumor suppressive effect was correlated well to the level of claudin-1 expression in these stable cell lines. The number of tumors was lower when the level of exogenously expressed claudin-1 was higher (Fig. 4.11 & 4.12). These results show that restoration of claudin-1 expression contributes to the tumor suppressive effect in the tumorigenic mouse gastric epithelial cell lines.

GIF5 (gm)	clone1 (gm)	clone2 (gm)
0.62	NA	NA
0.65	NA	NA
0.44	NA	NA
0.83	0.06	NA
0.7	NA	NA
0.9	NA	NA
0.29	NA	NA
0.39	NA	NA
0.32	NA	NA
0.57	NA	NA

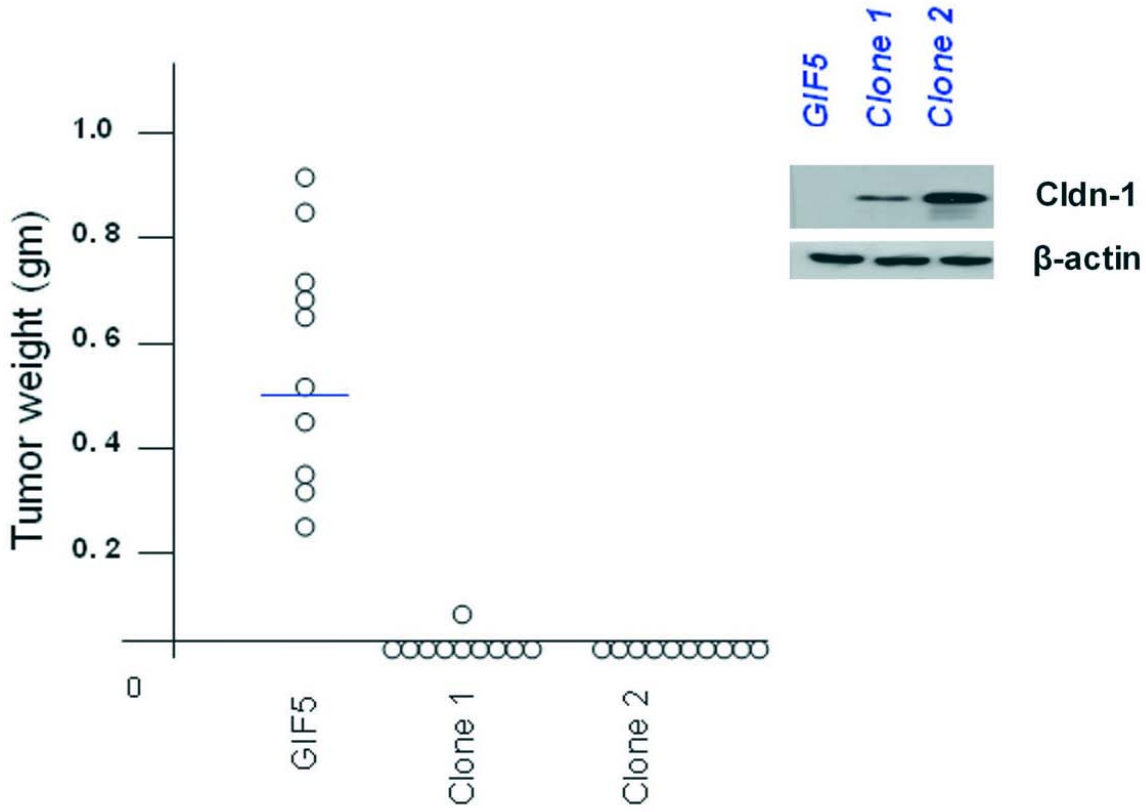

Figure 4.11: Nude mice assay in *Runx3*-/- GIF5 cell line. GIF5 stable cell lines expressing exogenous mclaudin-1 (clone 1 and 2), and GIF5 control cell line stably expressing pcDNA3.1 were used. GIF5 stable cell lines expressing mclaudin-1 highly reduced tumorigenicity in nude mice as compared to control GIF5 cells, indicating the possible role of claudin-1 as a tumor suppressor, functioning as a target of *RUNX3*. NA: no tumor observed.

GIF14 (gm)	clone2 (gm)	clone3 (gm)
0.26	NA	NA
0.27	0.05	NA
0.05	NA	NA
0.13	NA	NA
0.17	NA	NA
0.2	0.13	NA
0.24	0.17	NA
NA	NA	NA
NA	NA	NA
NA	NA	NA

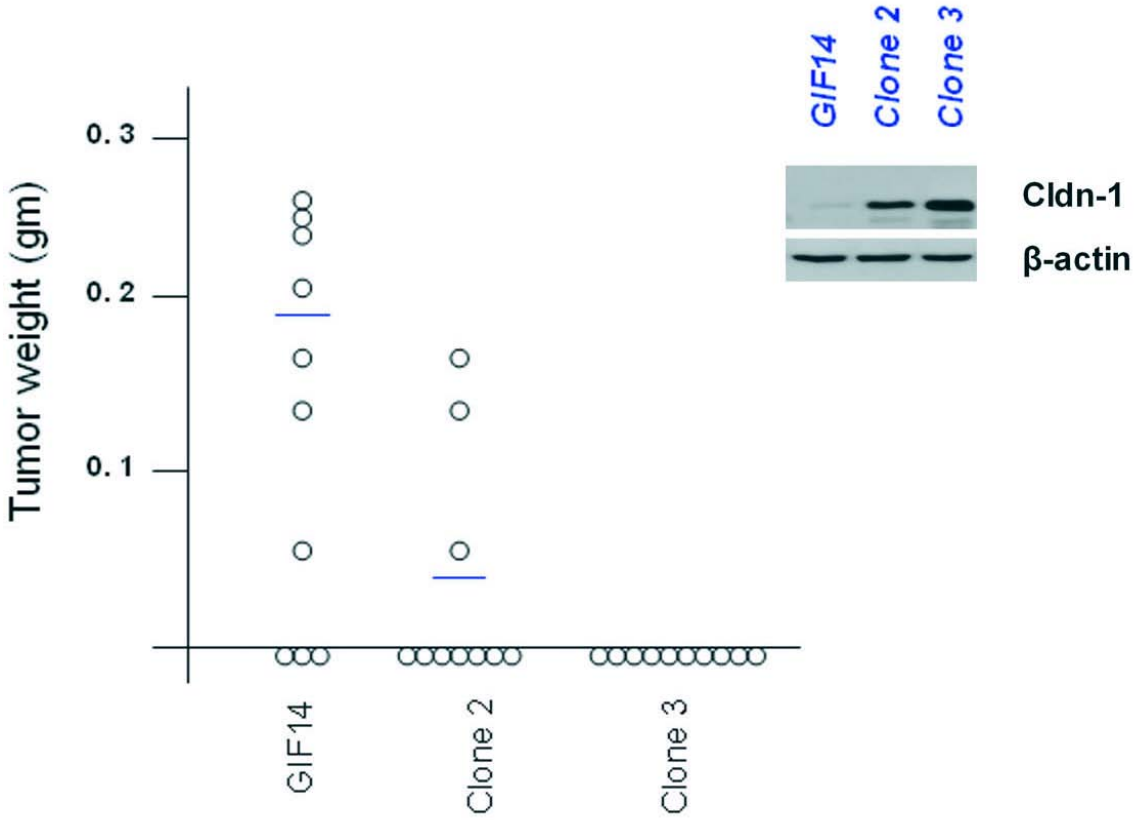

Figure 4.12: Nude mice assay in *Runx3*-/- GIF14 cell line. GIF14 stable cell lines expressing exogenous mclaudin-1 (clone 2 and 3), and GIF14 control cell line stably expressing pcDNA3.1 were used. GIF14 stable cell lines expressing mclaudin-1 highly reduced tumorigenicity in nude mice as compared to control GIF14 cells, indicating the possible role of claudin-1 as a tumor suppressor, functioning as a target of *RUNX3*. NA: no tumor observed.

SNU16 (gm)	clone8 (gm)	clone9 (gm)
NA	NA	0.04
NA	0.13	0.04
NA	0.06	0.1
NA	0.02	0.14
NA	0.17	0.17
NA	0.18	0.18
NA	0.25	0.21
0.14	0.14	0.21
0.1	0.31	0.2
NA	0.27	0.36

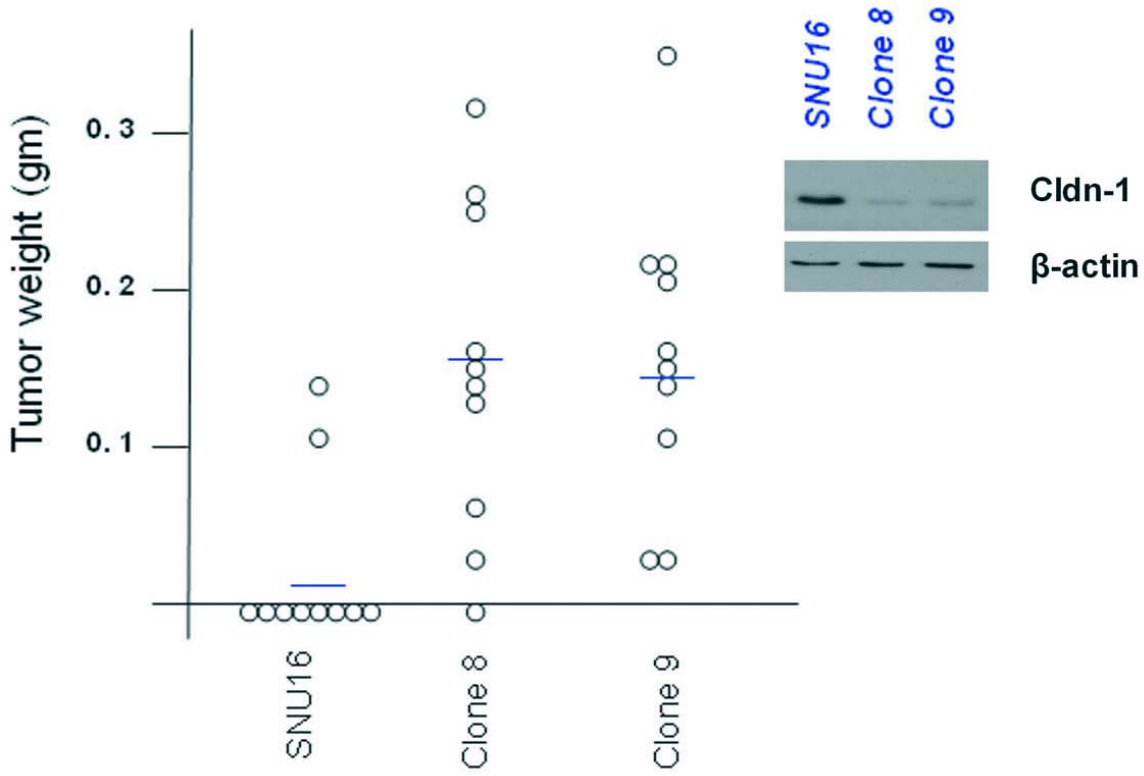

Figure 4.13: Nude mice assay in the SNU16 human gastric cancer cells. SNU16 stable cell lines whereby endogenous claudin-1 was stably knocked-down (clone 8 and 9), and SNU16 control cell line stably expressing pCDNA3.1 were used. Knock-down of hclaudin-1 in SNU16 stable cell lines enhances tumorigenicity as compared to the control SNU16 cells, supporting the role of *claudin-1* as a tumor suppressor. NA: no tumor observed.

4.1.8.2 Reduced claudin-1 Expression Enhances Tumorigenicity

The effect of reduction of claudin-1 expression on tumorigenicity was then examined. SNU16 stable cell line with reduced level of claudin-1 was generated using the antisense DNA against claudin-1. Consistence with the observations in GIF5 and GIF14, reduction of claudin-1 enhanced tumorigenicity in nude mice (Fig. 4.13). These observations collectively show that claudin-1 has the tumor suppressive property in gastric epithelial cells, whereby its restoration helps to lower the incidence of tumor formation.

4.1.9 Claudin-1 and RUNX3 Expression in Human Gastric Cancer Samples

A total of 52 gastric cancer samples were analyzed for the expression of RUNX3 and claudin-1. Figure 4.14 shows the expression pattern of RUNX3 and claudin-1 in normal human adult gastric mucosa. Both RUNX3 and claudin-1 are expressed most strongly in chief cells and surface epithelial cells and to a lesser degree in parietal cells. RUNX3 stains the nucleus whereas claudin-1 stains at cell-cell boundaries and in the cytoplasm.

Table 4.1 and 4.2 show a summary of RUNX3 and claudin-1 expression in the 52 gastric cancer cases whereby 29 samples (55.8%) were differentiated type whereas 23 samples (44.2%) were diffuse (undifferentiated) type. RUNX3 expression that was detected in nucleus was scored as positive, whereas no expression or those in the

cytoplasm was scored as negative. Base on the results, these samples were categorized into three groups according to the expression of RUNX3 and claudin-1, whereby 15 samples (28.8%) expressed both RUNX3 and claudin-1 (Fig. 4.15A); 17 samples (32.7%) neither express RUNX3 nor claudin-1 (Fig. 4.15B); and 20 samples (38.5%) expressed only claudin-1 but not RUNX3 (Fig. 4.16).

RUNX3 was only expressed in a total of 15 samples (28.8%) and it was interesting to observe that claudin-1 was also expressed in all these cases. This suggests that when RUNX3 was present, claudin-1 was also induced. Besides, it was also interesting to note that all 32.7% of samples that stain negatively for claudin-1 was in fact in the subset of RUNX3 negative cases, indicating that loss of RUNX3 expression also inhibited the expression of claudin-1. These results collectively show that expression of claudin-1 and RUNX3 is correlated in approximately 61.5% (28.8% + 32.7%) of the gastric cancer cases.

The third group of results showed that claudin-1 was expressed in the absence of RUNX3 (38.5%). This suggested that claudin-1 was also regulated by factors other than RUNX3. However, as shown in Figure 4.16, in samples that RUNX3 was absent, claudin-1 expression level also appeared to be lower as compared to samples with RUNX3 expression. This observation was consistent throughout the three types of tissues that were analyzed, namely the poorly-differentiated, the well-differentiated and the diffuse type of gastric cancer. This suggested that RUNX3 plays a crucial role in the regulation and expression of claudin-1 in the human gastric cancer samples.

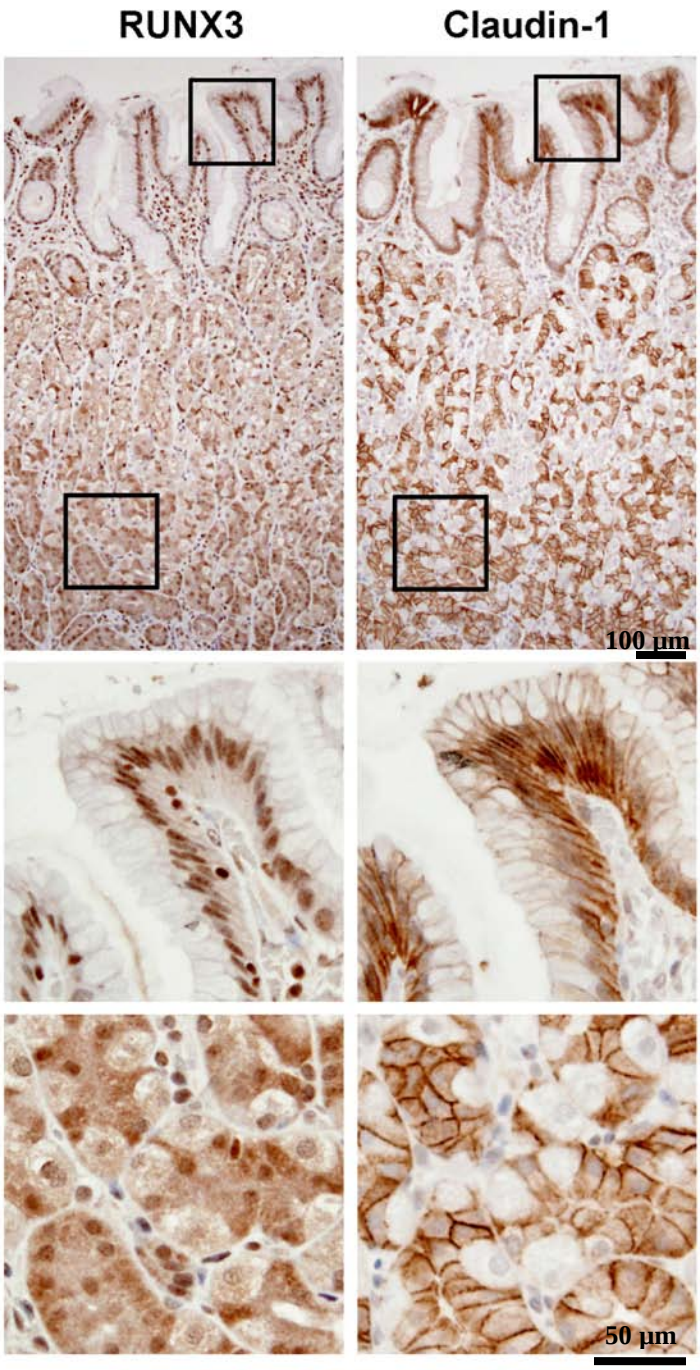

Figure 4.14: Expression pattern of claudin-1 and RUNX3 in normal human gastric sample. Both RUNX3 and claudin-1 are expressed most strongly in chief cells and surface epithelial cells and to a lesser degree in parietal cells. RUNX3 stains the nucleus whereas claudin-1 stains at cell-cell boundaries and in the cytoplasm.

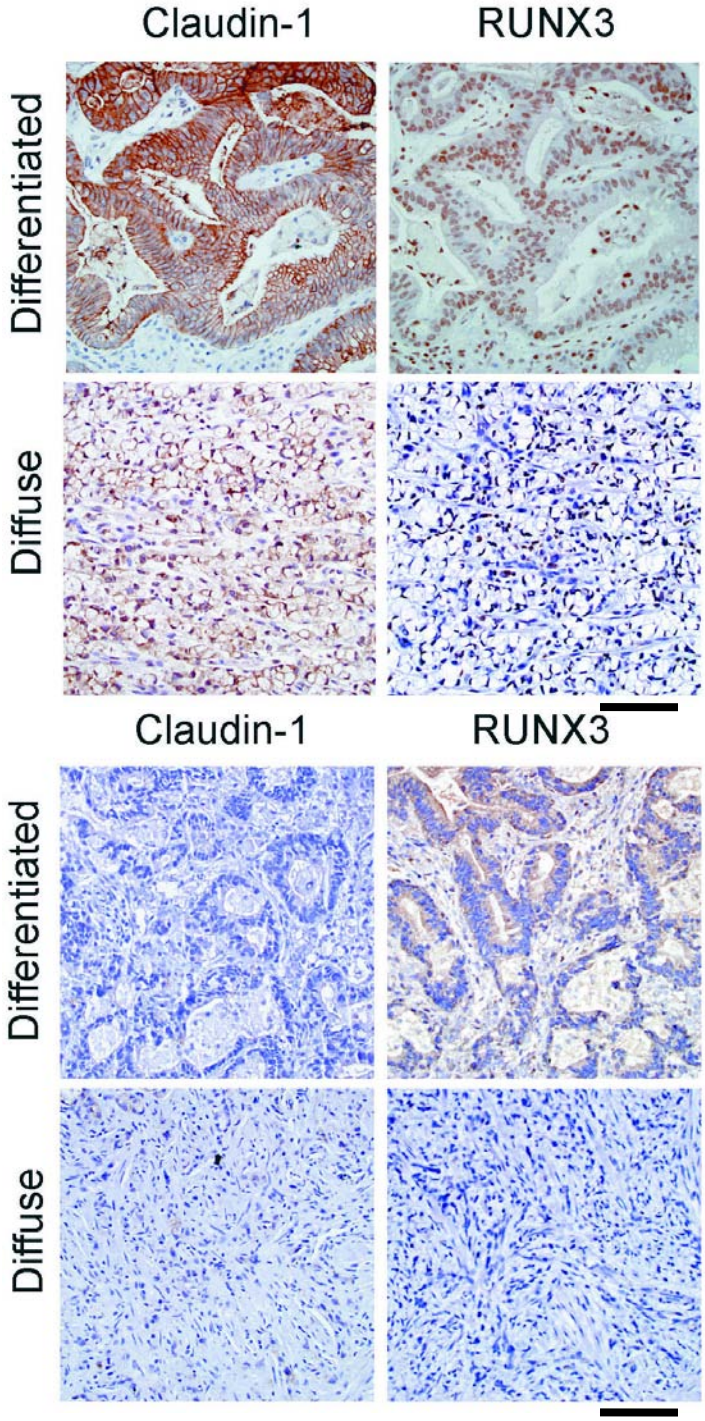

Figure 4.15: RUNX3 and claudin-1 expression pattern in differentiated and diffuse type of human gastric cancers. (A) 15 samples (28.8%) expressed both RUNX3 and claudin-1. (B) 17 samples (32.7%) did not express both RUNX3 and claudin-1. Scale bar, 100 µm.

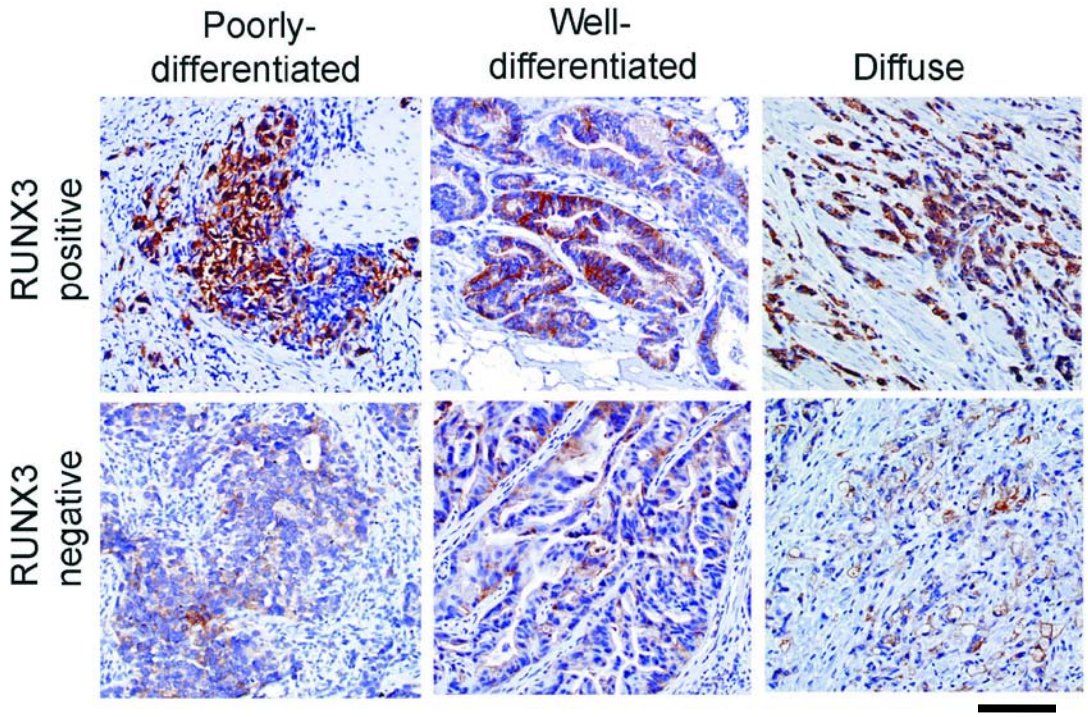

Figure 4.16: Staining pattern of claudin-1 in the RUNX3 positive and negative cases from the poorly-differentiated, well-differentiated and diffuse type of gastric cancer. A total of 38.5% cases express only claudin-1 but not RUNX3. When RUNX3 was absent, claudin-1 expression also appeared to be lower as compared to those with RUNX3 expression. This suggested that claudin-1 expression is RUNX3 dependent. Scale bar, 100 μm.

Table 4.1: RUNX3 vs claudin-1 expression in 52 gastric cancers

	Sample	Claudin-1	RUNX3		Sample	Claudin-1	RUNX3
U	GT24	N	N	U	GT53	P	P
U	GT25	N	N	D	GT54	P	N
U	GT26	P	P	D	GT55	P	N
U	GT27-1	N	N	U	GT57	P	P
U	GT27-2	N	N	D	GT61	N	N
U	GT30	P	N	U	GT63	P	N
U	GT31	N	N	D	GT64	N	N
U	GT32	N	N	U	GT67	P	N
U	GT34	N	N	D	GT69	N	N
D	GT37	N	N	D	GT71	N	N
D	GT39	N	N	D	GT73	P	N
D	GT40	P	P	U	GT76	P	P
D	GT42	P	N	U	G10	P	P
D	GT44	N	N	D	G54	P	N
U	G00104	P	N	D	G55	P	N
U	G00143	P	P	D	G84	P	N
U	G01032	P	P	D	G111	P	N
U	G01058	P	N	D	G118	P	N
D	G02005	P	N	D	G136	P	P
D	G04142	P	N	D	G148	P	N
D	G04202	P	P	D	G0102	P	P
U	G04197	P	P	D	G0155	P	N
D	GT2	N	N	U	G0158	P	P
U	GT4	N	N	D	G0182	P	N
D	GT51	N	N	U	G0204	P	P
D	GT52	P	P	D	G0250	P	N

P = positive; N = negative

U = Diffuse; D = Differentiated

^ RUNX3 negative samples included cytoplasmic positive cases

Table 4.2: RUNX3 vs claudin-1 expression in differentiated and diffuse type of gastric cancers

	RUNX3 negative, n (%)	RUNX3 positive, n (%)	Claudin-1 negative, n (%)	Claudin-1 positive, n (%)
Differentiated (n=29)	24 (83.0)	5 (17.0)	9 (31.0)	20 (69.0)
Diffuse (n=23)	13 (56.5)	10 (43.5)	8 (35.0)	15 (65.0)
Total (n=52)	37 (71.2)	15 (28.8)	17 (32.7)	35 (67.3)

4.2 Discussions

Due to the lack of cell-cell contact and polarity in *Runx3*$^{-/-}$ mice, the possible role of *RUNX3* in this function was investigated by screening several TJ proteins and the E-cadherin AJ protein to check their correlation with *RUNX3*. E-cadherin AJ molecule was included in the screen as dysfunction of E-cadherin has been a well-known cause of gastric carcinogenesis (213, 214). Results showed that *RUNX3* transcriptionally regulated the expression of claudin-1. Claudin-1 was also shown to have tumor suppressive activity. Therefore, a part of tumor suppressor activity of *RUNX3* is likely to be to positively regulate the expression of claudin-1.

Various claudin genes including *claudin-1* have been reported to play a role in gastric cancer. Recently, it was reported that diffuse type of gastric carcinomas shows lack of claudin-1 and claudin-4 expression (169). A tissue microarray study shows a lower expression of claudin-1, -3, -4 and ZO-1 in diffuse type of gastric cancer (165). Study by Lee et al. also observed that loss of claudin-4 promotes the advancement of gastric adenocarcinoma (155).

Quantitative RT-PCR method also revealed the down-regulation of claudin-18 in intestinal type of gastric cancer, which was postulated to be an early event in gastric carcinogenesis (166). Claudin-23 on the other hand, was found to be down-regulated in the intestinal type of gastric cancer (167). All these genes were hence thought to be tumor suppressor genes in gastric cancer, though their mechanisms were not clearly understood. Results using GIF and SNU16 cells however showed no

regulation of claudin-3, -4 and ZO-1 by RUNX3. RT-PCR results on SNU16 and AS SNU16 cells also did not show clear correlation between claudin-18 and -23 with RUNX3 (data not shown). It is possible that other than claudin-1, the expression of these proteins must be regulated by genes other than *RUNX3*.

Claudin-1 knockout mice confirmed its important role in maintaining the barrier integrity in the epidermis (143). The up- and down-regulation of claudin-1 expression have been well-documented in cancers. Decreased expression of claudin-1 has been linked to the induction of tumor spheroids and recurrence status in breast cancer (170, 215). On the other hand, upregulation of claudin-1 expression contributes to colorectal carcinogenesis (164, 178, 216). Overexpression of claudin-1 was also linked to the development of intestinal neoplasia (217). Two main signaling pathways have been described to regulate claudin-1 expression. The increased expression of claudin-1 in the β-catenin-Tcf / LEF signaling pathway was found to play a role in colorectal carcinogenesis (164). On the other hand, *claudin-1* was identified as a direct downstream target gene of the Snail family of transcription factors, in the MAPK pathway. In human epithelial cells and invasive human breast tumors, high levels of Snail and Slug were correlated with low levels of claudin-1 expression, indicating the Snail family transcription factors as repressors of *claudin-1* (188).

It is worth noting that a similar characteristic wrinkled skin appearance was observed in the *Runx3* knockout mice (unpublished observation) as those observed in the *claudin-1* knockout mice. The wrinkled skin appearance, a result from the loss of

epidermal barrier function, causes the *claudin-1* knockout mice to die within 1 day of birth (143). 75% of *Runx3* knockout mice died in the first day after birth, and none survived beyond 10 days. Though it was postulated that the *Runx3* knockout mice may have died from starvation (23), the precise reason was not known. It could also be possible that lost of epidermal barrier function in the skin also contributed to the death of *Runx3* knockout mice as those observed in *claudin-1* knockout mice. These observations indicated a possible correlation between *RUNX3* and *claudin-1* expression in the gastric epithelial cells which was worth investigating.

Induction of claudin-1 expression by TGF-β is regulated at transcriptional level, as confirmed by RT-PCR and western analysis. The nuclear import of transcription factors is an essential factor in many signaling pathways to allow access of transcription factors to their target genes. Transcription factors such as the signal tranducers and activators of transcription (STAT) and Smads, require receptor-mediated phosphorylation for conversion to their active state. The unstimulated forms of these proteins remain in the cytoplasm (218). Thus, transcription factors localized in the cytoplasm are thought to be in a basal, inactive state. TGF-β was recognized as the factor that stimulates nuclear translocation of RUNX3, thus switching the inactive form of RUNX3 to their active counterpart (97). This allows RUNX3 to physically bind to the promoter of their target genes, hence activating their expression, as observed in the case of claudin-1 induction upon stimulation by TGF-β.

It has been well documented that transcription factors like *Snail* and *Slug* act as repressors of claudin-1 expression in epithelial cells (188). Snail family genes are

transcription factors that play a central role in epithelial-mesenchymal transition (EMT), a process that occurs during cancer progression. During EMT, epithelial cells lose polarity. Though SNU16 cell line appeared to be unsuitable for the study of claudin-1 promoter assay in this study, it opens up new areas which could be explored to investigate possible connection between RUNX3 and Snail family transcription factor in the regulation of gastric epithelial cells. If their interaction is true, it would be interesting to observe how two antagonizing pathways could work together in the regulation and maintenance of epithelial cells.

It has been postulated that TJ functions are altered during cancer progression due to loss of claudins expression. In non-tumorigenic epithelial tissues, TJ functions to regulate the flow of solutes between cell membranes, such as growth factors and cytokines. When TJ barrier functions are interrupted, growth factors and cytokines freely penetrate from the surrounding tissue, increasing paracellular flux of growth factors, which subsequently give rise to auto- and paracrine stimulation of tumorigenic epithelial cells. This lowering of diffusion barrier leads to an improved nutrient supply and adds to the selective advantage for developing tumor cells (191).

This model could well explain the results in tumorigenicity assay using nude mice, whereby reintroduction of claudin-1 may have restored tight junction functions, thus reducing paracellular flux of growth factors, and minimizing tumorigenic epithelial cells and tumor formation. Collagen gel assay showed no reconstitution of cell polarity in GIF5 and GIF14 cells expressing exogenous claudin-1 (data not shown). Thus, the reduction of tumorigenicity could have worked through

mechanisms other than preserving the cell polarity, like the reconstitution of TJ barrier function. To confirm this, the use of electronmicroscopy technique (EM) may be needed for a detailed observation of the TJ strands.

CHAPTER 5 CONCLUSIONS AND FUTURE PERSPECTIVE

For the first time, these findings supported the unsuspected role of *RUNX3* as a tumor suppressor in gastric carcinogenesis through its direct regulation of tight junction protein, claudin-1. Claudin-1 also appears to be a tumor suppressor in the gastric system. It is also the first detailed report describing the regulation of claudin-1 by TGF-β signaling pathway. Therefore, a signaling cascade involving TGF-β, RUNX3 and claudin-1 in the tumor suppression of gastric epithelial cells is proposed.

Based on the expression pattern of RUNX3 and claudin-1 in the human gastric cancer samples, RUNX3 was either not expressed or expressed but mislocalized in the cytoplasm as an inactive form in 71.2% (37/52) of the cases. RUNX3 negative cases were especially high (83%) in the differentiated type of gastric cancer. As such, RUNX3 is highly suitable to be used as a marker for diagnostic purposes. Claudin-1 was either not expressed (32.7%) or expressed at a minimal level (38.5%) in the human gastric cancer samples. Although its expression pattern correlated with the expression of RUNX3, usage of claudin-1 alone as a diagnostic marker is deemed not sufficient.

Unlike the staining pattern of RUNX3 which is easier to determine (in nucleus or cytoplasm), the claudin-1 expression level in the positive cases (high or low) may be harder to be determined by eye, unless a fixed parameter is utilized through the use of a software. Even then, a positive reference or normal tissue counterpart need to be tested alongside each time a sample is to be tested for claudin-1 expression. As

availability of normal tissue counterpart may not be feasible all the time, plus the fact that the expression level of claudin-1 may vary in between tissue samples, comparison of claudin-1 expression level in each patient tissue can become daunting and less accurate. Thus, it will be more meaningful to carry out RUNX3 and claudin-1 expression at the same time for diagnosis purposes. With this, markers with better diagnostic value may be developed through the use of RUNX3 and claudin-1.

REFERENCES

1. Parkin DM, Bray F, Ferlay J, Pisani P. Global cancer statistics, 2002. CA Cancer J Clin 2005; 55: 74-108.

2. Terry MB, Gaudet MM, Gammon MD. The epidemiology of gastric cancer. Semin Radiat Oncol 2002; 12: 111-27.

3. Correa P. Human gastric carcinogenesis: a multistep and multifactorial process--First American Cancer Society Award Lecture on Cancer Epidemiology and Prevention. Cancer Res 1992; 52: 6735-40.

4. Meining A, Morgner A, Miehlke S, Bayerdorffer E, Stolte M. Atrophy-metaplasia-dysplasia-carcinoma sequence in the stomach: a reality or merely an hypothesis? Best Pract Res Clin Gastroenterol 2001; 15: 983-98.

5. Leung SY, Yuen ST, Chung LP, Chu KM, Chan AS, Ho JC. hMLH1 promoter methylation and lack of hMLH1 expression in sporadic gastric carcinomas with high-frequency microsatellite instability. Cancer Res 1999; 59: 159-64.

6. Jung HY, Jung KC, Shim YH, Ro JY, Kang GH. Methylation of the hMLH1 promoter in multiple gastric carcinomas with microsatellite instability. Pathol Int 2001; 51: 445-51.

7. El-Rifai W, Powell SM. Molecular biology of gastric cancer. Semin Radiat Oncol 2002; 12: 128-40.

8. Hayden JD, Martin IG, Cawkwell L, Quirke P. The role of microsatellite instability in gastric carcinoma. Gut 1998; 42: 300-3.

9. Miyoshi E, Haruma K, Hiyama T, et al. Microsatellite instability is a genetic marker for the development of multiple gastric cancers. Int J Cancer 2001; 95: 350-3.

10. Bishop JM. Cancer genes come of age. Cell 1983; 32: 1018-20.

11. Nishizuka S, Tamura G, Terashima M, Satodate R. Loss of heterozygosity during the development and progression of differentiated adenocarcinoma of the stomach. J Pathol 1998; 185: 38-43.

12. Nishizuka S, Tamura G, Terashima M, Satodate R. Commonly deleted region on the long arm of chromosome 7 in differentiated adenocarcinoma of the stomach. Br J Cancer 1997; 76: 1567-71.

13. Sakata K, Tamura G, Nishizuka S, et al. Commonly deleted regions on the long arm of chromosome 21 in differentiated adenocarcinoma of the stomach. Genes Chromosomes Cancer 1997; 18: 318-21.

14. Sano T, Tsujino T, Yoshida K, et al. Frequent loss of heterozygosity on chromosomes 1q, 5q, and 17p in human gastric carcinomas. Cancer Res 1991; 51: 2926-31.

15. Jones PA, Laird PW. Cancer epigenetics comes of age. Nat Genet 1999; 21: 163-7.

16. Teitz T, Wei T, Valentine MB, et al. Caspase 8 is deleted or silenced preferentially in childhood neuroblastomas with amplification of MYCN. Nat Med 2000; 6: 529-35.

17. Brown R, Strathdee G. Epigenomics and epigenetic therapy of cancer. Trends Mol Med 2002; 8: S43-8.

18. Carneiro F, Sobrinho-Simoes M. The prognostic significance of amplification and overexpression of c-met and c-erb B-2 in human gastric carcinomas. Cancer 2000; 88: 238-40.

19. Ross JS, McKenna BJ. The HER-2/neu oncogene in tumors of the gastrointestinal tract. Cancer Invest 2001; 19: 554-68.

20. Mizutani T, Onda M, Tokunaga A, Yamanaka N, Sugisaki Y. Relationship of C-erbB-2 protein expression and gene amplification to invasion and metastasis in human gastric cancer. Cancer 1993; 72: 2083-8.

21. Yu J, Miehlke S, Ebert MP, et al. Expression of cyclin genes in human gastric cancer and in first degree relatives. Chin Med J (Engl) 2002; 115: 710-5.

22. Kozma L, Kiss I, Hajdu J, Szentkereszty Z, Szakall S, Ember I. C-myc amplification and cluster analysis in human gastric carcinoma. Anticancer Res 2001; 21: 707-10.

23. Li QL, Ito K, Sakakura C, et al. Causal relationship between the loss of RUNX3 expression and gastric cancer. Cell 2002; 109: 113-24.

24. Huang G, Shigesada K, Ito K, Wee HJ, Yokomizo T, Ito Y. Dimerization with PEBP2beta protects RUNX1/AML1 from ubiquitin-proteasome-mediated degradation. EMBO J 2001; 20: 723-33.

25. Perry C, Eldor A, Soreq H. Runx1/AML1 in leukemia: disrupted association with diverse protein partners. Leuk Res 2002; 26: 221-8.

26. Kagoshima H, Shigesada K, Satake M, et al. The Runt domain identifies a new family of heteromeric transcriptional regulators. Trends Genet 1993; 9: 338-41.

27. Bae SC, Takahashi E, Zhang YW, et al. Cloning, mapping and expression of PEBP2 alpha C, a third gene encoding the mammalian Runt domain. Gene 1995; 159: 245-8.

28. Downing JR. The AML1-ETO chimaeric transcription factor in acute myeloid leukaemia: biology and clinical significance. Br J Haematol 1999; 106: 296-308.

29. Ito Y. Molecular basis of tissue-specific gene expression mediated by the runt domain transcription factor PEBP2/CBF. Genes Cells 1999; 4: 685-96.

30. Okuda T, van Deursen J, Hiebert SW, Grosveld G, Downing JR. AML1, the target of multiple chromosomal translocations in human leukemia, is essential for normal fetal liver hematopoiesis. Cell 1996; 84: 321-30.

31. Wang Q, Stacy T, Binder M, Marin-Padilla M, Sharpe AH, Speck NA. Disruption of the Cbfa2 gene causes necrosis and hemorrhaging in the central nervous system and blocks definitive hematopoiesis. Proc Natl Acad Sci U S A 1996; 93: 3444-9.

32. Komori T, Yagi H, Nomura S, et al. Targeted disruption of Cbfa1 results in a complete lack of bone formation owing to maturational arrest of osteoblasts. Cell 1997; 89: 755-64.

33. Otto F, Thornell AP, Crompton T, et al. Cbfa1, a candidate gene for cleidocranial dysplasia syndrome, is essential for osteoblast differentiation and bone development. Cell 1997; 89: 765-71.

34. Daga A, Karlovich CA, Dumstrei K, Banerjee U. Patterning of cells in the Drosophila eye by Lozenge, which shares homologous domains with AML1. Genes Dev 1996; 10: 1194-205.

35. Kania MA, Bonner AS, Duffy JB, Gergen JP. The Drosophila segmentation gene runt encodes a novel nuclear regulatory protein that is also expressed in the developing nervous system. Genes Dev 1990; 4: 1701-13.

36. Rennert J, Coffman JA, Mushegian AR, Robertson AJ. The evolution of Runx genes I. A comparative study of sequences from phylogenetically diverse model organisms. BMC Evol Biol 2003; 3: 4.

37. Coffman JA, Kirchhamer CV, Harrington MG, Davidson EH. SpRunt-1, a new member of the runt domain family of transcription factors, is a positive regulator of the aboral ectoderm-specific CyIIIA gene in sea urchin embryos. Dev Biol 1996; 174: 43-54.

38. Tracey WD, Jr., Pepling ME, Horb ME, Thomsen GH, Gergen JP. A Xenopus homologue of aml-1 reveals unexpected patterning mechanisms leading to the formation of embryonic blood. Development 1998; 125: 1371-80.

39. Burns CE, DeBlasio T, Zhou Y, Zhang J, Zon L, Nimer SD. Isolation and characterization of runxa and runxb, zebrafish members of the runt family of transcriptional regulators. Exp Hematol 2002; 30: 1381-9.

40. Crosier PS, Kalev-Zylinska ML, Hall CJ, Flores MV, Horsfield JA, Crosier KE. Pathways in blood and vessel development revealed through zebrafish genetics. Int J Dev Biol 2002; 46: 493-502.

41. Kataoka H, Ochi M, Enomoto K, Yamaguchi A. Cloning and embryonic expression patterns of the zebrafish Runt domain genes, runxa and runxb. Mech Dev 2000; 98: 139-43.

42. Nam S, Jin YH, Li QL, et al. Expression pattern, regulation, and biological role of runt domain transcription factor, run, in Caenorhabditis elegans. Mol Cell Biol 2002; 22: 547-54.

43. Ito Y. RUNX genes in development and cancer: regulation of viral gene expression and the discovery of RUNX family genes. Adv Cancer Res 2008; 99: 33-76.

44. Kagoshima H, Shigesada K, Kohara Y. RUNX regulates stem cell proliferation and differentiation: insights from studies of C. elegans. J Cell Biochem 2007; 100: 1119-30.

45. Speck NA, Gilliland DG. Core-binding factors in haematopoiesis and leukaemia. Nat Rev Cancer 2002; 2: 502-13.

46. Song WJ, Sullivan MG, Legare RD, et al. Haploinsufficiency of CBFA2 causes familial thrombocytopenia with propensity to develop acute myelogenous leukaemia. Nat Genet 1999; 23: 166-75.

47. Osato M. Point mutations in the RUNX1/AML1 gene: another actor in RUNX leukemia. Oncogene 2004; 23: 4284-96.

48. Osato M, Asou N, Abdalla E, et al. Biallelic and heterozygous point mutations in the runt domain of the AML1/PEBP2alphaB gene associated with myeloblastic leukemias. Blood 1999; 93: 1817-24.

49. Prokunina L, Castillejo-Lopez C, Oberg F, et al. A regulatory polymorphism in PDCD1 is associated with susceptibility to systemic lupus erythematosus in humans. Nat Genet 2002; 32: 666-9.

50. Tokuhiro S, Yamada R, Chang X, et al. An intronic SNP in a RUNX1 binding site of SLC22A4, encoding an organic cation transporter, is associated with rheumatoid arthritis. Nat Genet 2003; 35: 341-8.

51. North T, Gu TL, Stacy T, et al. Cbfa2 is required for the formation of intra-aortic hematopoietic clusters. Development 1999; 126: 2563-75.

52. Yokomizo T, Ogawa M, Osato M, et al. Requirement of Runx1/AML1/PEBP2alphaB for the generation of haematopoietic cells from endothelial cells. Genes Cells 2001; 6: 13-23.

53. Lee B, Thirunavukkarasu K, Zhou L, et al. Missense mutations abolishing DNA binding of the osteoblast-specific transcription factor OSF2/CBFA1 in cleidocranial dysplasia. Nat Genet 1997; 16: 307-10.

54. Mundlos S, Otto F, Mundlos C, et al. Mutations involving the transcription factor CBFA1 cause cleidocranial dysplasia. Cell 1997; 89: 773-9.

55. Stewart M, Terry A, Hu M, et al. Proviral insertions induce the expression of bone-specific isoforms of PEBP2alphaA (CBFA1): evidence for a new myc collaborating oncogene. Proc Natl Acad Sci U S A 1997; 94: 8646-51.

56. Taniuchi I, Osato M, Egawa T, et al. Differential requirements for Runx proteins in CD4 repression and epigenetic silencing during T lymphocyte development. Cell 2002; 111: 621-33.

57. Woolf E, Xiao C, Fainaru O, et al. Runx3 and Runx1 are required for CD8 T cell development during thymopoiesis. Proc Natl Acad Sci U S A 2003; 100: 7731-6.

58. Fainaru O, Woolf E, Lotem J, et al. Runx3 regulates mouse TGF-beta-mediated dendritic cell function and its absence results in airway inflammation. EMBO J 2004; 23: 969-79.

59. Inoue K, Ozaki S, Shiga T, et al. Runx3 controls the axonal projection of proprioceptive dorsal root ganglion neurons. Nat Neurosci 2002; 5: 946-54.

60. Levanon D, Bettoun D, Harris-Cerruti C, et al. The Runx3 transcription factor regulates development and survival of TrkC dorsal root ganglia neurons. EMBO J 2002; 21: 3454-63.

61. Goel A, Arnold CN, Tassone P, et al. Epigenetic inactivation of RUNX3 in microsatellite unstable sporadic colon cancers. Int J Cancer 2004; 112: 754-9.

62. Kang GH, Lee S, Lee HJ, Hwang KS. Aberrant CpG island hypermethylation of multiple genes in prostate cancer and prostatic intraepithelial neoplasia. J Pathol 2004; 202: 233-40.

63. Kang S, Kim JW, Kang GH, et al. Polymorphism in folate- and methionine-metabolizing enzyme and aberrant CpG island hypermethylation in uterine cervical cancer. Gynecol Oncol 2005; 96: 173-80.

64. Kato N, Tamura G, Fukase M, Shibuya H, Motoyama T. Hypermethylation of the RUNX3 gene promoter in testicular yolk sac tumor of infants. Am J Pathol 2003; 163: 387-91.

65. Kim TY, Lee HJ, Hwang KS, et al. Methylation of RUNX3 in various types of human cancers and premalignant stages of gastric carcinoma. Lab Invest 2004; 84: 479-84.

66. Li QL, Kim HR, Kim WJ, et al. Transcriptional silencing of the RUNX3 gene by CpG hypermethylation is associated with lung cancer. Biochem Biophys Res Commun 2004; 314: 223-8.

67. Mori T, Nomoto S, Koshikawa K, et al. Decreased expression and frequent allelic inactivation of the RUNX3 gene at 1p36 in human hepatocellular carcinoma. Liver Int 2005; 25: 380-8.

68. Nakase Y, Sakakura C, Miyagawa K, et al. Frequent loss of RUNX3 gene expression in remnant stomach cancer and adjacent mucosa with special reference to topography. Br J Cancer 2005; 92: 562-9.

69. Oshimo Y, Oue N, Mitani Y, et al. Frequent loss of RUNX3 expression by promoter hypermethylation in gastric carcinoma. Pathobiology 2004; 71: 137-43.

70. Sakakura C, Hagiwara A, Miyagawa K, et al. Frequent downregulation of the runt domain transcription factors RUNX1, RUNX3 and their cofactor CBFB in gastric cancer. Int J Cancer 2005; 113: 221-8.

71. Schulmann K, Sterian A, Berki A, et al. Inactivation of p16, RUNX3, and HPP1 occurs early in Barrett's-associated neoplastic progression and predicts progression risk. Oncogene 2005; 24: 4138-48.

72. Tamura G. Promoter methylation status of tumor suppressor and tumor-related genes in neoplastic and non-neoplastic gastric epithelia. Histol Histopathol 2004; 19: 221-8.

73. Wada M, Yazumi S, Takaishi S, et al. Frequent loss of RUNX3 gene expression in human bile duct and pancreatic cancer cell lines. Oncogene 2004; 23: 2401-7.

74. Xiao WH, Liu WW. Hemizygous deletion and hypermethylation of RUNX3 gene in hepatocellular carcinoma. World J Gastroenterol 2004; 10: 376-80.

75. Yanagawa N, Tamura G, Oizumi H, Takahashi N, Shimazaki Y, Motoyama T. Promoter hypermethylation of tumor suppressor and tumor-related genes in non-small cell lung cancers. Cancer Sci 2003; 94: 589-92.

76. Blobe GC, Schiemann WP, Lodish HF. Role of transforming growth factor beta in human disease. N Engl J Med 2000; 342: 1350-8.

77. Massague J, Blain SW, Lo RS. TGFbeta signaling in growth control, cancer, and heritable disorders. Cell 2000; 103: 295-309.

78. Derynck R, Akhurst RJ, Balmain A. TGF-beta signaling in tumor suppression and cancer progression. Nat Genet 2001; 29: 117-29.

79. Wakefield LM, Roberts AB. TGF-beta signaling: positive and negative effects on tumorigenesis. Curr Opin Genet Dev 2002; 12: 22-9.

80. Tang B, Bottinger EP, Jakowlew SB, et al. Transforming growth factor-beta1 is a new form of tumor suppressor with true haploid insufficiency. Nat Med 1998; 4: 802-7.

81. Shull MM, Ormsby I, Kier AB, et al. Targeted disruption of the mouse transforming growth factor-beta 1 gene results in multifocal inflammatory disease. Nature 1992; 359: 693-9.

82. Hanai J, Chen LF, Kanno T, et al. Interaction and functional cooperation of PEBP2/CBF with Smads. Synergistic induction of the immunoglobulin germline Calpha promoter. J Biol Chem 1999; 274: 31577-82.

83. Alliston T, Choy L, Ducy P, Karsenty G, Derynck R. TGF-beta-induced repression of CBFA1 by Smad3 decreases cbfa1 and osteocalcin expression and inhibits osteoblast differentiation. EMBO J 2001; 20: 2254-72.

84. Shi Y, Massague J. Mechanisms of TGF-beta signaling from cell membrane to the nucleus. Cell 2003; 113: 685-700.

85. Muraoka M, Konishi M, Kikuchi-Yanoshita R, et al. p300 gene alterations in colorectal and gastric carcinomas. Oncogene 1996; 12: 1565-9.

86. Gayther SA, Batley SJ, Linger L, et al. Mutations truncating the EP300 acetylase in human cancers. Nat Genet 2000; 24: 300-3.

87. Suganuma T, Kawabata M, Ohshima T, Ikeda MA. Growth suppression of human carcinoma cells by reintroduction of the p300 coactivator. Proc Natl Acad Sci U S A 2002; 99: 13073-8.

88. Ito Y. Oncogenic potential of the RUNX gene family: 'overview'. Oncogene 2004; 23: 4198-208.

89. Bangsow C, Rubins N, Glusman G, et al. The RUNX3 gene--sequence, structure and regulated expression. Gene 2001; 279: 221-32.

90. Robertson AJ, Dickey CE, McCarthy JJ, Coffman JA. The expression of SpRunt during sea urchin embryogenesis. Mech Dev 2002; 117: 327-30.

91. Weith A, Brodeur GM, Bruns GA, et al. Report of the second international workshop on human chromosome 1 mapping 1995. Cytogenet Cell Genet 1996; 72: 114-44.

92. Guo WH, Weng LQ, Ito K, et al. Inhibition of growth of mouse gastric cancer cells by Runx3, a novel tumor suppressor. Oncogene 2002; 21: 8351-5.

93. Fukamachi H, Ito K. Growth regulation of gastric epithelial cells by Runx3. Oncogene 2004; 23: 4330-5.

94. Fukamachi H. Runx3 controls growth and differentiation of gastric epithelial cells in mammals. Dev Growth Differ 2006; 48: 1-13.

95. Fukamachi H, Ito K, Ito Y. Runx3-/- gastric epithelial cells differentiate into intestinal type cells. Biochem Biophys Res Commun 2004; 321: 58-64.

96. Furihata C, Tatematsu M, Saito M, et al. Rare occurrence of ras and p53 gene mutations in mouse stomach tumors induced by N-methyl-N-nitrosourea. Jpn J Cancer Res 1997; 88: 363-8.

97. Ito K, Liu Q, Salto-Tellez M, et al. RUNX3, a novel tumor suppressor, is frequently inactivated in gastric cancer by protein mislocalization. Cancer Res 2005; 65: 7743-50.

98. Wei D, Gong W, Oh SC, et al. Loss of RUNX3 expression significantly affects the clinical outcome of gastric cancer patients and its restoration causes drastic suppression of tumor growth and metastasis. Cancer Res 2005; 65: 4809-16.

99. Miyazono K, Maeda S, Imamura T. Coordinate regulation of cell growth and differentiation by TGF-beta superfamily and Runx proteins. Oncogene 2004; 23: 4232-7.

100. Ito Y, Miyazono K. RUNX transcription factors as key targets of TGF-beta superfamily signaling. Curr Opin Genet Dev 2003; 13: 43-7.

101. Schuster N, Krieglstein K. Mechanisms of TGF-beta-mediated apoptosis. Cell Tissue Res 2002; 307: 1-14.

102. Atfi A, Buisine M, Mazars A, Gespach C. Induction of apoptosis by DPC4, a transcriptional factor regulated by transforming growth factor-beta through stress-activated protein kinase/c-Jun N-terminal kinase (SAPK/JNK) signaling pathway. J Biol Chem 1997; 272: 24731-4.

103. Yamamura Y, Hua X, Bergelson S, Lodish HF. Critical role of Smads and AP-1 complex in transforming growth factor-beta -dependent apoptosis. J Biol Chem 2000; 275: 36295-302.

104. Teramoto T, Kiss A, Thorgeirsson SS. Induction of p53 and Bax during TGF-beta 1 initiated apoptosis in rat liver epithelial cells. Biochem Biophys Res Commun 1998; 251: 56-60.

105. Chalaux E, Lopez-Rovira T, Rosa JL, et al. A zinc-finger transcription factor induced by TGF-beta promotes apoptotic cell death in epithelial Mv1Lu cells. FEBS Lett 1999; 457: 478-82.

106. Chipuk JE, Bhat M, Hsing AY, Ma J, Danielpour D. Bcl-xL blocks transforming growth factor-beta 1-induced apoptosis by inhibiting cytochrome c release and not by directly antagonizing Apaf-1-dependent caspase activation in prostate epithelial cells. J Biol Chem 2001; 276: 26614-21.

107. Yano T, Ito K, Fukamachi H, et al. The RUNX3 tumor suppressor upregulates Bim in gastric epithelial cells undergoing transforming growth factor beta-induced apoptosis. Mol Cell Biol 2006; 26: 4474-88.

108. Alexandrow MG, Moses HL. Transforming growth factor beta and cell cycle regulation. Cancer Res 1995; 55: 1452-7.

109. Chi XZ, Yang JO, Lee KY, et al. RUNX3 suppresses gastric epithelial cell growth by inducing p21(WAF1/Cip1) expression in cooperation with transforming growth factor {beta}-activated SMAD. Mol Cell Biol 2005; 25: 8097-107.

110. Mitic LL, Anderson JM. Molecular architecture of tight junctions. Annu Rev Physiol 1998; 60: 121-42.

111. Schneeberger EE, Lynch RD. Structure, function, and regulation of cellular tight junctions. Am J Physiol 1992; 262: L647-61.

112. Gonzalez-Mariscal L, Nava P. Tight junctions, from tight intercellular seals to sophisticated protein complexes involved in drug delivery, pathogens interaction and cell proliferation. Adv Drug Deliv Rev 2005; 57: 811-4.

113. Mitic LL, Van Itallie CM, Anderson JM. Molecular physiology and pathophysiology of tight junctions I. Tight junction structure and function: lessons from mutant animals and proteins. Am J Physiol Gastrointest Liver Physiol 2000; 279: G250-4.

114. Lechner F, Sahrbacher U, Suter T, et al. Antibodies to the junctional adhesion molecule cause disruption of endothelial cells and do not prevent leukocyte influx into the meninges after viral or bacterial infection. J Infect Dis 2000; 182: 978-82.

115. Gow A, Southwood CM, Li JS, et al. CNS myelin and sertoli cell tight junction strands are absent in Osp/claudin-11 null mice. Cell 1999; 99: 649-59.

116. Baechner D, Liehr T, Hameister H, et al. Widespread expression of the peripheral myelin protein-22 gene (PMP22) in neural and non-neural tissues during murine development. J Neurosci Res 1995; 42: 733-41.

117. Martin-Padura I, Lostaglio S, Schneemann M, et al. Junctional adhesion molecule, a novel member of the immunoglobulin superfamily that distributes at intercellular junctions and modulates monocyte transmigration. J Cell Biol 1998; 142: 117-27.

118. Stevenson BR, Siliciano JD, Mooseker MS, Goodenough DA. Identification of ZO-1: a high molecular weight polypeptide associated with the tight junction (zonula occludens) in a variety of epithelia. J Cell Biol 1986; 103: 755-66.

119. Jesaitis LA, Goodenough DA. Molecular characterization and tissue distribution of ZO-2, a tight junction protein homologous to ZO-1 and the Drosophila discs-large tumor suppressor protein. J Cell Biol 1994; 124: 949-61.

120. Haskins J, Gu L, Wittchen ES, Hibbard J, Stevenson BR. ZO-3, a novel member of the MAGUK protein family found at the tight junction, interacts with ZO-1 and occludin. J Cell Biol 1998; 141: 199-208.

121. Bowerman B, Ingram MK, Hunter CP. The maternal par genes and the segregation of cell fate specification activities in early Caenorhabditis elegans embryos. Development 1997; 124: 3815-26.

122. Ebnet K, Suzuki A, Horikoshi Y, et al. The cell polarity protein ASIP/PAR-3 directly associates with junctional adhesion molecule (JAM). EMBO J 2001; 20: 3738-48.

123. Guo S, Kemphues KJ. A non-muscle myosin required for embryonic polarity in Caenorhabditis elegans. Nature 1996; 382: 455-8.

124. Hamazaki Y, Itoh M, Sasaki H, Furuse M, Tsukita S. Multi-PDZ domain protein 1 (MUPP1) is concentrated at tight junctions through its possible interaction with claudin-1 and junctional adhesion molecule. J Biol Chem 2002; 277: 455-61.

125. Yamamoto T, Harada N, Kano K, et al. The Ras target AF-6 interacts with ZO-1 and serves as a peripheral component of tight junctions in epithelial cells. J Cell Biol 1997; 139: 785-95.

126. Mandai K, Nakanishi H, Satoh A, et al. Afadin: A novel actin filament-binding protein with one PDZ domain localized at cadherin-based cell-to-cell adherens junction. J Cell Biol 1997; 139: 517-28.

127. Citi S, Sabanay H, Jakes R, Geiger B, Kendrick-Jones J. Cingulin, a new peripheral component of tight junctions. Nature 1988; 333: 272-6.

128. Keon BH, Schafer S, Kuhn C, Grund C, Franke WW. Symplekin, a novel type of tight junction plaque protein. J Cell Biol 1996; 134: 1003-18.

129. Briehl MM, Miesfeld RL. Isolation and characterization of transcripts induced by androgen withdrawal and apoptotic cell death in the rat ventral prostate. Mol Endocrinol 1991; 5: 1381-8.

130. Katahira J, Inoue N, Horiguchi Y, Matsuda M, Sugimoto N. Molecular cloning and functional characterization of the receptor for Clostridium perfringens enterotoxin. J Cell Biol 1997; 136: 1239-47.

131. Katahira J, Sugiyama H, Inoue N, Horiguchi Y, Matsuda M, Sugimoto N. Clostridium perfringens enterotoxin utilizes two structurally related membrane proteins as functional receptors in vivo. J Biol Chem 1997; 272: 26652-8.

132. Bronstein JM, Popper P, Micevych PE, Farber DB. Isolation and characterization of a novel oligodendrocyte-specific protein. Neurology 1996; 47: 772-8.

133. Morita K, Sasaki H, Fujimoto K, Furuse M, Tsukita S. Claudin-11/OSP-based tight junctions of myelin sheaths in brain and Sertoli cells in testis. J Cell Biol 1999; 145: 579-88.

134. Furuse M, Fujita K, Hiiragi T, Fujimoto K, Tsukita S. Claudin-1 and -2: novel integral membrane proteins localizing at tight junctions with no sequence similarity to occludin. J Cell Biol 1998; 141: 1539-50.

135. Morita K, Furuse M, Fujimoto K, Tsukita S. Claudin multigene family encoding four-transmembrane domain protein components of tight junction strands. Proc Natl Acad Sci U S A 1999; 96: 511-6.

136. Van Itallie CM, Anderson JM. Claudins and epithelial paracellular transport. Annu Rev Physiol 2006; 68: 403-29.

137. Asano A, Asano K, Sasaki H, Furuse M, Tsukita S. Claudins in Caenorhabditis elegans: their distribution and barrier function in the epithelium. Curr Biol 2003; 13: 1042-6.

138. Behr M, Riedel D, Schuh R. The claudin-like megatrachea is essential in septate junctions for the epithelial barrier function in Drosophila. Dev Cell 2003; 5: 611-20.

139. Heiskala M, Peterson PA, Yang Y. The roles of claudin superfamily proteins in paracellular transport. Traffic 2001; 2: 93-8.

140. Loh YH, Christoffels A, Brenner S, Hunziker W, Venkatesh B. Extensive expansion of the claudin gene family in the teleost fish, Fugu rubripes. Genome Res 2004; 14: 1248-57.

141. Furuse M, Sasaki H, Tsukita S. Manner of interaction of heterogeneous claudin species within and between tight junction strands. J Cell Biol 1999; 147: 891-903.

142. Furuse M, Tsukita S. Claudins in occluding junctions of humans and flies. Trends Cell Biol 2006; 16: 181-8.

143. Furuse M, Hata M, Furuse K, et al. Claudin-based tight junctions are crucial for the mammalian epidermal barrier: a lesson from claudin-1-deficient mice. J Cell Biol 2002; 156: 1099-111.

144. Hoevel T, Macek R, Mundigl O, Swisshelm K, Kubbies M. Expression and targeting of the tight junction protein CLDN1 in CLDN1-negative human breast tumor cells. J Cell Physiol 2002; 191: 60-8.

145. Tepass U. Claudin complexities at the apical junctional complex. Nat Cell Biol 2003; 5: 595-7.

146. Tsukita S, Furuse M. The structure and function of claudins, cell adhesion molecules at tight junctions. Ann N Y Acad Sci 2000; 915: 129-35.

147. Tsukita S, Furuse M. Claudin-based barrier in simple and stratified cellular sheets. Curr Opin Cell Biol 2002; 14: 531-6.

148. Tanaka M, Kamata R, Sakai R. EphA2 phosphorylates the cytoplasmic tail of Claudin-4 and mediates paracellular permeability. J Biol Chem 2005; 280: 42375-82.

149. D'Souza T, Agarwal R, Morin PJ. Phosphorylation of claudin-3 at threonine 192 by cAMP-dependent protein kinase regulates tight junction barrier function in ovarian cancer cells. J Biol Chem 2005; 280: 26233-40.

150. Itoh M, Furuse M, Morita K, Kubota K, Saitou M, Tsukita S. Direct binding of three tight junction-associated MAGUKs, ZO-1, ZO-2, and ZO-3, with the COOH termini of claudins. J Cell Biol 1999; 147: 1351-63.

151. Cordenonsi M, D'Atri F, Hammar E, et al. Cingulin contains globular and coiled-coil domains and interacts with ZO-1, ZO-2, ZO-3, and myosin. J Cell Biol 1999; 147: 1569-82.

152. Bazzoni G, Martinez-Estrada OM, Orsenigo F, Cordenonsi M, Citi S, Dejana E. Interaction of junctional adhesion molecule with the tight junction components ZO-1, cingulin, and occludin. J Biol Chem 2000; 275: 20520-6.

153. Fanning AS, Jameson BJ, Jesaitis LA, Anderson JM. The tight junction protein ZO-1 establishes a link between the transmembrane protein occludin and the actin cytoskeleton. J Biol Chem 1998; 273: 29745-53.

154. Hewitt KJ, Agarwal R, Morin PJ. The claudin gene family: expression in normal and neoplastic tissues. BMC Cancer 2006; 6: 186.

155. Lee SK, Moon J, Park SW, Song SY, Chung JB, Kang JK. Loss of the tight junction protein claudin 4 correlates with histological growth-pattern and differentiation in advanced gastric adenocarcinoma. Oncol Rep 2005; 13: 193-9.

156. Kramer F, White K, Kubbies M, Swisshelm K, Weber BH. Genomic organization of claudin-1 and its assessment in hereditary and sporadic breast cancer. Hum Genet 2000; 107: 249-56.

157. Resnick MB, Konkin T, Routhier J, Sabo E, Pricolo VE. Claudin-1 is a strong prognostic indicator in stage II colonic cancer: a tissue microarray study. Mod Pathol 2005; 18: 511-8.

158. Kominsky SL, Argani P, Korz D, et al. Loss of the tight junction protein claudin-7 correlates with histological grade in both ductal carcinoma in situ and invasive ductal carcinoma of the breast. Oncogene 2003; 22: 2021-33.

159. Long H, Crean CD, Lee WH, Cummings OW, Gabig TG. Expression of Clostridium perfringens enterotoxin receptors claudin-3 and claudin-4 in prostate cancer epithelium. Cancer Res 2001; 61: 7878-81.

160. Ikenouchi J, Matsuda M, Furuse M, Tsukita S. Regulation of tight junctions during the epithelium-mesenchyme transition: direct repression of the gene expression of claudins/occludin by Snail. J Cell Sci 2003; 116: 1959-67.

161. Medici D, Hay ED, Goodenough DA. Cooperation between snail and LEF-1 transcription factors is essential for TGF-beta1-induced epithelial-mesenchymal transition. Mol Biol Cell 2006; 17: 1871-9.

162. Mima S, Tsutsumi S, Ushijima H, et al. Induction of claudin-4 by nonsteroidal anti-inflammatory drugs and its contribution to their chemopreventive effect. Cancer Res 2005; 65: 1868-76.

163. Michl P, Barth C, Buchholz M, et al. Claudin-4 expression decreases invasiveness and metastatic potential of pancreatic cancer. Cancer Res 2003; 63: 6265-71.

164. Miwa N, Furuse M, Tsukita S, Niikawa N, Nakamura Y, Furukawa Y. Involvement of claudin-1 in the beta-catenin/Tcf signaling pathway and its frequent upregulation in human colorectal cancers. Oncol Res 2001; 12: 469-76.

165. Resnick MB, Gavilanez M, Newton E, et al. Claudin expression in gastric adenocarcinomas: a tissue microarray study with prognostic correlation. Hum Pathol 2005; 36: 886-92.

166. Sanada Y, Oue N, Mitani Y, Yoshida K, Nakayama H, Yasui W. Down-regulation of the claudin-18 gene, identified through serial analysis of gene expression data analysis, in gastric cancer with an intestinal phenotype. J Pathol 2006; 208: 633-42.

167. Katoh M, Katoh M. CLDN23 gene, frequently down-regulated in intestinal-type gastric cancer, is a novel member of CLAUDIN gene family. Int J Mol Med 2003; 11: 683-9.

168. Johnson AH, Frierson HF, Zaika A, et al. Expression of tight-junction protein claudin-7 is an early event in gastric tumorigenesis. Am J Pathol 2005; 167: 577-84.

169. Soini Y. Expression of claudins 1, 2, 3, 4, 5 and 7 in various types of tumours. Histopathology 2005; 46: 551-60.

170. Morohashi S, Kusumi T, Sato F, et al. Decreased expression of claudin-1 correlates with recurrence status in breast cancer. Int J Mol Med 2007; 20: 139-43.

171. Kominsky SL, Vali M, Korz D, et al. Clostridium perfringens enterotoxin elicits rapid and specific cytolysis of breast carcinoma cells mediated through tight junction proteins claudin 3 and 4. Am J Pathol 2004; 164: 1627-33.

172. Cheung ST, Leung KL, Ip YC, et al. Claudin-10 expression level is associated with recurrence of primary hepatocellular carcinoma. Clin Cancer Res 2005; 11: 551-6.

173. Rangel LB, Agarwal R, D'Souza T, et al. Tight junction proteins claudin-3 and claudin-4 are frequently overexpressed in ovarian cancer but not in ovarian cystadenomas. Clin Cancer Res 2003; 9: 2567-75.

174. Al Moustafa AE, Alaoui-Jamali MA, Batist G, et al. Identification of genes associated with head and neck carcinogenesis by cDNA microarray comparison between matched primary normal epithelial and squamous carcinoma cells. Oncogene 2002; 21: 2634-40.

175. Cohn ML, Goncharuk VN, Diwan AH, Zhang PS, Shen SS, Prieto VG. Loss of claudin-1 expression in tumor-associated vessels correlates with acquisition of metastatic phenotype in melanocytic neoplasms. J Cutan Pathol 2005; 32: 533-6.

176. Nichols LS, Ashfaq R, Iacobuzio-Donahue CA. Claudin 4 protein expression in primary and metastatic pancreatic cancer: support for use as a therapeutic target. Am J Clin Pathol 2004; 121: 226-30.

177. Agarwal R, D'Souza T, Morin PJ. Claudin-3 and claudin-4 expression in ovarian epithelial cells enhances invasion and is associated with increased matrix metalloproteinase-2 activity. Cancer Res 2005; 65: 7378-85.

178. Dhawan P, Singh AB, Deane NG, et al. Claudin-1 regulates cellular transformation and metastatic behavior in colon cancer. J Clin Invest 2005; 115: 1765-76.

179. Turksen K, Troy TC. Permeability barrier dysfunction in transgenic mice overexpressing claudin 6. Development 2002; 129: 1775-84.

180. Mankertz J, Hillenbrand B, Tavalali S, Huber O, Fromm M, Schulzke JD. Functional crosstalk between Wnt signaling and Cdx-related transcriptional activation in the regulation of the claudin-2 promoter activity. Biochem Biophys Res Commun 2004; 314: 1001-7.

181. Polette M, Gilles C, Nawrocki-Raby B, et al. Membrane-type 1 matrix metalloproteinase expression is regulated by zonula occludens-1 in human breast cancer cells. Cancer Res 2005; 65: 7691-8.

182. Reichert M, Muller T, Hunziker W. The PDZ domains of zonula occludens-1 induce an epithelial to mesenchymal transition of Madin-Darby canine kidney I cells. Evidence for a role of beta-catenin/Tcf/Lef signaling. J Biol Chem 2000; 275: 9492-500.

183. Kinugasa T, Sakaguchi T, Gu X, Reinecker HC. Claudins regulate the intestinal barrier in response to immune mediators. Gastroenterology 2000; 118: 1001-11.

184. Feldman G, Kiely B, Martin N, Ryan G, McMorrow T, Ryan MP. Role for TGF-beta in cyclosporine-induced modulation of renal epithelial barrier function. J Am Soc Nephrol 2007; 18: 1662-71.

185. Howe KL, Reardon C, Wang A, Nazli A, McKay DM. Transforming growth factor-beta regulation of epithelial tight junction proteins enhances barrier function

and blocks enterohemorrhagic Escherichia coli O157:H7-induced increased permeability. Am J Pathol 2005; 167: 1587-97.

186. Chen Y, Lu Q, Schneeberger EE, Goodenough DA. Restoration of tight junction structure and barrier function by down-regulation of the mitogen-activated protein kinase pathway in ras-transformed Madin-Darby canine kidney cells. Mol Biol Cell 2000; 11: 849-62.

187. Lan M, Kojima T, Osanai M, Chiba H, Sawada N. Oncogenic Raf-1 regulates epithelial to mesenchymal transition via distinct signal transduction pathways in an immortalized mouse hepatic cell line. Carcinogenesis 2004; 25: 2385-95.

188. Martinez-Estrada OM, Culleres A, Soriano FX, et al. The transcription factors Slug and Snail act as repressors of Claudin-1 expression in epithelial cells. Biochem J 2006; 394: 449-57.

189. Ohkubo T, Ozawa M. The transcription factor Snail downregulates the tight junction components independently of E-cadherin downregulation. J Cell Sci 2004; 117: 1675-85.

190. Singh AB, Harris RC. Epidermal growth factor receptor activation differentially regulates claudin expression and enhances transepithelial resistance in Madin-Darby canine kidney cells. J Biol Chem 2004; 279: 3543-52.

191. Mullin JM. Epithelial barriers, compartmentation, and cancer. Sci STKE 2004; 2004: pe2.

192. Swisshelm K, Macek R, Kubbies M. Role of claudins in tumorigenesis. Adv Drug Deliv Rev 2005; 57: 919-28.

193. Thiery JP. Epithelial-mesenchymal transitions in tumour progression. Nat Rev Cancer 2002; 2: 442-54.

194. Peinado H, Quintanilla M, Cano A. Transforming growth factor beta-1 induces snail transcription factor in epithelial cell lines: mechanisms for epithelial mesenchymal transitions. J Biol Chem 2003; 278: 21113-23.

195. Bolos V, Peinado H, Perez-Moreno MA, Fraga MF, Esteller M, Cano A. The transcription factor Slug represses E-cadherin expression and induces epithelial to mesenchymal transitions: a comparison with Snail and E47 repressors. J Cell Sci 2003; 116: 499-511.

196. Yang J, Mani SA, Donaher JL, et al. Twist, a master regulator of morphogenesis, plays an essential role in tumor metastasis. Cell 2004; 117: 927-39.

197. Kurrey NK, K A, Bapat SA. Snail and Slug are major determinants of ovarian cancer invasiveness at the transcription level. Gynecol Oncol 2005; 97: 155-65.

198. Wang Z, Mandell KJ, Parkos CA, Mrsny RJ, Nusrat A. The second loop of occludin is required for suppression of Raf1-induced tumor growth. Oncogene 2005; 24: 4412-20.

199. Wang Z, Wade P, Mandell KJ, et al. Raf 1 represses expression of the tight junction protein occludin via activation of the zinc-finger transcription factor slug. Oncogene 2007; 26: 1222-30.

200. Radisky DC, Levy DD, Littlepage LE, et al. Rac1b and reactive oxygen species mediate MMP-3-induced EMT and genomic instability. Nature 2005; 436: 123-7.

201. Zavadil J, Cermak L, Soto-Nieves N, Bottinger EP. Integration of TGF-beta/Smad and Jagged1/Notch signalling in epithelial-to-mesenchymal transition. EMBO J 2004; 23: 1155-65.

202. Wang Z, Li Y, Banerjee S, Sarkar FH. Emerging role of Notch in stem cells and cancer. Cancer Lett 2008.

203. Bhowmick NA, Ghiassi M, Bakin A, et al. Transforming growth factor-beta1 mediates epithelial to mesenchymal transdifferentiation through a RhoA-dependent mechanism. Mol Biol Cell 2001; 12: 27-36.

204. Townsend TA, Wrana JL, Davis GE, Barnett JV. Transforming growth factor-beta-stimulated endocardial cell transformation is dependent on Par6c regulation of RhoA. J Biol Chem 2008; 283: 13834-41.

205. Levayer R, Lecuit T. Breaking down EMT. Nat Cell Biol 2008; 10: 757-9.

206. Taddei A, Giampietro C, Conti A, et al. Endothelial adherens junctions control tight junctions by VE-cadherin-mediated upregulation of claudin-5. Nat Cell Biol 2008; 10: 923-34.

207. Potempa S, Ridley AJ. Activation of both MAP kinase and phosphatidylinositide 3-kinase by Ras is required for hepatocyte growth factor/scatter factor-induced adherens junction disassembly. Mol Biol Cell 1998; 9: 2185-200.

208. Theard D, Steiner M, Kalicharan D, Hoekstra D, van Ijzendoorn SC. Cell polarity development and protein trafficking in hepatocytes lacking E-cadherin/beta-catenin-based adherens junctions. Mol Biol Cell 2007; 18: 2313-21.

209. Harten SK, Shukla D, Barod R, et al. Regulation of Renal Epithelial Tight Junctions by the VHL Tumor Suppressor Gene Involves Repression of Occludin and Claudin 1 and Is Independent of E-Cadherin. Mol Biol Cell 2008.

210. Lehembre F, Yilmaz M, Wicki A, et al. NCAM-induced focal adhesion assembly: a functional switch upon loss of E-cadherin. EMBO J 2008; 27: 2603-15.

211. Tsukada T, Tomooka Y, Takai S, et al. Enhanced proliferative potential in culture of cells from p53-deficient mice. Oncogene 1993; 8: 3313-22.

212. Kamachi Y, Ogawa E, Asano M, et al. Purification of a mouse nuclear factor that binds to both the A and B cores of the polyomavirus enhancer. J Virol 1990; 64: 4808-19.

213. Becker KF, Atkinson MJ, Reich U, et al. E-cadherin gene mutations provide clues to diffuse type gastric carcinomas. Cancer Res 1994; 54: 3845-52.

214. Tamura G, Sakata K, Nishizuka S, et al. Inactivation of the E-cadherin gene in primary gastric carcinomas and gastric carcinoma cell lines. Jpn J Cancer Res 1996; 87: 1153-9.

215. Hoevel T, Macek R, Swisshelm K, Kubbies M. Reexpression of the TJ protein CLDN1 induces apoptosis in breast tumor spheroids. Int J Cancer 2004; 108: 374-83.

216. Shiou SR, Singh AB, Moorthy K, et al. Smad4 regulates claudin-1 expression in a transforming growth factor-beta-independent manner in colon cancer cells. Cancer Res 2007; 67: 1571-9.

217. Boudreau F, Lussier CR, Mongrain S, et al. Loss of cathepsin L activity promotes claudin-1 overexpression and intestinal neoplasia. FASEB J 2007.

218. Xu L, Massague J. Nucleocytoplasmic shuttling of signal transducers. Nat Rev Mol Cell Biol 2004; 5: 209-19.

APPENDIX 1

GENOMIC STRUCTURE OF *Runx3*, STRUCTURE OF THE TARGETING VECTOR FOR HOMOLOGOUS RECOMBINATION, AND THE GENE STRUCTURE OF THE TARGETED LOCUS

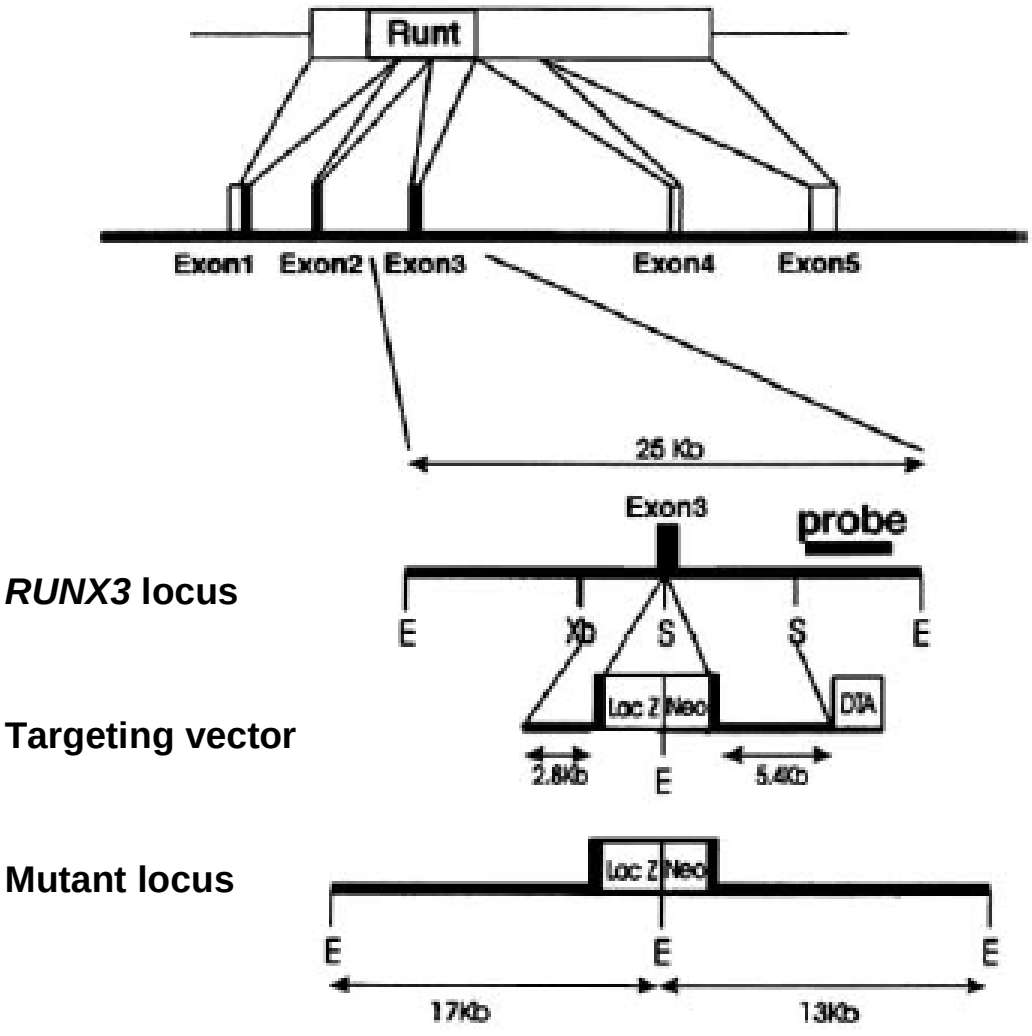

APPENDIX 2

FULL LENGTH SEQUENCE OF hCLAUDIN-1 PROMOTER (1530 bp)

(RUNX BINDING SITES HIGHLIGHTED IN YELLOW)

CCCTGGGATACAACACGAACATGGTCTTGTCCTAAACAGCTGATAGGAGAAAGACAG
TATTCACTGTGTTAATCTCAGTCCAAATTAATTGTCTTCATCTAGCTCCTGTCTTAC
ATTCTTCATTGCTTGTCCCTAAATCCTAGCACGGCCAAGTCCTTTAGTTTTAAGCCT
ACATGAAAGGCATCCAGGGAGAGCCAGGTGGAAATGAAGGTGGTGGGGCTTGGCCTT
TCTTCCCATTCCCACCTTGAGAATTTGCACCTTTCCTTCTCTGTCACCAACTAGCAG
TTGCCATGGTATATAAGGGTATATCTTATTTTATCCTTAATATGTTTATTTCTGCTT
CCAAGATGCTTCTGTTTTTACTAAAACCATAGAAGCTTCCCCTCCCACCACACTCGC
ACCACACACAAAAAGCAGTTGGAAAAACATTTCAATGATTCCTAACCACAACAGCAC
TTCTGACTAACTACAAAGAAGGAAGCTTTGGAGAAACATAGAGGGAAACTACAGTCC
CAGCGAGACCGAAACCGGAGGGGTGAGATAGCCAGTCACAGTAAAAGCTGGAACCAG
AGCCCAGACTTCCTCAACTCCAGCCCAGTCCTTTTGCCACTGGGGAAACGCTGTTTA
CATGTCCTCACCTGCGACGAACAACATTTGATAACTCACAAAATTAACACCTTTCAG
GGAGAGCGGGGCACTGGCCAGGTCCCTCTGATAATGAATTGCTGCTCTAAGACATAA
CTGCTGTGGGGAGGAGGTTGGTGTTTGGCGGGGAAGGGCTGCTAGCCTGCAGTTTCA
TAAGGACAATAATACATCAAAAAGGACAATCATAGATCAAAGGGGATATTTTGGGTC
AACTTGATATGTAGTGGAAAGCAGATTGGGAGGGGAGCCAAGTACTGGATATGCTCC
GTGCGTGAGTGTGTCTGTGTGTGTGTGTGTGTGTGTGTGTAAATCATGTTGCTCTCT
GGGTCTGTTTCCCAATCTGTAGAGTGTAAAAGTCTCTGAGGCTCCTTGCAGAGACAA
GTGATGGAACGACCTTGACAGAAGAGAGCAGAGAGAGGAAAGAAGGGGGAGGAAGCC
AAGCAAAGGAGAGAGAAATGGTGTGATGGGGGAGGAGACGCGGAGTTGGGTAGAAAT
GCCTTTTAATAAGATATTGGGAAAAAAGTATTAAACCTAAAACTGCAGCTCTTGAAG
GATCATTTTTTCATCTTTGTGTTAGGATTTACAAGTACAGTGCATAGTAATTTTTGG
ATAATTGGAGTGAATGAATGAAAAGCGTGAAACGCCTTACAGGAGCGAGAAGATCCA
CGAGAGAAAGCGAGCAGGGACGCAGCTCTGGTGCCTGGTCCTGCCGGGTGGTCCCCA
CGCCGCCAGCCGCGCGTTCCCCAACCGGGCGCTCCCGGCGCCCTCTCGGTGAGCCGC
CCTGAAACCGCCAGGGGGCGCTCCCCGGCTGCCGGGGCTGAGGCGGGCGGAGCTGCT
TTAAATCGCGGCGCCCAGCGGTTCTGCGTCTCAGTTCCCGAGCCTGGG

APPENDIX 3

pGL3 VECTOR FOR CLONING OF PROMOTER

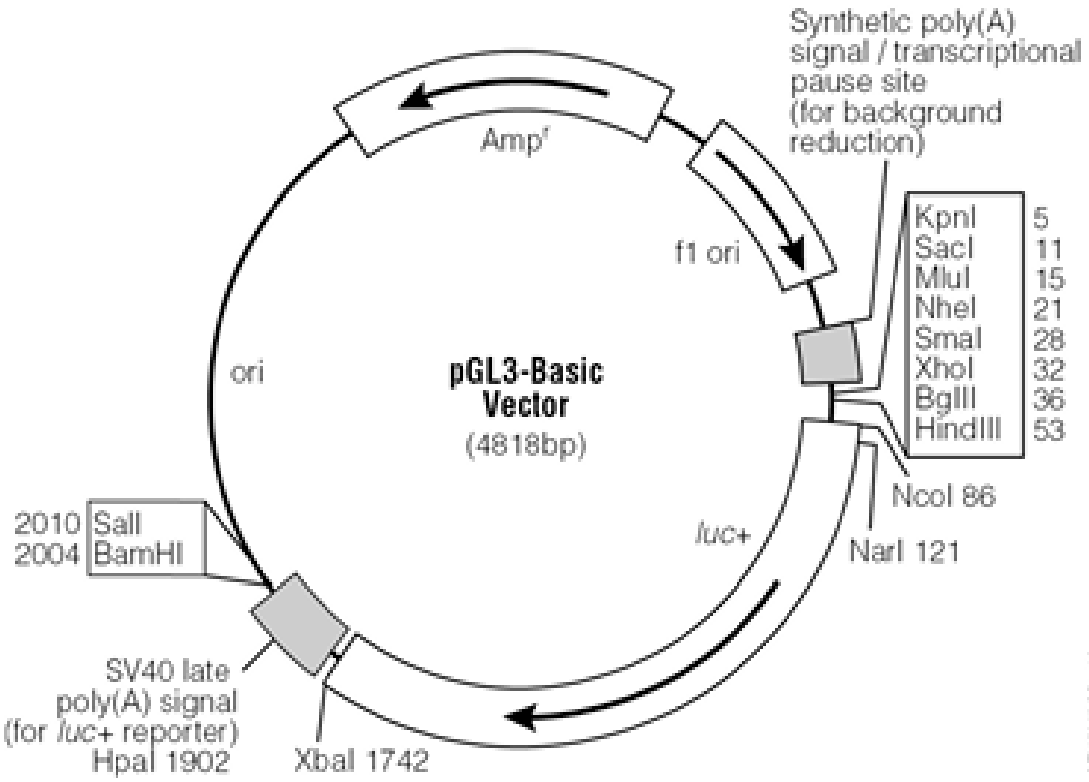

APPENDIX 4

pRLSV40 VECTOR

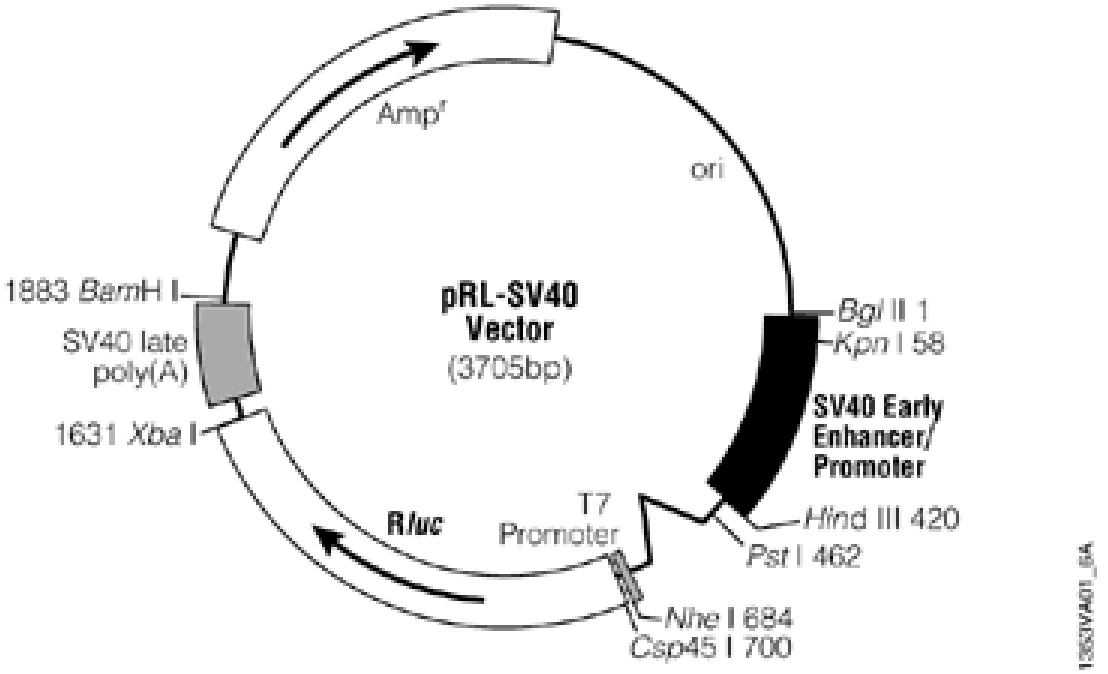

Note: The SV40 promoter was removed at the *Bgl* II and *Hind* III restriction sites and ligated through blunt-end ligation.

APPENDIX 5

Human *RUNX3* cDNA

(nucleotide 1-1784; Genbank accession no. Z35278)

gccgctgttatgcgtattcccgtagacccaagcaccagccgccgcttcacacctccctcc
ccggccttcccctgcggcggcggcggcggcaagatgggcgagaacagcggcgcgctg
agcgcgcaggcggccgtggggcccggagggcgcgcccggcccgaggtgcgctcgatg
gtggacgtgctggcggaccacgcaggcgagctcgtgcgcaccgacagccccaacttc
ctctgctccgtgctgccctcgcactggcgctgcaacaagacgctgcccgtcgccttc
aaggtggtggcattgggggacgtgccggatggtacggtggtgactgtgatggcaggc
aatgacgagaactactccgctgagctgcgcaatgcctcggccgtcatgaagaaccag
gtggccaggttcaacgaccttcgcttcgtgggccgcagtgggcgagggaagagtttc
accctgaccatcactgtgttcaccaaccccacccaagtggcgacctaccaccgagcc
atcaaggtgaccgtggacggaccccgggagcccagacggcaccggcagaagctggag
gaccagaccaagccgttccctgaccgctttggggacctggaacggctgcgcatgcgg
gtgacaccgagcacacccagcccccgaggctcactcagcaccacaagccacttcagc
agccagccccagaccccaatccaaggcacctcggaactgaacccattctccgacccc
cgccagtttgaccgctccttccccacgctgccaaccctcacggagagccgcttccca
gaccccaggatgcattatcccggggccatgtcagctgccttcccctacagcgccacg
ccctcgggcacgagcatcagcagcctcagcgtggcgggcatgccggccaccagccgc
ttccaccatacctacctcccgccaccctacccgggggccccgcagaaccagagcggg
cccttccaggccaacccgtccccctaccacctctactacgggacatcctctggctcc
taccagttctccatggtggccggcagcagcagtgggggcgaccgctcacctacccgc
atgctggcctcttgcaccagcagcgctgcctctgtcgccgccggcaacctcatgaac
cccagcctgggcggccagagtgatggcgtggaggccgacggcagccacagcaactca
cccacggccctgagcacgccaggccgcatggatgaggccgtgtggcggccctactga
ccgccctggtggactcctcccgctggaggcggggaccctaacaaccttcaagaccag
tgatgggccggctccgaggctccgggcgggaatgggacctgcgctccagggtggtct
cggtcccagggtggtcccagctggtgggagcctctggctgcatctgtgcagccacat
ccttgtacagaggcataggttaccacccccaccccggcccgggatactgcccccggc
ccagatcctggccgtctcatcccatacttctgtggggaatcagcctcctgccacccc
cccggaaggacctcactgtctccagctatgcccagtgctgcatgggacccatgtctc
ctgggacagaggccatctctcttccagagagaggcagcattggcccacaggataagc
ctcaggccctgggaaacctcccgacccctgcaccttcgttggagcccctgcatcccc
tgggtccagccccctctgcatttacacagatttgagtcagaactggaaagtgtcccc
caccccccaccaccc

APPENDIX 6

FULL LENGTH SEQUENCE OF mCLAUDIN-1

OPEN READING FRAME (636 bp)

atggccaacgcggggctgcagctgctgggtttcatcctggcttctctgggatggatc
ggctccatcgtcagcactgccctgccccagtggaagatttactcctatgctggggac
aacatcgtgaccgctcaggccatctacgagggactgtggatgtcctgcgtttcgcaa
agcaccgggcagatacagtgcaaagtcttcgactccttgctgaatctgaacagtact
ttgcaggcaacccgagccttgatggtaattggcatcctgctggggctgatcgcaatc
tttgtgtccaccattggcatgaagtgcatgaggtgcctggaagatgatgaggtgcag
aagatgtggatggctgtcattgggggcataatattttaatttcaggtctggcgaca
ttagtggccacagcatggtatggaaacagaattgttcaagaattctatgacccttg
acccccatcaatgccaggtatgaatttggccaggccctctttactggctgggccgct
gcctccctctgccttctgggaggtgtcctactttcctgctcctgtccccggaaaaca
acctcttacccaacaccacggccttatcccaagccaacaccttctagtgggaaagac
tatgtgtga

APPENDIX 7

FULL LENGTH SEQUENCE OF hCLAUDIN-1

OPEN READING FRAME (636 bp)

atggccaacgcggggctgcagctgttgggcttcattctcgccttcctgggatggatc
ggcgccatcgtcagcactgccctgccccagtggaggatttactcctatgccggcgac
aacatcgtgaccgcccaggccatgtacgaggggctgtggatgtcctgcgtgtcgcag
agcaccgggcagatccagtgcaaagtctttgactccttgctgaatctgagcagcaca
ttgcaagcaacccgtgccttgatggtggttggcatcctcctgggagtgatagcaatc
tttgtggccaccgttggcatgaagtgtatgaagtgcttggaagacgatgaggtgcag
aagatgaggatggctgtcattgggggtgcgatatttcttcttgcaggtctggctatt
ttagttgccacagcatggtatggcaatagaatcgttcaagaattctatgaccctatg
accccagtcaatgccaggtacgaatttggtcaggctctcttcactggctgggctgct
gcttctctctgccttctgggaggtgccctactttgctgttcctgtccccgaaaaaca
acctcttacccaacaccaaggccctatccaaaacctgcaccttccagcgggaaagac
tacgtgtga